Quantum steering ellipsoids

Antony Milne

Imperial College London

Department of Physics

16 December 2016

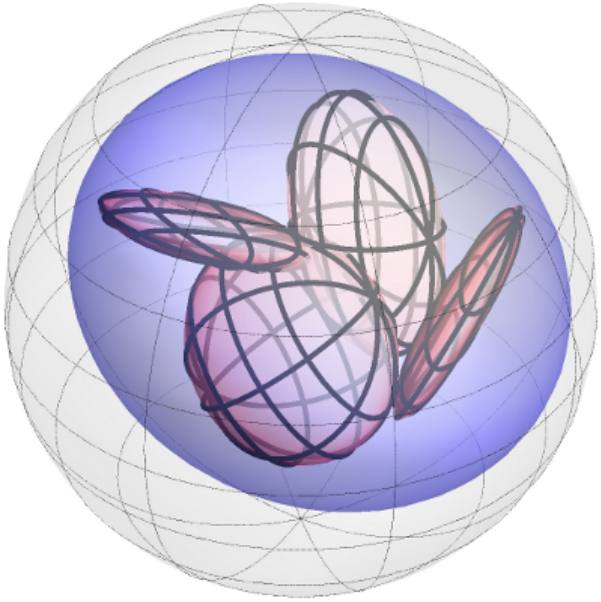

Supervisors: David Jennings and Terry Rudolph

Submitted for the degree of Doctor of Philosophy

DECLARATION

The research presented in this thesis was completed by me, and the work of any other people is appropriately referenced.

Antony Milne, 16 December 2016

Abstract

Graphical representations are invaluable for visualising physical systems and processes. In quantum information theory, the Bloch vector representation of a single qubit is ubiquitous, but visualising higher-dimensional quantum systems is far less straightforward. The quantum steering ellipsoid provides a method for geometrically representing the state of two qubits, the most fundamental system for studying quantum correlations. This thesis constitutes a significant development of the steering ellipsoid formalism. As well as offering new insight into the study of two-qubit states, we extend this powerful geometric approach to explore scenarios beyond two qubits.

We find necessary and sufficient conditions for when an ellipsoid inside the Bloch ball describes a valid (i.e. positive semidefinite) two-qubit state. Combined with the notion of ellipsoid chirality, this enables a geometric characterisation of entanglement. We find a family of 'maximally obese' two-qubit states whose ellipsoids have maximal volume. These states have optimal correlation properties within the set of all two-qubit states with a single maximally mixed marginal. We study a three-qubit scenario and discover that ellipsoid volume obeys an elegant monogamy of steering relationship. From this we can derive the Coffman-Kundu-Wootters (CKW) inequality for concurrence monogamy, providing an intuitive geometric derivation of this classic result.

Remarkably, we find that steering ellipsoids offer a fresh perspective on questions beyond quantum state space. Entanglement witnesses are also very naturally represented and classified using the formalism. This gives a physical interpretation to any ellipsoid inside the Bloch ball as a block positive two-qubit operator, which we may then classify further. We can also use steering ellipsoids to derive some highly nontrivial results in classical Euclidean geometry, extending Euler's inequality for the circumradius and inradius of a triangle.

PUBLISHED WORK

Much of this thesis is based on the following publications, although material has been expanded and reworked throughout:

- Ref. [1]: A. Milne, S. Jevtic, D. Jennings, H. Wiseman, and T. Rudolph, "Quantum steering ellipsoids, extremal physical states and monogamy," New J. Phys. 16, 083017 (2014).
- Ref. [2]: A. Milne, D. Jennings, S. Jevtic, and T. Rudolph, "Quantum correlations of two-qubit states with one maximally mixed marginal," Phys. Rev. A 90, 024302 (2014).
- Ref. [3]: A. Milne, D. Jennings, and T. Rudolph, "Geometric representation of two-qubit entanglement witnesses," Phys. Rev. A 92, 012311 (2015).
- Ref. [4]: A. Milne, "The Euler and Grace-Danielsson inequalities for nested triangles and tetrahedra: a derivation and generalisation using quantum information theory," J. Geom. 106, 455–463 (2015).

The interested reader may also wish to refer to the following:

- Ref. [5]: X. Hu, A. Milne, B. Zhang, and H. Fan, "Quantum coherence of steered states," Sci. Rep. **6**, 19365 (2016).
- Ref. [6]: S. Cheng, A. Milne, M. J. W. Hall, and H. M. Wiseman, "Volume monogamy of quantum steering ellipsoids for multi-qubit systems," Phys. Rev. A 94, 042105 (2016).

The work published in these papers was led by others and is not included in this thesis.

ACKNOWLEDGEMENTS

Firstly, I would like to thank my supervisors David Jennings and Terry Rudolph. I am privileged to have completed a PhD under the guidance of two exceptional quantum information theorists, and I have learnt a great deal from them both. I have also enjoyed collaborations with several other first rate scientists. Sania Jevtic, Howard Wiseman and Chau Nguyen are especially worthy of mention for their contributions to the steering ellipsoid formalism.

I am very lucky to have been part of the Centre for Doctoral Training in Controlled Quantum Dynamics, and many of my happiest memories from the past four years are of times shared with the members of Cohort 4. During the last year, Kamil Korzekwa and Matteo Lostaglio have shown me a world beyond ellipsoids, and it has been a pleasure to work with them. Moreover, their company as officemates and friends is a large part of what has made my PhD such a wonderful experience. I am also greatly indebted to all the administrative staff of Whiteley 115, in particular Miranda Smith and Lisa Cheung, for their support and friendship.

Finally, and most importantly, I wish to acknowledge my parents. They have always encouraged my academic work, and during my PhD they have also generously provided me with food and shelter. I am extremely grateful for all they have done.

Contents

FIGURES

THEOREMS

PICTORIAL OVERVIEW

We begin the thesis with an introduction to Schrödinger's notion of *quantum steering*. Chapter 1 outlines the steering scenario: when Alice and Bob share a two-qubit state ρ, a local measurement by Bob alters Alice's local state from ρ_A to ρ'_A. Alice's Bloch vector changes accordingly as $\boldsymbol{a} \mapsto \boldsymbol{a}'$.

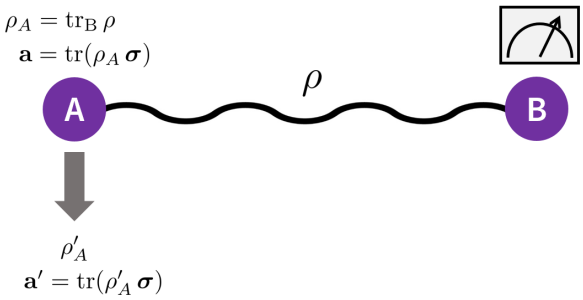

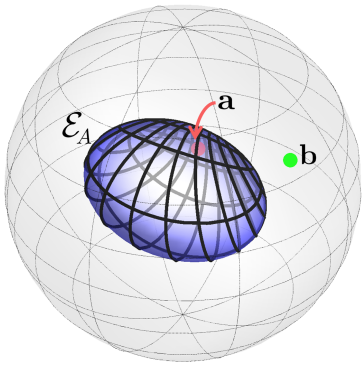

This concept is the basis of the steering ellipsoid formalism for two-qubit states. In analogy to the Bloch sphere picture for a single qubit, we can represent a two-qubit state using the Bloch vectors $\boldsymbol{a}$ and $\boldsymbol{b}$ and Alice's steering ellipsoid $\mathcal{E}_A$. This gives the set of all Bloch vectors $\boldsymbol{a}'$ to which Alice can be remotely steered by Bob. Chapter 2 gives a full derivation of the steering ellipsoid.

We then proceed to characterise the steering ellipsoid. Chapter 3 formulates conditions for when an ellipsoid represents a valid two-qubit state and explores how entanglement is manifest in the representation. We investigate the separable-entangled and physical-unphysical boundaries, and then in Chapter 4 present a family of ellipsoids that have maximal volume for the ellipsoid centre.

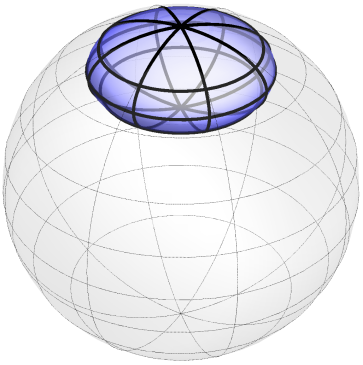

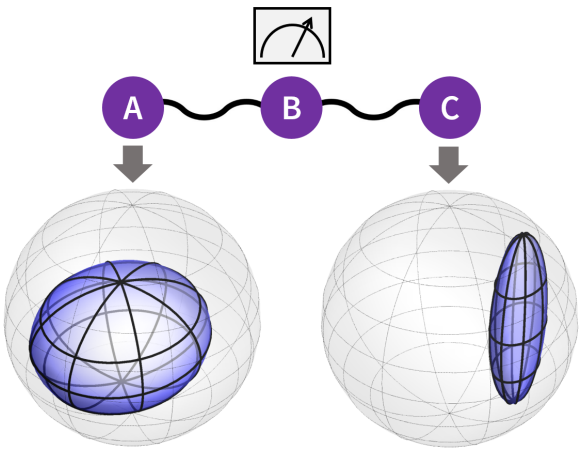

This reveals the family of *maximally obese* two-qubit states, which forms the basis for much of the work in Chapters 5 and 6. These states are found to have optimal quantum correlation properties. We study a three-qubit scenario in which Bob can steer Alice and Charlie to ellipsoids $\mathcal{E}_A$ and $\mathcal{E}_C$. This yields a remarkable *monogamy of steering* relationship in terms of the ellipsoid volumes: $\sqrt{V_A} + \sqrt{V_C} \leq \sqrt{\frac{4\pi}{3}}$.

In Chapter 7 we show that the steering ellipsoid formalism can be extended to represent more than just quantum states. Ellipsoids that do not describe states instead correspond to *entanglement witnesses*. We investigate how properties such as witness optimality are manifest in the ellipsoid representation and provide a new geometric classification for two-qubit block positive operators.

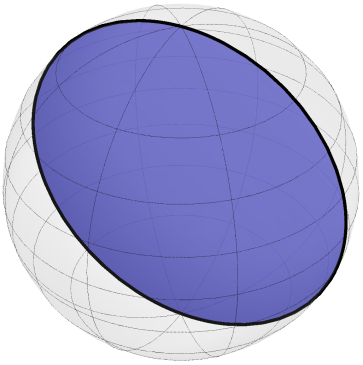

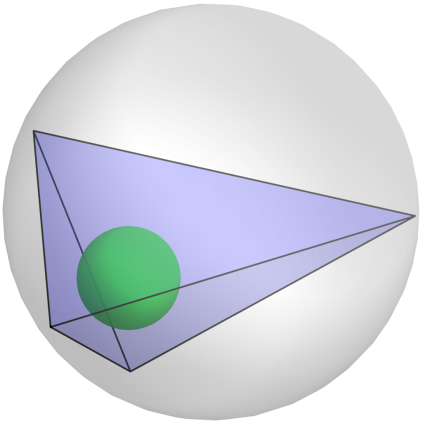

Finally, we show in Chapter 8 that steering ellipsoids can be used to derive results in pure Euclidean geometry. We provide a physically-motivated derivation of known (but highly nontrivial) inequalities concerning the existence of a tetrahedron nested between two spheres. Remarkably, the steering ellipsoid also enables us to formulate results that are entirely new to the field of classical Euclidean elementary geometry.

CHAPTER 1

BACKGROUND

In this introductory chapter, we motivate the study of quantum steering ellipsoids and provide an outline of the formalism. We consider what are the desirable features of a graphical representation and explain why the Bloch vector is an effective visualisation tool for single qubit states. The steering ellipsoid is then introduced as an extension of the Bloch vector picture to two-qubit states.

We show how the steering ellipsoid can be found and review known results relating ellipsoid geometry to physical properties of a two-qubit state. For example, the *nested tetrahedron condition* states that a two-qubit state is separable if and only if its steering ellipsoid fits inside a tetrahedron inside the Bloch ball. We thus demonstrate steering ellipsoids to be an intuitive and physically meaningful representation scheme.

We also consider alternative methods for visualising two-qubit states and discuss how the steering ellipsoid can be generalised to higher dimensions. This chapter is intended to give a reasonably non-technical and readable introduction to quantum steering ellipsoids; a thorough mathematical treatment of the formalism, including a full derivation, will be provided in Chapter 2.

1.1 NOTATION

We begin by introducing some terminology that will be used throughout the thesis. This background material may be found in any standard reference text on quantum information, e.g. Ref. [7].

A quantum system is associated with a Hilbert space $\mathcal{H}$, and the *state* of the system is described by a *density operator* ρ acting on $\mathcal{H}$. We denote by $\mathrm{L}(\mathcal{H})$ the set of linear operators on $\mathcal{H}$, so that $\rho \in \mathrm{L}(\mathcal{H})$. By definition, ρ must be Hermitian ($\rho = \rho^\dagger$), unit trace ($\mathrm{tr}\,\rho = 1$) and positive semidefinite ($\rho \geq 0$). We will use $\hat{\rho}$ to denote an unnormalised density matrix.

A density operator can be expressed as a probabilistic ensemble via a convex decomposition $\{p_i, \rho_i\}$, with p_i probabilities (i.e. $\sum_i p_i = 1$ and $p_i \geq 0$) and each ρ_i a distinct density matrix: $\rho = \sum_i p_i \rho_i$. Any mixed state ρ has infinitely many convex decompositions, while a pure state has a unique decomposition $\rho = |\psi\rangle\langle\psi|$, with $|\psi\rangle \in \mathcal{H}$. When a quantum system is shared between remote parties, local *reduced states* can be found using the partial trace operation: say that ρ is shared between Alice and Bob; then $\rho_A = \mathrm{tr}_B\,\rho$ gives Alice's reduced state and $\rho_B = \mathrm{tr}_A\,\rho$ gives Bob's.

A *measurement* in quantum mechanics is described by the POVM (positive operator valued measurement) formalism. A POVM is a set of n *measurement outcomes* $\left\{M_{i|j}\right\}_{i=1}^{n}$ that satisfy $M_{i|j} \geq 0$ and $\sum_i M_{i|j} = \mathbb{1}$. The index j labels the choice of POVM, whilst the index i labels the outcome obtained.

When Bob performs the local measurement j on his half of the bipartite state ρ, he obtains at random an outcome $M_{i|j}$. Alice's local state will 'collapse' as follows:

$$\rho_A \mapsto \hat{\rho}_A^{i|j} = \mathrm{tr}_B\left[\rho\left(\mathbb{1}\otimes M_{i|j}\right)\right], \tag{1.1}$$

where $\mathbb{1}$ is the identity operator. Alice's normalised state will be $\rho_A^{i|j} = \hat{\rho}_A^{i|j}/p_{i|j}$, where the normalisation constant $p_{i|j} = \mathrm{tr}\left[\rho\left(\mathbb{1}\otimes M_{i|j}\right)\right]$ gives the probability of Bob obtaining outcome i given that he has performed POVM j. This transformation is referred to as *steering*: Bob's local measurement has remotely steered Alice's state. Note that, since $\sum_i M_{i|j} = \mathbb{1}$, Alice's unconditioned state $\rho_A = \sum_i \hat{\rho}_A^{i|j}$ is not affected by Bob's choice of measurement – a manifestation of the no signalling principle.

1.2 STEERING

The notion of steering originated as a response by Schrödinger to the famous EPR (Einstein-Podolsky-Rosen) paper of 1935 [8]. Schrödinger both coined the term 'steering' and provided

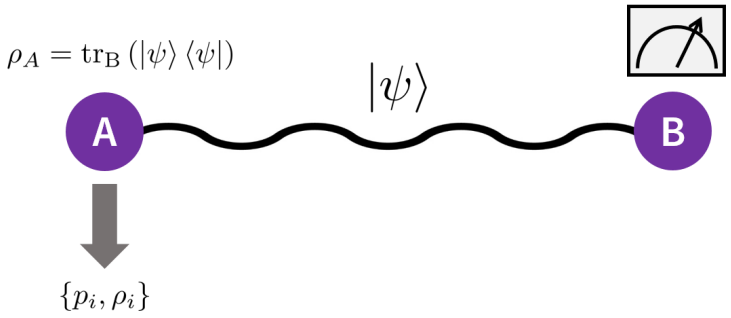

Figure 1.1: According to the Schrödinger-HJW theorem, when Alice and Bob share the state $|\psi\rangle$, Bob's measurement can steer Alice to the convex decomposition $\{p_i, \rho_i\}$ if and only if $\rho_A = \sum_i p_i \rho_i$.

the first proof of what is sometimes called the *pure state steering theorem* [9, 10]: when Alice and Bob share a pure entangled state then by performing a suitable measurement, Bob has 'a non-vanishing probability of driving [Alice's] system into any state he chooses'.[1] In fact, Schrödinger found this behaviour 'very disconcerting' and doubted whether the notion of steering could really be true.

Unaware of Schrödinger's work, Hughston, Jozsa and Wootters rediscovered the steering theorem in 1993 [12], building on earlier work by Gisin [13] (for a more detailed discussion of the history, see Ref. [14]). The pure state steering theorem is thus sometimes known as the *Schrödinger-HJW theorem*. We give this below, expressed in modern terminology, and illustrate it in Figure 1.1.

Theorem 1.1: Schrödinger-HJW theorem

When Alice and Bob share a pure bipartite state $|\psi\rangle$, a measurement by Bob can steer Alice's system to the convex decomposition $\{p_i, \rho_i\}$ if and only if $\rho_A = \sum_i p_i \rho_i$, where $\rho_A = \mathrm{tr}_B(|\psi\rangle\langle\psi|)$.

The proof may be found in any of the historical references given above or, perhaps most clearly using modern quantum information notation, in Ref. [15].

It was not until 2007 that the notion of so-called EPR-steerability was formalised and extended to mixed states by Wiseman et al. in Refs. [16, 17]. A quantum state can demonstrate the steering effect that so troubled Schrödinger if and only if we cannot write

$$\hat{\rho}_A^{i|j} = \sum_\lambda p_\lambda \, p_{i|j,\lambda} \, \phi_\lambda \tag{1.2}$$

[1] Throughout this thesis, we adopt the steering ellipsoid convention set in Ref. [11] that Bob is the steering party and Alice is the steered party. Note that literature on EPR-steering generally takes Alice to be the steering party instead.

for all measurement outcomes $M_{i|j}$. Here p_λ and $p_{i|j,\lambda}$ are probability distributions involving a *local hidden variable* (LHV) λ, and ϕ_λ is a *local hidden state* (LHS) for Alice. If we can write (1.2) then Bob's steering of Alice could be explained simply by underlying classical correlation between Alice's LHS and Bob's LHV.[1] Otherwise, we are demonstrating genuine quantum steering, and the state ρ is *steerable* from Bob to Alice.

The development of a modern formulation of EPR-steering has led to a remarkable resurgence of interest in the phenomenon, and there is now an ever-growing body of work devoted to examining all the varied facets of quantum steering. To name but a few, topics include the formulation of steering inequalities, experimental demonstrations of steering, development of a resource theory of steering, investigations into the use of steering in quantum key distribution and subchannel discrimination, and the quantification of steerability. For a recent review of these topics and many more, the reader is referred to Ref. [18].

In the quantum steering ellipsoid picture we consider a slightly different and complementary perspective to the EPR-steering approach given above. Instead of considering the existence of a local hidden state model, we focus instead on the set of reduced states to which Alice can be steered by Bob's measurement. It is this perspective that will allow us to develop a powerful tool for visualising two-qubit states.

1.3 VISUALISATION OF QUANTUM STATES

Given a Hilbert space $\mathcal{H}$ of dimension d, the number of real parameters required to specify a quantum state ρ is $d^2 - 1$.[2] For the case of a qubit ($d = 2$), the three parameters can easily be visualised as a Bloch vector [19]. For higher-dimensional systems, however, there is no simple geometric picture; already for the system of two qubits it is a significant challenge to geometrically represent all 15 parameters.

In the following section we recall the Bloch vector representation of a single qubit state. We then present the quantum steering ellipsoid representation for two-qubit states. A useful visualisation scheme for quantum states should reveal physical properties of the quantum state through the representation's geometric features. Ideally, the scheme should also be faithful, allowing any state to be represented as well as providing a method for uniquely reconstructing ρ from the representation. We will see that the steering ellipsoid formalism, like the Bloch

[1] This places steering as a form of correlation intermediate between Bell-nonlocality and entanglement. A state is Bell-nonlocal if joint measurement probabilities cannot be explained by a LHV for Alice and Bob; a state is entangled if joint measurement probabilities cannot be explained by a LHS for Alice and Bob. For pure states, entanglement, steerability and Bell-nonlocality are all equivalent; for mixed states, the hierarchy is strict [16, 17].

[2] A general linear operator on the Hilbert space is given by $\rho \in \mathbb{C}^{d\times d}$ and has $2d^2$ real parameters. The constraint $\mathrm{tr}\,\rho = 1$ and Hermiticity reduce this to $d^2 - 1$.

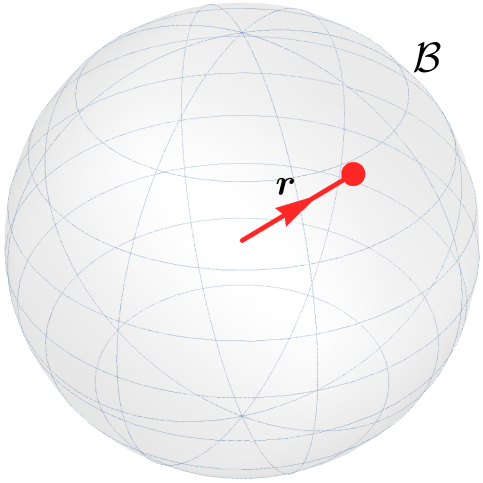

Figure 1.2: The Bloch vector representation of a single qubit state: $\boldsymbol{r}$ lies inside the unit ball $\mathcal{B}$.

vector picture, achieves both of these desiderata. At the end of the chapter we present some alternative schemes for visualising two-qubit states and discuss the representation of systems beyond two qubits.

1.4 VISUALISING A SINGLE QUBIT: THE BLOCH VECTOR

The single qubit system is the most fundamental unit in quantum information theory, analogous to a bit in classical information [7]. A single qubit state ρ acts on $\mathcal{H} = \mathbb{C}^2$. The identity matrix $\mathbb{1}$ and the Pauli matrices $\boldsymbol{\sigma} = (\sigma_x, \sigma_y, \sigma_z)$ form a basis for the set of Hermitian operators on $\mathcal{H}$.[1] We may thus parametrise the state of a qubit as

$$\rho = \tfrac{1}{2}(\mathbb{1} + \boldsymbol{r} \cdot \boldsymbol{\sigma}), \tag{1.3}$$

where $\boldsymbol{r} \in \mathbb{R}^3$ is the *Bloch vector*. Equivalently, letting $\sigma_0 = \mathbb{1}$, we may write[2]

$$\rho = \frac{1}{2}\sum_{\mu=0}^{3} r_\mu \sigma_\mu, \tag{1.4}$$

with $r_\mu = \mathrm{tr}(\rho\,\sigma_\mu)$, and consider instead the four-vector $\boldsymbol{R} = (r_0, \boldsymbol{r})$. This notation will be extremely useful when we derive the form of the steering ellipsoid using four-dimensional geometry in Chapter 2.

Note that by construction ρ is unit trace ($r_0 = 1$). The constraint of positivity, $\rho \geq 0$, is equivalent to $r \leq 1$, where $r := |\boldsymbol{r}|$. We can thus identify the Bloch vector of a single qubit state as a point inside the unit ball $\mathcal{B}$ (see Figure 1.2).

[1] Under the Hilbert-Schmidt inner product $(A, B) := \mathrm{tr}(A^\dagger B)$ this is in fact an orthonormal basis after normalisation.

[2] We adopt the general convention that Greek indices run from 0 to 3 whilst Latin indices run from 1 to 3.

We could of course have represented ρ by a different set of three parameters, which could then be depicted using some other geometric picture. The significance of the Bloch vector representation, and the reason for its ubiquity, is that there is substantial physical meaning underlying the representation. Some interesting physical properties of a single qubit state and the corresponding geometric interpretation in the Bloch vector picture are given below.

- The purity of a state is given by $\mathrm{tr}(\rho^2) = \frac{1}{2}(1 + r^2)$ and thus directly relates to the magnitude of the Bloch vector. In particular, any pure state lies on the Bloch *sphere*, i.e. the surface of the Bloch ball, denoted $\partial\mathcal{B}$. The maximally mixed state $\rho = \frac{1}{2}\mathbb{1}$ is given by the origin.
- Orthogonal pure states are given by antipodal points on the Bloch sphere.
- The expectation of some observable A corresponding to four-vector $(a_0, \boldsymbol{a})$ is $\mathrm{tr}(\rho\, A) = \frac{1}{2}(a_0 + \boldsymbol{a} \cdot \boldsymbol{r})$. In particular, note that if A is the spin operator along some unit direction $\hat{\boldsymbol{a}}$ then the expectation value is simply given by an inner product: $\mathrm{tr}(\rho\, A) = \boldsymbol{r} \cdot \hat{\boldsymbol{a}}$. The probability of obtaining the measurement outcome corresponding to ± 1 is $\frac{1}{2}(1 \pm \boldsymbol{r} \cdot \hat{\boldsymbol{a}})$. Finding these probabilities geometrically corresponds to projecting the Bloch vector onto $\hat{\boldsymbol{a}}$ and then comparing the lengths of line segments.
- Unitary operations on the qubit correspond to rotations of the Bloch vector.

1.5 VISUALISING TWO QUBITS: THE STEERING ELLIPSOID

Most of the interesting features in quantum information theory arise only when we consider multiple qubits and how they interact. In particular, entanglement between qubits is a key resource that lies at the heart of almost all quantum information protocols. More fundamentally, the nature of quantum correlations underlies many results in the foundations of quantum mechanics. Indeed, in the same paper in which he introduced the notion of steering, Schrödinger famously described entanglement as 'not ... *one* but rather *the* characteristic trait of quantum mechanics' [9].

A system of two qubits is the most fundamental unit for studying such correlations. A two-qubit state $\rho \in \mathrm{L}(\mathbb{C}^2 \otimes \mathbb{C}^2)$ can be expressed in the basis $(\mathbb{1}, \boldsymbol{\sigma})^{\otimes 2}$ as

$$\rho = \frac{1}{4}(\mathbb{1} \otimes \mathbb{1} + \boldsymbol{a} \cdot \boldsymbol{\sigma} \otimes \mathbb{1} + \mathbb{1} \otimes \boldsymbol{b} \cdot \boldsymbol{\sigma} + \sum_{i,j=1}^{3} T_{ij}\, \sigma_i \otimes \sigma_j). \tag{1.5}$$

Alternatively, using the four-vector notation, we can write

$$\rho = \frac{1}{4} \sum_{\mu,\nu=0}^{3} \Theta_{\mu\nu}\, \sigma_\mu \otimes \sigma_\nu, \tag{1.6}$$

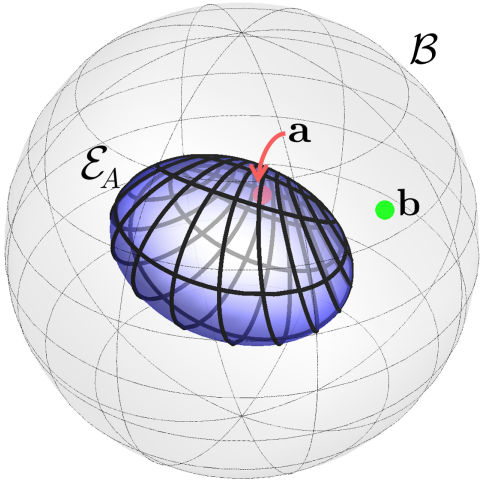

Figure 1.3: An example of the geometric data that describes a two-qubit state: Alice's steering ellipsoid $\mathcal{E}_A$ and the two local Bloch vectors $\boldsymbol{a}$ and $\boldsymbol{b}$ inside the Bloch ball $\mathcal{B}$.

with $\Theta_{\mu\nu} = \mathrm{tr}(\rho\, \sigma_\mu \otimes \sigma_\nu)$. As a block matrix we have $\Theta = \left(\begin{smallmatrix} 1 & \boldsymbol{b}^\intercal \\ \boldsymbol{a} & T \end{smallmatrix}\right)$.

A two-qubit state is thus described by two Bloch vectors $\boldsymbol{a}$ and $\boldsymbol{b}$ and a correlation matrix $T \in \mathbb{R}^{3\times 3}$. The Bloch vectors describe local behaviour of Alice's and Bob's individual qubits, whilst any interesting non-local behaviour associated with the two-qubit state is encoded in the correlation matrix. Note that ρ is unit trace and Hermitian by construction. However, finding constraints to ensure that ρ is positive semidefinite and hence represents a physical quantum state is a much less trivial task than it was for a single qubit. We will find such conditions in Chapter 3; for now we assume that $\rho \geq 0$ in order to facilitate a reasonably non-technical presentation.

1.5.1 DEFINITION

Visualising the two Bloch vectors is straightforward: $\boldsymbol{a}$ and $\boldsymbol{b}$ can simply be represented as points inside the Bloch ball $\mathcal{B}$. The structure of correlations between Alice and Bob will be captured by Alice's steering ellipsoid, which we denote $\mathcal{E}_A$. This ellipsoid will always lie inside the Bloch ball; we write this as $\mathcal{E}_A \subseteq \mathcal{B}$. Thus the geometric data associated with a single qubit state was a Bloch vector $\boldsymbol{r}$; the geometric data associated with a two-qubit state is $(\boldsymbol{a}, \boldsymbol{b}, \mathcal{E}_A)$. Figure 1.3 illustrates a typical example.

We have already outlined the phenomenon of steering: when Alice and Bob share a correlated state then Bob's local measurement can *steer* Alice's local state as $\rho_A \mapsto \rho'_A$, as in (1.1).[1]

[1]We will not generally be interested in which POVM a measurement outcome is associated with, and so we drop the label $i|j$ and refer to a measurement outcome simply as M and the steered state as ρ'_A.

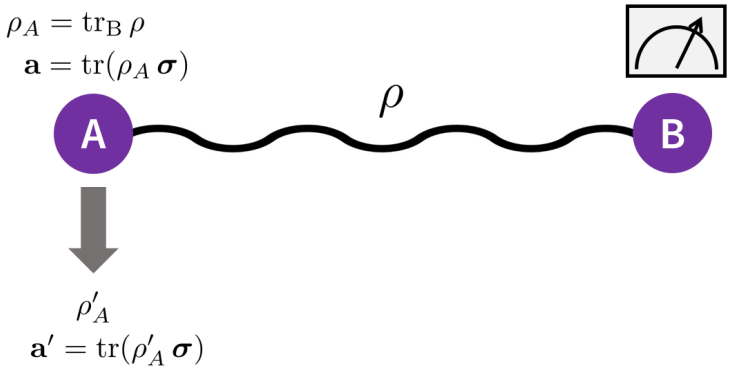

Figure 1.4: When Alice and Bob share a two-qubit state ρ, Bob's local measurement remotely steers Alice's Bloch vector from $\boldsymbol{a}$ to $\boldsymbol{a}'$. This phenomenon is the basis for the steering ellipsoid representation.

For a two-qubit state, Bob's measurement will alter Alice's local Bloch vector as

$$\boldsymbol{a} = \mathrm{tr}(\rho_A\,\boldsymbol{\sigma}) \mapsto \boldsymbol{a}' = \mathrm{tr}(\rho'_A\,\boldsymbol{\sigma}). \tag{1.7}$$

Alice's steered Bloch vector $\boldsymbol{a}'$ depends on the measurement outcome M that Bob obtains. The two-qubit steering scenario is illustrated in Figure 1.4).

Alice's steering ellipsoid $\mathcal{E}_A$ may then be defined as follows:

Definition of the steering ellipsoid

$\mathcal{E}_A$ is the set of Bloch vectors to which Alice can be steered with non-zero probability given all possible local measurement outcomes for Bob:

$$\mathcal{E}_A = \left\{ \boldsymbol{a}' = \mathrm{tr}(\rho'_A\,\boldsymbol{\sigma}) \;\middle|\; \rho'_A = \frac{\mathrm{tr}_B\left[\rho\,(\mathbb{1}\otimes M)\right]}{\mathrm{tr}\left[\rho\,(\mathbb{1}\otimes M)\right]}, M \in \mathrm{POVM} \right\}.$$

The steering ellipsoid was initially presented in work by Verstraete [20] and Shi et al. [21, 22], before a more thorough study by Jevtic et al. uncovered many more features of the representation [11]. Some of these key features will be highlighted after we outline some of the steering ellipsoid's most fundamental properties.

1.5.2 PURE AND MIXED STATES

Let us firstly consider the simplest case of a pure two-qubit state $\rho = |\psi\rangle\langle\psi|$. This is called a *product state* if it can be written as $|\psi\rangle = |\phi\rangle \otimes |\nu\rangle$, where $|\phi\rangle$ and $|\nu\rangle$ are pure states for Alice and Bob. Any state that cannot be written in this way is *entangled*.

When ρ is a product state then no steering is possible, and Alice's steering ellipsoid is just a point: $\mathcal{E}_A = \boldsymbol{a}$. However, when Alice and Bob share a pure entangled two-qubit state, one finds that Alice's qubit can be steered to any state (pure or mixed) inside the Bloch ball, so that

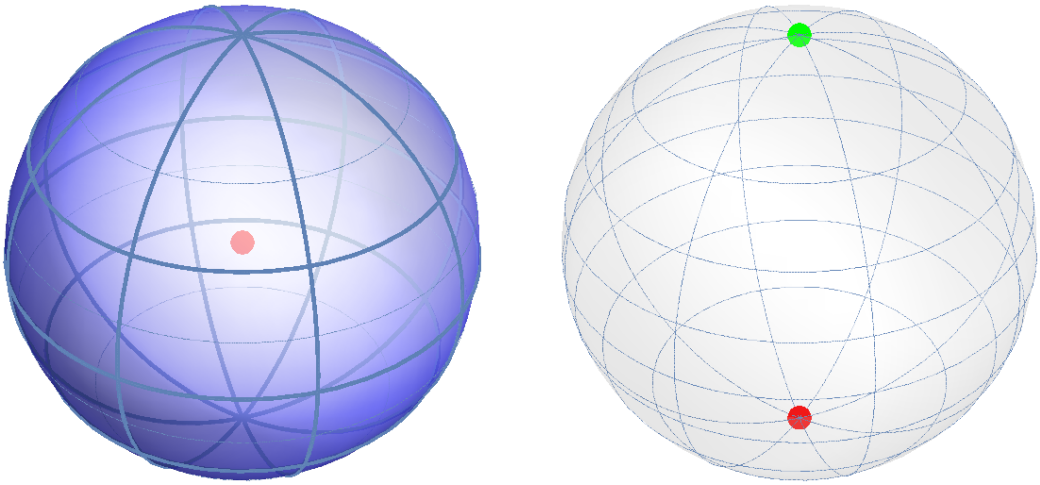

Figure 1.5: For a pure two-qubit state, the steering ellipsoid is either the Bloch ball (left) or a point (right), corresponding to an entangled state and a product state respectively. The entangled state shown here is the Bell state $|\psi^-\rangle = (|01\rangle - |10\rangle)/\sqrt{2}$; in terms of the Pauli basis representation (1.5), we have $\boldsymbol{a} = \boldsymbol{b} = \mathbf{0}$ and $T = \mathrm{diag}(-1, -1, -1)$. The product state shown here is $|10\rangle$, for which we have $\boldsymbol{a} = (0, 0, -1)$, $\boldsymbol{b} = (0, 0, 1)$ and $T = \mathrm{diag}(0, 0, 0)$.

$\mathcal{E}_A = \mathcal{B}$. This expresses in geometric terms the surprising result of Theorem 1.1 applied to two-qubit states. It should be emphasised that $\mathcal{E}_A = \mathcal{B}$ for *all* pure entangled two-qubit states and not for just, say, maximally entangled states. Steering ellipsoids for pure states are illustrated in Figure 1.5.

The case of a mixed state is much more interesting (see Figure 1.6). A bipartite state ρ is described as *separable* if it admits a convex decomposition $\{p_i, \phi_i \otimes \nu_i\}$, where ϕ_i and ν_i are local states for Alice and Bob. Any state that does not admit such a decomposition is entangled. The steering ellipsoid for a mixed two-qubit state cannot be the whole Bloch sphere: $\mathcal{E}_A \subsetneq \mathcal{B}$.

Ref. [11] found the relationship $\dim \mathcal{E}_A = \mathrm{rank}\, \Theta - 1$ that relates the dimension of the steering ellipsoid to the two-qubit Pauli basis matrix Θ. Hence a steering ellipsoid can be degenerate, i.e. an ellipse, line or a point (as it was for a pure product state). Any entangled state ρ must have full rank Θ and hence a fully three-dimensional steering ellipsoid [11]; a degenerate $\mathcal{E}_A$ will describe a separable state.

1.5.3 GEOMETRIC DESCRIPTION

Note that Bob's steering ellipsoid $\mathcal{E}_B$ can be defined analogously using the set of states to which he can be steered by Alice's measurement, and it would be equally valid to consider instead the geometric data $(\boldsymbol{a}, \boldsymbol{b}, \mathcal{E}_B)$. Although $\mathcal{E}_A$ and $\mathcal{E}_B$ can be quite different, we always have $\dim \mathcal{E}_A = \dim \mathcal{E}_B$. Unless stated otherwise, we will consider Alice's steering ellipsoid and drop the label A so that $\mathcal{E} \equiv \mathcal{E}_A$. Note that Alice's Bloch vector must be contained within her

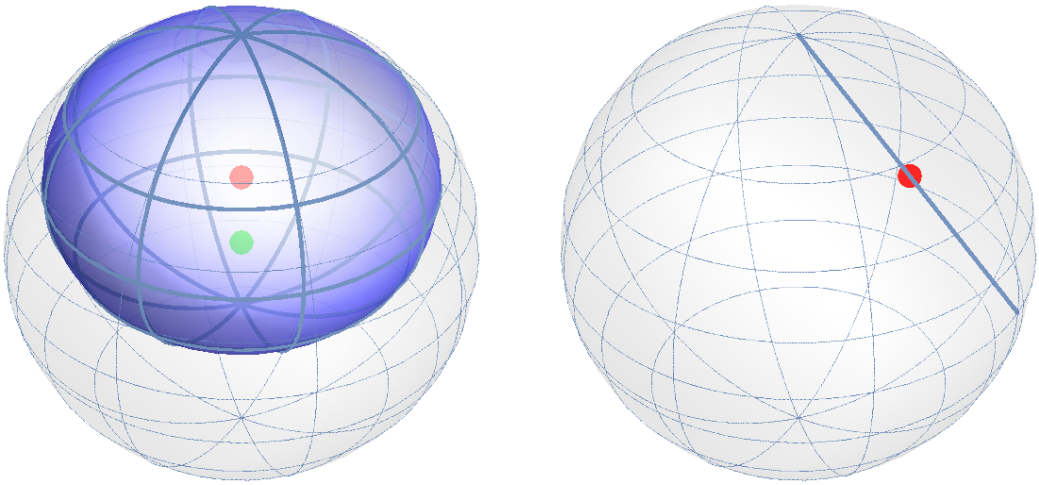

Figure 1.6: For a mixed two-qubit state, the steering ellipsoid cannot be the whole Bloch ball. We picture here an example of an entangled state (left) and a separable state (right). The entangled state has $\boldsymbol{a} = (0, 0, 1/3)$, $\boldsymbol{b} = \boldsymbol{0}$, $T = \mathrm{diag}(\sqrt{2/3}, \sqrt{2/3}, -2/3)$ and is an example of a *maximally obese* state that will be discussed in Section 4.4. The separable state shown is $\rho = (|00\rangle\langle 00| + |{+}{+}\rangle\langle {+}{+}|)/2$, where $|+\rangle = (|0\rangle + |1\rangle)/\sqrt{2}$. This has $\boldsymbol{a} = \boldsymbol{b} = (1/2, 0, 1/2)$, $T = \mathrm{diag}(1/2, 0, 1/2)$, and the steering ellipsoid is a line.

steering ellipsoid so that we always have $\boldsymbol{a} \in \mathcal{E}_A$ (Bob steers Alice to this state when he obtains the trivial measurement outcome $\mathbb{1}$).

Recall that a two-qubit state is given by 15 real parameters: 3 for each of the Bloch vectors $\boldsymbol{a}$ and $\boldsymbol{b}$, and 9 for the correlation matrix T. It is instructive to consider how the geometric data $(\boldsymbol{a}, \boldsymbol{b}, \mathcal{E})$ matches up with this parameter count. The Bloch vectors are directly given, whilst the remaining 9 parameters are encoded in the steering ellipsoid as follows: 3 parameters give the vector $\boldsymbol{c}$ describing the centre of $\mathcal{E}$, 3 parameters give the lengths of the axes of $\mathcal{E}$, and 3 parameters give the orientation of these axes (the Euler angles of $\mathcal{E}$). The lengths and orientation of the axes can be encoded using the eigenvalues and eigenvectors of a symmetric matrix $Q \in \mathbb{R}^{3\times 3}$.

Full expressions for $\boldsymbol{c}$ and Q will be found in Section 2.1.4; for now, we simply note that the geometric description of $\mathcal{E}$ can be conveniently expressed using $(\boldsymbol{c}, Q)$. Indeed, since the interesting features of two-qubit states concern the correlations encoded in $\mathcal{E}$, much of our work will focus on the geometry of $\mathcal{E}$ only, and we will often characterise a state using only $(\boldsymbol{c}, Q)$; it is taken that $\boldsymbol{a}$ and $\boldsymbol{b}$ could be represented as points inside $\mathcal{B}$ without explicitly showing them.

1.5.4 FAITHFULNESS

The faithfulness of the steering ellipsoid representation is proven in Ref. [11]. We note here a slight technicality associated with reconstructing ρ from the geometric data $(\boldsymbol{a}, \boldsymbol{b}, \mathcal{E})$. Consider, for example, the case that ρ is some maximally entangled pure state; any such state has $\boldsymbol{a} = \boldsymbol{b} = \boldsymbol{0}$ and $\mathcal{E} = \mathcal{B}$. It would therefore seem that we cannot distinguish between these states using the geometric data alone.

The ambiguity arises from the fact that a local unitary operation by Bob does not alter the set of states contained in $\mathcal{E}$, and we can provide a resolution by also specifying Bob's choice of basis. One way to do this within the steering ellipsoid formalism is to give the directions of the axes of $\mathcal{E}$ explicitly rather than showing the surface $\partial\mathcal{E}$ alone. Alternatively, one could colour in red, green and blue the points where these axes meet $\partial\mathcal{E}$ [23]. These methods indicate which measurement outcome for Bob is associated with which steered state for Alice and resolve the ambiguity of Bob's basis choice. Hence, if $\mathcal{E}$ is considered to be described by its axes rather than as the set of enclosed Bloch vectors then the geometric data $(\boldsymbol{a}, \boldsymbol{b}, \mathcal{E})$ does indeed give a faithful description of ρ.

It should be noted that, although every two-qubit state ρ can be described by the geometric data $(\boldsymbol{a}, \boldsymbol{b}, \mathcal{E})$, not every set of geometric data will necessarily describe a two-qubit state. This is intimately related to the task of finding constraints for the positivity of ρ. In fact, in Chapter 7, we will find that the steering ellipsoid formalism goes beyond representing two-qubit states alone, and that the geometric data corresponding to an operator ρ for which $\rho \ngeq 0$ describes an entanglement witness.

1.5.5 IMPORTANT PROPERTIES

Let us briefly review some of the geometric features of the steering ellipsoid formalism found in Ref. [11]. Perhaps the most remarkable result is the *nested tetrahedron condition*, which will form the basis of the work in Chapter 8.

Nested tetrahedron condition

$\mathcal{E}$ corresponds to a separable state if and only if there exists a (possibly degenerate) tetrahedron circumscribed about $\mathcal{E}$ and inscribed in $\mathcal{B}$.

In other words, a separable state is described by a steering ellipsoid that fits inside a tetra-

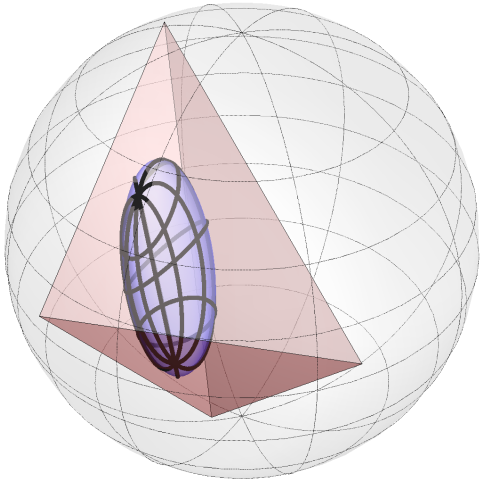

Figure 1.7: An example of the nested tetrahedron condition: the steering ellipsoid must describe a separable two-qubit state, since it fits inside a tetrahedron whose vertices lie inside the Bloch ball. (Adapted from Ref. [11].)

hedron whose vertices are inside the Bloch ball, as shown in Figure 1.7.[1] We will outline a derivation of the nested tetrahedron condition in Chapter 8. For now, we note that the convex decomposition of two-qubit separable state can be decomposed into a sum of four terms, $\rho = \sum_{i=1}^{4} p_i \phi_i \otimes \nu_i$ [24]; the states ϕ_i will have Bloch vectors corresponding to the vertices of the nested tetrahedron.

This nested tetrahedron condition provides a beautiful connection between steering ellipsoid geometry and the most important property of a two-qubit state. It is also possible to find an algebraic condition for the entanglement of a state in terms of rotational invariants of the ellipsoid parameters $(\boldsymbol{c}, Q)$. This identifies three geometric contributions to the entanglement of ρ: the distance of the steering ellipsoid centre from the origin (c), the size of the ellipsoid (given by terms such as $\det Q$ and $\mathrm{tr}\, Q$) and the *skew* $\boldsymbol{c}^{\mathsf{T}} Q \boldsymbol{c}$.

Ref. [11] also gives geometric conditions for a two-qubit state to have quantum discord, a measure which goes beyond entanglement and aims to capture the total extent of quantum correlations [25, 26]. Specifically, ρ is zero discord for Alice if and only if her steering ellipsoid is a segment of a diameter.[2]

We thus see that the steering ellipsoid picture is endowed with considerable physical significance, as important properties of a two-qubit state are manifest in the geometry of the representation. Some of the work in this thesis seeks to build on this perspective by devel-

[1] As we shall see when we investigate this condition, this tetrahedron is far from unique. In fact, owing to Poncelet's porism, the existence of such a nested tetrahedron implies the existence of an entire continuous family of such tetrahedra.

[2] Note that, unlike entanglement, discord is an asymmetric notion: there exist states which are zero discord for Alice but non-zero discord for Bob, i.e. states for which $\mathcal{E}_A$ is a segment of a diameter and $\mathcal{E}_B$ is not (although $\mathcal{E}_B$ must still be some 1-dimensional line segment).

oping further interpretations of the geometric properties of steering ellipsoids. In particular, in Chapter 5 we will see the significance of ellipsoid volume, and then in Chapter 6 we will investigate other functions that describe the size of the steering ellipsoid.

1.6 ALTERNATIVE REPRESENTATIONS OF TWO-QUBIT STATES

It should be noted that other systems for geometrically representing two-qubit states have been developed. However, to the best of our knowledge, there is no method that is comparable to the steering ellipsoid in providing a faithful, intuitive and physically relevant picture. In particular, a key feature of the steering ellipsoid representation is that it is based on the familiar Bloch vector picture for a single-qubit, and all the relevant data can be visualised on a single Bloch sphere. This is certainly not to say that alternative schemes are without value; rather, the most appropriate representation should be chosen according to the context. We give here a brief summary of these alternatives.

- For visualising pure two-qubit states various methods have been proposed. The formal mathematical extension of the Bloch sphere gives a 7-dimensional sphere [27], which clearly does not provide an accessible visual representation. Alternatively, pure states can be visualised by considering a simplex whose vertices are the computational basis states, but this cannot be easily extended to mixed states [19].
- For mixed states, Avron et al. have developed a scheme which partitions two-qubit states into SLOCC (stochastic local operations and classical communication) equivalence classes [28, 29]. This provides a geometric perspective on a number of results, in particular entanglement and Bell nonlocality. However, partitioning into equivalence classes represents a significant coarse-graining and hence the scheme is far from faithful.
- There is a well-known scheme for visualising *T states* [30], the set of two-qubit states for which the marginals are maximally mixed ($\boldsymbol{a} = \boldsymbol{b} = \boldsymbol{0}$). A T state may be represented by a 3D correlation vector. However, in addition to not being faithful, this scheme does not use the Bloch sphere and it is difficult to develop any intuition for what this correlation vector means.
- Perhaps most notable as a scheme offering similar features to the steering ellipsoid picture is the work of Gamel [31]. This scheme represents any two-qubit state using a set of vectors on two entangled Bloch spheres. This is very recent work, and it remains to be seen exactly how far the formalism can be exploited to study physical properties of two-qubit states.

1.7 EXTENSIONS TO HIGHER DIMENSIONS

Although the steering ellipsoid was originally conceived as a tool for visualising two-qubit states, it is very natural to consider whether it can be extended to higher dimensional quantum systems. Consider an n-partite quantum system, where the dimension of each local Hilbert space is given by d_i, with $i = 1, \ldots, n$. The composite Hilbert space is $\mathcal{H} = \bigotimes_i \mathbb{C}^{d_i}$ and has dimension $d = \prod_i d_i$. For a two-qubit system, we have $n = 2$ and $d_1 = d_2 = 2$, so that $d = 4$. Recall that the number of real parameters required to specify a d-dimensional quantum state is $d^2 - 1$. It should therefore be possible to use the same steering ellipsoid construction to faithfully represent the quantum state of any system for which $d \leq 4$. Furthermore, we may also be able to extend the formalism to provide a (possibly unfaithful) representation for systems with $d > 4$.

Most simply, we might use steering ellipsoids to visualise single-party states for a qutrit ($d = 3$) and a ququart ($d = 4$). The Hilbert space associated with a ququart, $\mathcal{H} = \mathbb{C}^4$, is isomorphic to that of two qubits, and one could directly map the computational basis states of a ququart onto the two qubit system (e.g. $|0\rangle \to |00\rangle, |1\rangle \to |01\rangle, |2\rangle \to |10\rangle, |3\rangle \to |11\rangle$). For a qutrit, there is 'room to spare' in the two-qubit Hilbert space, and one might map to the symmetric subspace as $|0\rangle \to |00\rangle, |1\rangle \to |11\rangle, |2\rangle \to |01\rangle + |10\rangle$. Hence, by embedding a single-party state in a two qubit system, we could in principle provide a faithful representation of qutrits and ququarts. However, the scheme appears rather contrived: we lose the physical interpretation of one party remotely steering another, and it is not immediately clear what the value of such a representation might be.

A higher dimensional single-party system can of course be represented by generalising the notion of the Bloch vector. For example, analogous to the expression for the state of a qubit $\rho = \frac{1}{2}(\mathbb{1} + \boldsymbol{r}\cdot\boldsymbol{\sigma})$, we can write the state of a qutrit as $\rho = \frac{1}{3}(\mathbb{1} + \boldsymbol{r}\cdot\boldsymbol{\lambda}) \in \mathrm{L}(\mathbb{C}^3)$, where $\boldsymbol{r} \in \mathbb{R}^8$ is the *generalised Bloch vector* and $\boldsymbol{\lambda}$ denotes the set of Gell-Mann matrices. However, whilst the Pauli matrices yield the 3D Bloch ball $\mathcal{B}$, the structure of the Gell-Mann matrices is more complex and the corresponding 8-dimensional generalised Bloch vector space does not benefit from such simple underlying symmetries. The structure of this space is in fact highly non-trivial and has been investigated in detail by a number of authors (see, e.g., [32–34]). In particular, the space of operators for which $\rho \geq 0$ is very complicated and is generally characterised by taking different cross-sections through the space. Moreover, unitary operations on the qutrit do not correspond to straightforward rotations of $\boldsymbol{r}$ [31]. The utility of the generalised Bloch vector is thus rather limited as an intuitive tool for visualising higher dimensional single-party

states.

For a bipartite state ($n = 2$) where Alice holds a qudit ($d_1 > 2$) and Bob holds a qubit ($d_2 = 2$), a generalised steering ellipsoid $\mathcal{E}_A$ can still be found in the generalised Bloch sphere. Ref. [11] discusses how results for the two-qubit steering ellipsoid partially carry over into this generalised scenario (for example, the nested tetrahedron condition will still be sufficient but no longer necessary for separability). However, owing to the difficulty of visualising the generalised Bloch vector, such qudit-qubit scenarios have not been investigated in detail.

Finally, we might consider multipartite states ($n > 2$) in which every party holds a qubit ($d_i = 2$). For such a state ρ, we can consider the set of steering ellipsoids that describe the reduced two-qubit density matrices $\rho_{ij} = \mathrm{tr}_{\backslash ij}\,\rho$, where $\mathrm{tr}_{\backslash ij}$ denotes the partial trace over all systems except qubits i and j. The simplest case, $n = 3$, will be explored in Chapter 5. We shall see that when Alice, Bob and Charlie each hold a qubit, the steering ellipsoids that describe ρ_{AB}, ρ_{BC} and ρ_{CA} obey certain monogamy properties; these relations have recently been extended to scenarios with $n > 3$ [6].

SUMMARY AND DISCUSSION OF CHAPTER 1

We have seen how the notion of steering, originally conceived by Schrödinger in 1935, can be used as the basis of a graphical representation for two-qubit states. The steering ellipsoid $\mathcal{E}$ describes the set of states to which Alice can be steered given all possible measurements by Bob; together with the local Bloch vectors, this information provides a faithful representation. All the geometric data can be depicted inside a single Bloch sphere, giving us an intuitive picture that naturally extends the Bloch vector scheme for a single-qubit state.

The steering ellipsoid can represent both pure and mixed states. $\mathcal{E}$ for a pure entangled state is the whole Bloch ball $\mathcal{B}$, whilst a mixed state is entangled if and only if $\mathcal{E}$ does not fit inside a tetrahedron inside $\mathcal{B}$. In addition to entanglement, quantum discord is also manifest through the geometric properties of $\mathcal{E}$. In this thesis we will find that further quantum correlation measures such as fully entangled fraction and CHSH nonlocality also have natural interpretations in the steering ellipsoid picture. Before investigating the formalism in detail, however, we first provide a full derivation of the steering ellipsoid.

CHAPTER 2

4D BICONES AND 3D ELLIPSOIDS

In this chapter we derive expressions for the parameters $(\boldsymbol{c}, Q)$ that give the centre and semi-axes of the steering ellipsoid $\mathcal{E}$ for a two-qubit state ρ with Bloch vectors $\boldsymbol{a}$ and $\boldsymbol{b}$ and correlation matrix T. There are two possible routes for the derivation:

(1) Perform a *canonical filter* to transform a two-qubit state ρ into a canonical state $\widetilde{\rho}$ for which $\widetilde{\boldsymbol{b}} = \boldsymbol{0}$. The steering ellipsoid is invariant under this transformation, and finding $\mathcal{E}$ for a canonical state is algebraically much more straightforward than for a general state with non-vanishing $\boldsymbol{b}$. One can then convert the canonical expressions for $(\boldsymbol{c}, Q)$ back into terms of the original non-canonical $\boldsymbol{a}, \boldsymbol{b}$ and T.

(2) Work directly with a general two-qubit state ρ and use geometric considerations. The set of *steering outcomes* for ρ is a skewed bicone in 4D Euclidean space. When projected onto the Bloch ball $\mathcal{B}$, this skewed bicone yields $\mathcal{E}$. Projective geometry then gives expressions for $(\boldsymbol{c}, Q)$ in terms of $\boldsymbol{a}, \boldsymbol{b}$ and T.

Method (1) is the 'traditional' method initially suggested in work by Verstraete [20] and Shi et al. [21, 22]. Jevtic et al. provided the clearest and most complete derivation using this approach, giving for the first time general expressions for $(\boldsymbol{c}, Q)$ [11]. Method (2) was recently developed by Nguyen and Vu [35], but the derivation given there does not proceed all the way to an explicit parametrisation of $\mathcal{E}$. Here we present a derivation using the novel geometric picture of Nguyen and Vu and extend their work to produce expressions for $(\boldsymbol{c}, Q)$.[1]

Although the steering ellipsoid can be derived without use of the canonical filter, we will find the concept of canonical states to be essential anyway. Following our derivation of the steering ellipsoid, we describe the significance of the canonical transformation and show how it can be used to derive a standard form of two-qubit state. This family of canonical states will be the basis of much of the subsequent work in this thesis.

[1] The author is very grateful to Chau Nguyen for his assistance with the derivation presented in this chapter.

2.1 DERIVATION OF THE STEERING ELLIPSOID

2.1.1 4D BICONE OF MEASUREMENT OUTCOMES

We begin by recalling the 4D notation used in Section 1.4 for single-qubit states. Any Hermitian operator $A \in \mathrm{L}(\mathbb{C}^2)$ may be written in the Pauli basis $(\mathbb{1}, \boldsymbol{\sigma})$ as

$$A = \frac{1}{2} \sum_{\mu=0}^{3} a_\mu \sigma_\mu, \tag{2.1}$$

where $a_\mu = \mathrm{tr}(A\,\sigma_\mu)$. We can then identify A with a (column) vector in 4D Euclidean space: $\boldsymbol{A} = (a_0, \boldsymbol{a}) \in \mathbb{R}^4$. Note that the zero operator O corresponds to the origin $\boldsymbol{O} = (0, \boldsymbol{0})$, whilst the identity operator $\mathbb{1}$ corresponds to $\boldsymbol{I} = (2, \boldsymbol{0})$. For convenience, we will slightly abuse notation and often treat an operator A and its four-vector representation $\boldsymbol{A}$ as equivalent objects without further remark; thus a set $\mathcal{A} := \{A\}$ may be directly described as $\mathcal{A} := \{\boldsymbol{A}\}$.

Consider now the set of positive operators $\mathcal{M}^+ := \{M \mid M \geq 0\}$. In the Euclidean picture, $M \geq 0$ if and only if the corresponding $\boldsymbol{M} = (m_0, \boldsymbol{m})$ satisfies $m_0 \geq 0$ and $m^2 \leq m_0^2$, where $m := |\boldsymbol{m}|$. Thus we have

$$\mathcal{M}^+ := \left\{\boldsymbol{M} \mid m_0 \geq 0, m^2 \leq m_0^2\right\}. \tag{2.2}$$

This is a convex cone with vertex O [19].[1] We call $\mathcal{M}^+$ the forward light cone at O.[2] Consider also the set of operators $\mathcal{M}^- := \{M \mid M \leq \mathbb{1}\}$, which corresponds to the backward light cone at $\mathbb{1}$. The set $\mathcal{M} := \mathcal{M}^+ \cap \mathcal{M}^-$ is a *bicone*.[3]

We now show that this 4D bicone has an immediate interpretation as the set of *measurement outcomes*. Recall that a general measurement in quantum mechanics is a POVM, given by a set of n measurement outcomes $\left\{M_{i|j}\right\}_{i=1}^{n}$ that satisfy $M_{i|j} \geq 0$ and $\sum_i M_{i|j} = \mathbb{1}$ [7]. Dropping the subscript $i|j$, which labels the choice of POVM j and the outcome obtained i, we can thus identify any measurement outcome M as an operator satisfying $0 \leq M \leq \mathbb{1}$, which by definition belongs to $\mathcal{M}$. Conversely, any $M \in \mathcal{M}$ can be associated with a measurement outcome for some POVM (take, for example, the POVM $\{M, \mathbb{1} - M\}$). Thus the bicone $\mathcal{M}$ is precisely the set of all single-qubit measurement outcomes.

One can similarly identify the equator of $\mathcal{M}$ as the set of single-qubit states. Note that

[1] $\mathcal{M}^+$ is a cone since $\forall M \in \mathcal{M}^+, \lambda \geq 0$ we have $\lambda M \in \mathcal{M}^+$; and it is convex since $\forall M_1, M_2 \in \mathcal{M}^+, 0 \leq \lambda \leq 1$ we have $\lambda M_1 + (1-\lambda) M_2 \in \mathcal{M}^+$.

[2] This terminology follows by analogy with special relativity after making the identification of the timelike component $m_0 \equiv ct$ and spacelike component $\boldsymbol{m} \equiv \boldsymbol{x}$ in Minkowski space. Later in Section 2.2.2, we shall see that this analogy extends further by giving a correspondence between local filtering operations and Lorentz transformations.

[3] Here we modify terminology compared to Ref. [35], which referred to $\mathcal{M}$ as a *double cone*. A double cone typically refers to two cones joined at the apex, whilst a bicone is formed by cones joined at the base.

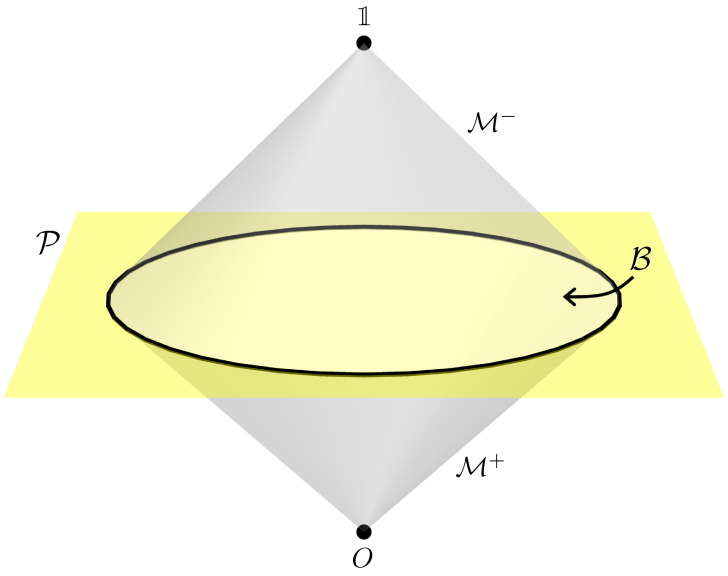

Figure 2.1: An illustration of the 4D Euclidean geometry. The timelike component runs vertically and the spacelike components are orthogonal to this. The bicone of measurement outcomes $\mathcal{M}$ is the intersection of the forward light cone at $O = (0, \mathbf{0})$ and the backward light cone at $\mathbb{1} = (2, \mathbf{0})$, i.e. $\mathcal{M} := \mathcal{M}^+ \cap \mathcal{M}^-$. The yellow hyperplane $\mathcal{P}$ is the Bloch hyperplane consisting of unit trace operators; this intersects the bicone at its equator to give the Bloch ball $\mathcal{B} = \mathcal{P} \cap \mathcal{M}$.

the trace of any operator M corresponds to its timelike component: $\operatorname{tr} M = m_0$. The 3D *Bloch hyperplane* is defined by $\mathcal{P} := \{M \mid m_0 = 1\}$. Denote by $\boldsymbol{R}$ the four-vector corresponding to a Hermitian operator ρ; this operator is a state if and only if $\rho \geq 0$ and $\operatorname{tr} \rho = 1$. A single-qubit density operator with Bloch vector $\boldsymbol{r}$ is thus given by $\boldsymbol{R} = (1, \boldsymbol{r}) \in \mathcal{M}^+$. The Bloch ball $\mathcal{B}$, which describes the set of all single-qubit states, thus corresponds to the intersection of $\mathcal{P}$ and $\mathcal{M}^+$. Owing to the symmetry of $\mathcal{M}$, this is precisely the equatorial ball of the measurement bicone: $\mathcal{B} = \mathcal{P} \cap \mathcal{M}$. The relevant geometry is illustrated in Figure 2.1.

A hyperplane parallel to $\mathcal{P}$ describes the set of Hermitian operators with some fixed trace; any operator in $\mathcal{M}^+$ thus corresponds to an unnormalised state $\hat{\rho}$ with corresponding four-vector $\hat{\boldsymbol{R}}$. A subnormalised state will have $\hat{r}_0 < 1$ and can be normalised by the operation

$$\hat{\rho} \mapsto \rho = \frac{\hat{\rho}}{\operatorname{tr} \hat{\rho}}. \tag{2.3}$$

Geometrically, this is a perspective projection onto the Bloch hyperplane with centre of projection O [36], i.e. a projection of $\hat{\boldsymbol{R}}$ from O onto $\mathcal{P}$. We write this as $\boldsymbol{R} = \mathbb{P}(\hat{\boldsymbol{R}})$ and illustrate the transformation in Figure 2.2. Recall that a pure state is an extremal point of the Bloch ball and lies on $\partial\mathcal{B}$; similarly, an unnormalised pure state will lie on $\partial\mathcal{M}^+$. The normalised maximally mixed state $\rho = \frac{1}{2}\mathbb{1}$ is at the centre of $\mathcal{B}$.

We have seen that a Hermitian operator on the single-qubit space $\mathcal{H} = \mathbb{C}^2$ corresponds to a vector in 4D Euclidean space $\mathbb{R}^4$. In figures, however, we draw geometric representations of

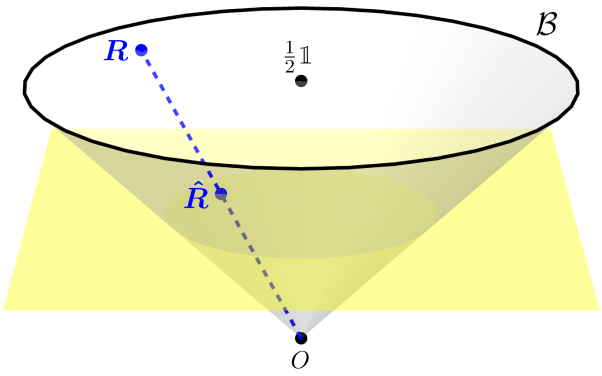

Figure 2.2: The projection of a point $\hat{\boldsymbol{R}} \in \mathcal{M}^+$ from O onto the Bloch ball $\mathcal{B}$. The yellow hyperplane describes the set of subnormalised operators with some given trace; projection of a subnormalised state onto $\mathcal{B}$ gives a normalised state with four-vector $\boldsymbol{R} = \mathbb{P}(\hat{\boldsymbol{R}})$. The maximally mixed state lies at the centre of $\mathcal{B}$.

objects in $\mathbb{R}^3$. This geometry in fact corresponds exactly to that of a *rebit*, i.e. a qubit with purely real entries, the basis of such operators being simply $(\mathbb{1}, \sigma_x, \sigma_z)$ [19]. We can thus develop an intuition for our complete 4D picture by considering the 3D space that we draw and simply 'adding' an extra spacelike component for σ_y. For example, in Figure 2.1, the Bloch hyperplane $\mathcal{P}$ is depicted as a 2D surface, and its intersection with the 3D bicone $\mathcal{M}$ gives a 2D circular 'Bloch disc' $\mathcal{B}$. Adding a dimension, we see that in the full 4D Euclidean space in which we are actually operating, the intersection $\mathcal{P} \cap \mathcal{M}$ will give a 3D ball $\mathcal{B}$.

2.1.2 4D SKEWED BICONE OF STEERING OUTCOMES

Using this 4D Euclidean picture, we now consider the steering scenario discussed in Section 1.3 and depicted in Figure 1.4. Say that Alice and Bob share a two-qubit state $\rho \in \mathrm{L}(\mathcal{H}_A \otimes \mathcal{H}_B)$, where $\mathcal{H}_A = \mathcal{H}_B = \mathbb{C}^2$. We write this as

$$\rho = \frac{1}{4} \sum_{\mu,\nu=0}^{3} \Theta_{\mu\nu}\, \sigma_\mu \otimes \sigma_\nu, \tag{2.4}$$

where $\Theta_{\mu\nu} = \mathrm{tr}(\rho\, \sigma_\mu \otimes \sigma_\nu)$ and the block matrix $\Theta = \left(\begin{smallmatrix} 1 & \boldsymbol{b}^\intercal \\ \boldsymbol{a} & T \end{smallmatrix}\right) \in \mathbb{R}^{4\times 4}$.

Alice's reduced state is given by $\rho_A = \mathrm{tr}_B\, \rho \in \mathrm{L}(\mathcal{H}_A)$, and her Bloch vector is $\boldsymbol{a} = \mathrm{tr}(\rho_A\, \boldsymbol{\sigma})$. When Bob performs some POVM and obtains outcome $M \in \mathrm{L}(\mathcal{H}_B)$, Alice's state is steered to ρ'_A. To be precise, Alice's subnormalised state will be $\hat{\rho}'_A = \mathrm{tr}_B\, [\rho\, (\mathbb{1} \otimes M)]$, where the normalisation $p_M = \mathrm{tr}\, \hat{\rho}'_A = \mathrm{tr}\, [\rho\, (\mathbb{1} \otimes M)]$ gives the probability of Bob obtaining measurement outcome M. Indeed, we define the *EPR map* when Bob steers Alice as [35]

$$\mathbb{S} : \mathrm{L}(\mathcal{H}_B) \mapsto \mathrm{L}(\mathcal{H}_A) : M \mapsto \mathrm{tr}_B\, [\rho\, (\mathbb{1} \otimes M)]\,. \tag{2.5}$$

In the four-vector picture, the EPR map can be realised as a straightforward matrix multi-

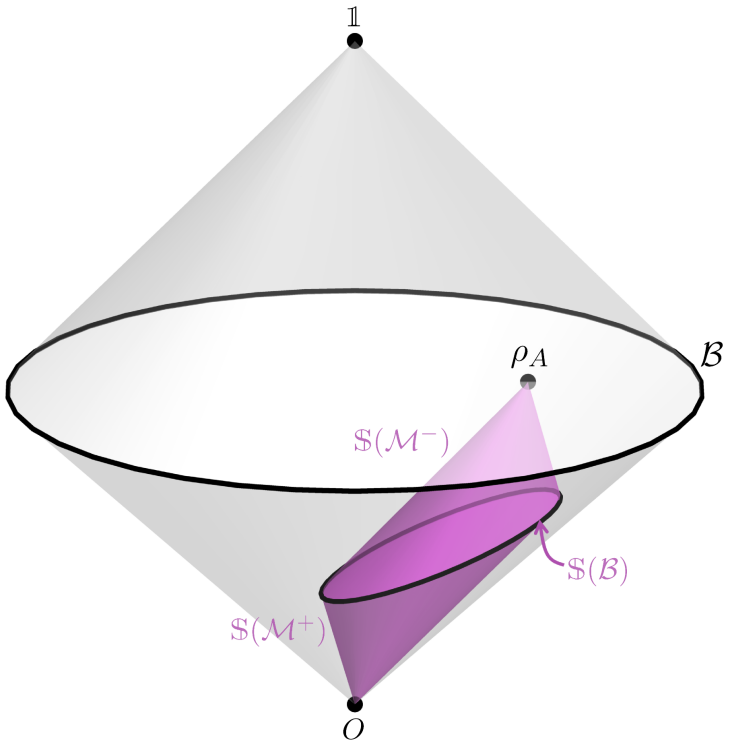

Figure 2.3: The skewed bicone of steering outcomes is the image of the EPR map $\mathbb{S}$ applied to $\mathcal{M}$. Here $\mathbb{S}(\mathcal{M})$ is shown in pink inside $\mathcal{M}$ (in fact, $\mathbb{S}(\mathcal{M})$ lies wholly within $\mathcal{M}^+$). The equator of $\mathbb{S}(\mathcal{M})$ is given by the image of the Bloch ball, $\mathbb{S}(\mathcal{B})$, and is not in general parallel to the Bloch hyperplane. The vertices of the skewed bicone are at $\mathbb{S}(O) = O$ and $\mathbb{S}(\mathbb{1}) = \rho_A \in \mathcal{B}$.

plication. As usual, we treat the four-vector representation as equivalent to the operator itself, $M \equiv \boldsymbol{M}$, and write $\mathbb{S}(\boldsymbol{M})$ to emphasise the geometric interpretation of the expression. Say that Bob obtains the measurement outcome $M = \frac{1}{2}\sum_{\nu=0}^{3} m_\nu \sigma_\nu$. Then

$$\begin{aligned}\mathbb{S}(\boldsymbol{M}) &= \frac{1}{4}\sum_{\mu,\nu=0}^{3} \Theta_{\mu\nu}\, \sigma_\mu \otimes \mathrm{tr}(M\,\sigma_\nu) \\ &= \frac{1}{2}\sum_{\mu=0}^{3}\left(\frac{1}{2}\sum_{\nu=0}^{3}\Theta_{\mu\nu} m_\nu\right)\sigma_\mu \\ &= \frac{1}{2}\Theta\boldsymbol{M}. \end{aligned} \tag{2.6}$$

Explicitly performing the matrix multiplication, we have $\mathbb{S}(\boldsymbol{M}) = \frac{1}{2}(m_0 + \boldsymbol{b}\cdot\boldsymbol{m}, m_0\boldsymbol{a} + T\boldsymbol{m})$.

We denote the image under the EPR map of a set $\mathcal{B} \subseteq \mathrm{L}(\mathcal{H}_B)$ similarly as $\mathbb{S}(\mathcal{B})$. The set of *steering outcomes* is the set of subnormalised states to which Alice can be steered given all possible measurement outcomes for Bob, and may thus be written as

$$\begin{aligned}\mathbb{S}(\mathcal{M}) &:= \{\mathbb{S}(M) \mid M \in \mathcal{M}\} \\ &= \{\mathrm{tr}_B\left[\rho\,(\mathbb{1}\otimes M)\right] \mid M \in \mathcal{M}\} \\ &= \left\{\tfrac{1}{2}\Theta\boldsymbol{M} \mid \boldsymbol{M} \in \mathcal{M}\right\}. \end{aligned} \tag{2.7}$$

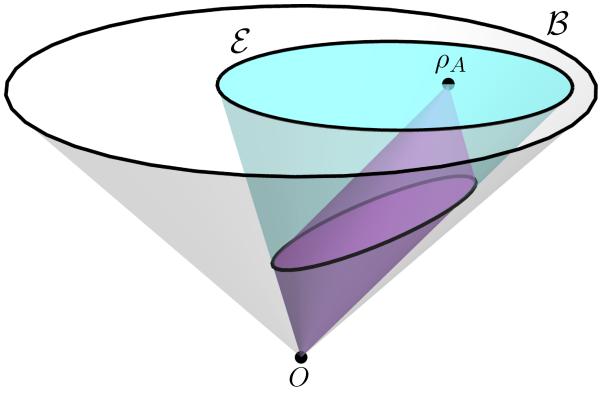

Figure 2.4: Alice's steering ellipsoid $\mathcal{E}$ is found by the projection of the steering outcomes skewed bicone onto $\mathcal{B}$, i.e. one applies the operation depicted in Figure 2.2 to every point inside $\mathbb{S}(\mathcal{M})$. The result of this projection is shown in blue. By convexity of $\mathbb{S}(\mathcal{M})$, we clearly need only project the equator of $\mathbb{S}(\mathcal{M})$, so that $\mathcal{E} = \mathbb{P}(\mathbb{S}(\mathcal{B}))$. This projection is equivalent to normalising the (necessarily positive) operators contained within $\mathbb{S}(\mathcal{M})$, yielding the set of normalised states $\mathcal{E} \subseteq \mathcal{B}$.

The EPR map is a linear transformation, so that the set of steering outcomes also forms a bicone. However, this bicone may now be *skewed*, i.e. the equator of $\mathbb{S}(\mathcal{M})$, which corresponds to the image of the Bloch ball $\mathbb{S}(\mathcal{B})$, is not in general parallel to $\mathcal{B}$. The two vertices of the bicone $\mathcal{M}$ transform as $\mathbb{S}(O) = O$ and $\mathbb{S}(\mathbb{1}) = \rho_A$. Hence the steering outcomes bicone $\mathbb{S}(\mathcal{M})$ has vertices at O and $\rho_A \in \mathcal{B}$, as shown in Figure 2.3.

2.1.3 3D STEERING ELLIPSOID

We now proceed to find Alice's steering ellipsoid $\mathcal{E} \subseteq \mathcal{B}$. We will show how $\mathcal{E}$ can be obtained by projecting the skewed bicone of steering outcomes onto the Bloch hyperplane, and then we will find explicit expressions for the parameters $(\boldsymbol{c}, Q)$ describing the centre and semiaxes of $\mathcal{E}$.

Recall that $\mathcal{E}$ is the set of Bloch vectors to which Alice can be steered given all possible local measurement outcomes for Bob. The set of steering outcomes gives precisely these states but unnormalised. We normalise a single-qubit state by performing the transformation given in (2.3), which geometrically corresponds to the perspective projection map $\mathbb{P}$. We thus have $\mathcal{E} = \mathbb{P}(\mathbb{S}(\mathcal{M}))$. By the convexity of $\mathbb{S}(\mathcal{M})$, we in fact need project only the image of $\mathcal{M}^+$, or indeed only the image of the Bloch ball (see Figure 2.4): $\mathcal{E} = \mathbb{P}(\mathbb{S}(\mathcal{B}))$.

Recall that $\boldsymbol{M} \in \mathcal{B}$ if and only if $m_0 = 1$ and $m \leq 1$; then $\mathbb{S}(\boldsymbol{M}) = \frac{1}{2}(1 + \boldsymbol{b}\cdot\boldsymbol{m}, \boldsymbol{a} + T\boldsymbol{m})$ gives Alice's subnormalised state $\hat{\rho}'_A$. Normalising this gives Alice's steered state as $\rho'_A = \mathbb{P}(\mathbb{S}(\boldsymbol{M})) = (1, \boldsymbol{a}')$, where

$$\boldsymbol{a}' = \frac{\boldsymbol{a} + T\boldsymbol{m}}{1 + \boldsymbol{b}\cdot\boldsymbol{m}} \tag{2.8}$$

is Alice's steered Bloch vector. We thus have:

The steering ellipsoid as a projection from 4D

Alice's steering ellipsoid is given by the projection of Bob's steering outcomes onto the Bloch hyperplane: $\mathcal{E} = \mathbb{P}(\mathbb{S}(\mathcal{M}))$. In terms of Bloch vectors, this gives

$$\mathcal{E} = \left\{ \boldsymbol{a}' = \frac{\boldsymbol{a} + T\boldsymbol{m}}{1 + \boldsymbol{b}\cdot\boldsymbol{m}} \;\middle|\; m \leq 1 \right\}.$$

This clearly corresponds to the definition of $\mathcal{E}$ given in Section 1.5.1, where we have now explicitly evaluated the expression for $\boldsymbol{a}'$.

That $\mathcal{E}$ is indeed an ellipsoid is not immediately obvious from this expression (except when $\boldsymbol{b} = \boldsymbol{0}$). However, we can gain some further understanding by considering the 3D geometry of the rebit scenario drawn in the figures. $\mathbb{S}(\mathcal{M}^+)$ is then a 3D cone whose base is not in general parallel to the Bloch disc $\mathcal{B}$. The intersection $\mathbb{S}(\mathcal{M}^+) \cap \mathcal{B}$ will therefore produce an elliptic conic section. In our 4D geometry, $\mathcal{E}$ will be the corresponding conic section but with an extra dimension, i.e. an ellipsoid. More formally, the equator of the steering outcomes bicone is $\mathbb{S}(\mathcal{B})$; this is the image of a linear map on $\mathcal{B}$ and so must be an ellipsoid. By projective geometry, $\mathcal{E} = \mathbb{P}(\mathbb{S}(\mathcal{B}))$ must then also be an ellipsoid.

The dimension of the steering ellipsoid, $\dim \mathcal{E}$, may easily be found using this 4D picture. From (2.7), we know that $\dim\, \mathbb{S}(\mathcal{M}) = \operatorname{rank} \Theta$. Since $\dim\, \mathbb{P}(\mathbb{S}(\mathcal{M})) = \dim\, \mathbb{S}(\mathcal{M}) - 1$, we have

$$\dim \mathcal{E} = \operatorname{rank} \Theta - 1. \tag{2.9}$$

This result has already been established algebraically in Ref. [11]; here we see that it follows immediately from a consideration of projective geometry.

We also note that for a non-degenerate steering ellipsoid, the surface $\partial\mathcal{E}$ corresponds to points for which $m = 1$, i.e. projective measurements, whilst the interior corresponds to points for which $m < 1$. When the steering ellipsoid has $\dim \mathcal{E} < 3$, the boundary $\partial\mathcal{E}$ again corresponds to points for which $m = 1$, but now the interior corresponds to points for which $m \leq 1$. In other words, the states on the boundary of Alice's steering ellipsoid can be obtained only when Bob performs a projective measurement; and only when this steering ellipsoid is degenerate can a projective measurement by Bob steer Alice to a point on the interior of $\mathcal{E}$.

2.1.4 PARAMETRISATION OF THE STEERING ELLIPSOID

Following the convention set in Ref. [11], we write the equation describing $\mathcal{E}$ (or, more precisely, $\partial\mathcal{E}$) as

$$(\boldsymbol{r} - \boldsymbol{c})^{\mathsf{T}} Q^{-1} (\boldsymbol{r} - \boldsymbol{c}) = 1. \tag{2.10}$$

Here $\boldsymbol{c}$ gives the centre of the steering ellipsoid and Q is a real symmetric matrix whose eigenvectors and eigenvalues give the orientation and squared lengths of the ellipsoid semiaxes. We aim to use our projective method to find the same expressions for $\boldsymbol{c}$ and Q that were originally given in Ref. [11], namely

$$\begin{aligned} \boldsymbol{c} &= \gamma^2(\boldsymbol{a} - T\boldsymbol{b}), \\ Q &= \gamma^2(T - \boldsymbol{a}\boldsymbol{b}^\intercal)(\mathbb{1} + \gamma^2\boldsymbol{b}\boldsymbol{b}^\intercal)(T^\intercal - \boldsymbol{b}\boldsymbol{a}^\intercal), \end{aligned} \tag{2.11}$$

where the Lorentz factor $\gamma = 1/\sqrt{1-b^2}$ and $\mathbb{1}$ is the 3×3 identity matrix. Before making the connection between the object $\mathcal{E} = \mathbb{P}(\mathbb{S}(\mathcal{M}))$ and its parametrisation $(\boldsymbol{c}, Q)$ we first establish a useful result on the matrix representation of a 3D conic section (i.e. paraboloids, hyperboloids and ellipsoids).

In homogeneous coordinates, we may write such a conic section as

$$\begin{pmatrix} 1 & \boldsymbol{r}^\intercal \end{pmatrix} \begin{pmatrix} z & \boldsymbol{u}^\intercal \\ \boldsymbol{u} & W \end{pmatrix} \begin{pmatrix} 1 \\ \boldsymbol{r} \end{pmatrix} = 0, \tag{2.12}$$

where W is the matrix of the associated quadratic form [37]. An ellipsoid corresponds to $\det W > 0$. For brevity we write $X := \left(\begin{smallmatrix} z & \boldsymbol{u}^\intercal \\ \boldsymbol{u} & W \end{smallmatrix}\right)$.

Lemma 2.1: Conversion from homogeneous coordinates to ellipsoid parameters
Given an ellipsoid (2.12), the parameters $(\boldsymbol{c}, Q)$ are encoded in X^{-1} as

$$X^{-1} = k \begin{pmatrix} 1 & \boldsymbol{c}^\intercal \\ \boldsymbol{c} & \boldsymbol{c}\boldsymbol{c}^\intercal - Q \end{pmatrix},$$

where $k := \det W / \det X$.

Proof. Define the quadratic function $x(\boldsymbol{r}) := (1, \boldsymbol{r})^\intercal X (1, \boldsymbol{r})$ so that (2.12) gives the 3D surface $x(\boldsymbol{r}) = 0$. The centre of an ellipsoid described by this quadratic form is given by the turning point of $x(\boldsymbol{r})$ [37]. Since $x(\boldsymbol{r}) = z + \boldsymbol{u}^\intercal\boldsymbol{r} + \boldsymbol{r}^\intercal\boldsymbol{u} + \boldsymbol{r}^\intercal W \boldsymbol{r}$ we have $\frac{\partial x}{\partial \boldsymbol{r}} = 2\boldsymbol{u} + 2W\boldsymbol{r}$ and hence the centre is $\boldsymbol{c} = -W^{-1}\boldsymbol{u}$.

Note that $x(\boldsymbol{r}) = (\boldsymbol{r} - \boldsymbol{c})^\intercal W (\boldsymbol{r} - \boldsymbol{c}) + z - \boldsymbol{c}^\intercal W \boldsymbol{c}$, and hence $x(\boldsymbol{r}) = 0$ becomes

$$(\boldsymbol{r} - \boldsymbol{c})^\intercal W (\boldsymbol{r} - \boldsymbol{c}) = \boldsymbol{c}^\intercal W \boldsymbol{c} - z.$$

Comparing this to (2.10) we see that $Q^{-1} = W/(\boldsymbol{c}^\intercal W \boldsymbol{c} - z)$. The denominator can be tided up by finding the determinant of the block matrix X:

$$\det X = z \det(W - z^{-1}\boldsymbol{u}\boldsymbol{u}^\intercal)$$

$$= z(1 - z^{-1}\boldsymbol{u}^\intercal W^{-1}\boldsymbol{u}) \det W$$
$$= (z - \boldsymbol{c}^\intercal W \boldsymbol{c}) \det W,$$

where we have used the matrix determinant lemma [38] and the observation that $\boldsymbol{u}^\intercal W^{-1}\boldsymbol{u} = \boldsymbol{c}^\intercal W \boldsymbol{c}$. Hence we find that $Q^{-1} = -kW$, where $k := \det W / \det X$.

Now that we have found $(\boldsymbol{c}, Q)$ in terms of the components of X, we shall demonstrate that precisely these expressions can conveniently be found in X^{-1}. Inverting the block matrix gives

$$X^{-1} = k \begin{pmatrix} 1 & -\boldsymbol{u}^\intercal W^{-1} \\ -W^{-1}\boldsymbol{u} & k^{-1}(W - z^{-1}\boldsymbol{u}\boldsymbol{u}^\intercal)^{-1} \end{pmatrix}.$$

The first column and row can immediately be identified with $\boldsymbol{c}$ and $\boldsymbol{c}^\intercal$ respectively. The matrix inverse in the 3×3 block may be evaluated using the Sherman-Morrison formula [38] to give

$$\begin{aligned}(W - z^{-1}\boldsymbol{u}\boldsymbol{u}^\intercal)^{-1} &= W^{-1} + \frac{W^{-1}\boldsymbol{u}\boldsymbol{u}^\intercal W^{-1}}{z - \boldsymbol{u}^\intercal W^{-1}\boldsymbol{u}} \\ &= W^{-1} + kW^{-1}\boldsymbol{u}\boldsymbol{u}^\intercal W^{-1} \\ &= k(-Q + \boldsymbol{c}\boldsymbol{c}^\intercal),\end{aligned}$$

giving the form of X^{-1} required. ■

We will now find the equation for $\mathcal{E}$ in the form (2.12) so that we can use this lemma to find $(\boldsymbol{c}, Q)$. Recall that $\mathcal{E}$ can be found by the projection of $\mathbb{S}(\mathcal{M})$ onto the Bloch hyperplane $\mathcal{P}$; equivalently, owing to the convexity of $\mathbb{S}(\mathcal{M})$, we may find the intersection $\mathcal{P} \cap \mathbb{S}(\mathcal{M}^+)$.

The cone of positive operators $\mathcal{M}^+$ (or, more precisely, the boundary $\partial\mathcal{M}^+$) is described by

$$\begin{pmatrix} r_0 & \boldsymbol{r}^\intercal \end{pmatrix} \begin{pmatrix} 1 & \boldsymbol{0}^\intercal \\ \boldsymbol{0} & -\mathbb{1} \end{pmatrix} \begin{pmatrix} r_0 \\ \boldsymbol{r} \end{pmatrix} = 0. \tag{2.13}$$

Recall that the EPR map acts on an operator $\boldsymbol{R} = (r_0, \boldsymbol{r})$ as $\mathbb{S}(\boldsymbol{R}) = \frac{1}{2}\Theta\boldsymbol{R}$. Hence the equation of the steered positive cone $\mathbb{S}(\mathcal{M}^+)$ is

$$\begin{pmatrix} r_0 & \boldsymbol{r}^\intercal \end{pmatrix} (\Theta^{-1})^\intercal \begin{pmatrix} 1 & \boldsymbol{0}^\intercal \\ \boldsymbol{0} & -\mathbb{1} \end{pmatrix} \Theta^{-1} \begin{pmatrix} r_0 \\ \boldsymbol{r} \end{pmatrix} = 0. \tag{2.14}$$

At the Bloch hyperplane, we have $r_0 = 1$ and hence the equation of $\mathcal{E}$ is $(1, \boldsymbol{r})^\intercal X (1, \boldsymbol{r}) = 0$, where $X := (\Theta^{-1})^\intercal \left(\begin{smallmatrix} 1 & \boldsymbol{0}^\intercal \\ \boldsymbol{0} & -\mathbb{1} \end{smallmatrix}\right) \Theta^{-1}$. Comparing to (2.12), we see that we can employ Lemma 2.1 without explicitly evaluating X but instead, more straightforwardly, finding X^{-1}. Indeed, we

find that

$$\begin{aligned} X^{-1} &= \Theta \begin{pmatrix} 1 & \mathbf{0}^\intercal \\ \mathbf{0} & -\mathbb{1} \end{pmatrix} \Theta^\intercal \\ &= \begin{pmatrix} 1 & \boldsymbol{b}^\intercal \\ \boldsymbol{a} & T \end{pmatrix} \begin{pmatrix} 1 & \mathbf{0}^\intercal \\ \mathbf{0} & -\mathbb{1} \end{pmatrix} \begin{pmatrix} 1 & \boldsymbol{a}^\intercal \\ \boldsymbol{b} & T^\intercal \end{pmatrix} \\ &= \begin{pmatrix} 1 - b^2 & \boldsymbol{a}^\intercal - \boldsymbol{b}^\intercal T^\intercal \\ \boldsymbol{a} - T\boldsymbol{b} & \boldsymbol{a}\boldsymbol{a}^\intercal - TT^\intercal \end{pmatrix}. \end{aligned} \tag{2.15}$$

Lemma 2.1 then gives $k = 1 - b^2 =: \gamma^{-2}$. Identifying the other components of X^{-1}, we find that $k\boldsymbol{c} = \boldsymbol{a} - T\boldsymbol{b}$ and $k(\boldsymbol{c}\boldsymbol{c}^\intercal - Q) = \boldsymbol{a}\boldsymbol{a}^\intercal - TT^\intercal$, so that

$$\begin{aligned} \boldsymbol{c} &= \gamma^2(\boldsymbol{a} - T\boldsymbol{b}), \\ Q &= \gamma^2(TT^\intercal - \boldsymbol{a}\boldsymbol{a}^\intercal) + \boldsymbol{c}\boldsymbol{c}^\intercal. \end{aligned} \tag{2.16}$$

Finally, using the identity $\gamma^2 \equiv 1 + \gamma^2 b^2$, the expression for Q can be rearranged to reproduce precisely the form presented in Ref. [11].

Parametrisation of the steering ellipsoid

Alice's steering ellipsoid $\mathcal{E}$ is parametrised by $(\boldsymbol{c}, Q)$, where

$$\begin{aligned} \boldsymbol{c} &= \gamma^2(\boldsymbol{a} - T\boldsymbol{b}), \\ Q &= \gamma^2(T - \boldsymbol{a}\boldsymbol{b}^\intercal)(\mathbb{1} + \gamma^2 \boldsymbol{b}\boldsymbol{b}^\intercal)(T^\intercal - \boldsymbol{b}\boldsymbol{a}^\intercal). \end{aligned}$$

The vector $\boldsymbol{c}$ gives the centre of $\mathcal{E}$; the eigenvectors and eigenvalues of the symmetric matrix Q give the orientation and squared lengths of the semiaxes.

As noted in Section 1.5.3, we focus on Alice's steering ellipsoid, but it would of course be equally valid to study the same scenario with the roles of Alice and Bob swapped. This amounts to the transformation $\Theta \mapsto \Theta^\intercal$, and so Bob's steering ellipsoid will be described by the above expressions but with $\boldsymbol{a} \leftrightarrow \boldsymbol{b}$ and $T \leftrightarrow T^\intercal$.

2.2 THE CANONICAL STEERING ELLIPSOID

In the above derivation, we have seen how to find the steering ellipsoid for any two-qubit state. However, much of the work in this thesis will use a particular sort of *canonical* two-qubit state for which Bob's marginal is maximally mixed. The significance of such states is that the steering ellipsoid is invariant under the canonical transformation, and so often, without loss of generality, we need study only the set of canonical two-qubit states. We now derive the form

of these canonical states by examining the effect of a SLOCC (stochastic local operations and classical communication) transformation in the four-vector picture.

2.2.1 LOCAL FILTERING OPERATIONS

When Alice and Bob perform a SLOCC operation (also known as a *local filter*), their two-qubit state ρ transforms according to the invertible map

$$\rho \mapsto \widetilde{\rho} = \frac{(S_A \otimes S_B)\,\rho\,(S_A \otimes S_B)^\dagger}{\mathrm{tr}\left[(S_A \otimes S_B)\,\rho\,(S_A \otimes S_B)^\dagger\right]}, \tag{2.17}$$

where $S_A, S_B \in \mathrm{GL}(2,\mathbb{C})$ [11].[1] Verstraete et al. showed that the effect of such a transformation on the Pauli basis representation Θ may be described by a Lorentz transformation [40]. Precisely, the above transformation corresponds, up to normalisation, to

$$\Theta \mapsto \widetilde{\Theta} = \Lambda_A \Theta \Lambda_B^\intercal, \tag{2.18}$$

where Λ_i are proper, orthochronous Lorentz transformations (i.e. $\det \Lambda_i = 1$ and $\Lambda_i^{00} \geq 1$) given by $\Lambda_i = \Upsilon(S_i \otimes S_i^*)\Upsilon^\dagger/|\det S_i|$ and

$$\Upsilon = \frac{1}{\sqrt{2}} \begin{pmatrix} 1 & 0 & 0 & 1 \\ 0 & 1 & 1 & 0 \\ 0 & i & -i & 0 \\ 1 & 0 & 0 & -1 \end{pmatrix}. \tag{2.19}$$

Consider in particular the case that only Bob performs a local filter, so that $\widetilde{\Theta} = \Theta\Lambda_B^\intercal$. The cone of positive operators is given by $\mathcal{M}^+ := \{M \mid M \geq 0\}$ and, following (2.7), its image under the EPR map is $\mathbb{S}(\mathcal{M}^+) = \left\{\frac{1}{2}\Theta \boldsymbol{M} \mid \boldsymbol{M} \in \mathcal{M}^+\right\}$. It is almost immediate to see that $\mathbb{S}(\mathcal{M}^+)$ is invariant under $\Theta \mapsto \widetilde{\Theta} = \Theta\Lambda_B^\intercal$. Since Λ_B, and hence $\Lambda_B^\intercal$, is orthochronous, it preserves the forward light cone: $\boldsymbol{M} \in \mathcal{M}^+$ if and only if $\Lambda_B^\intercal \boldsymbol{M} \in \mathcal{M}^+$. It follows that $\mathbb{S}(\mathcal{M}^+)$ and therefore Alice's steering ellipsoid $\mathcal{E}$ – which is given by the projection of $\mathbb{S}(\mathcal{M}^+)$ onto the Bloch hyperplane – is invariant under Bob's local filtering operation.[2]

2.2.2 CANONICAL TRANSFORMATION

Although $\mathcal{E}$ is invariant under any local filtering operation performed by Bob, a particular transformation will prove to be especially useful. This corresponds to $\rho \mapsto \widetilde{\rho}$ with $S_A = \mathbb{1}$ and

[1] Physically, SLOCC describes the set of operations that allow for a probabilistic, reversible transformation under LOCC [39] Note that projective measurements, which belong to LOCC but are irreversible, are excluded.

[2] It should be stressed, however, that $\mathbb{S}(\mathcal{M}^-)$, and hence Alice's skewed bicone of steering outcomes $\mathbb{S}(\mathcal{M})$, is *not* invariant under Bob's local filtering operation. It should also be noted that although Bob's local filtering operation alters his steering ellipsoid, it leaves EPR-steerability of Bob by Alice invariant [41, 42].

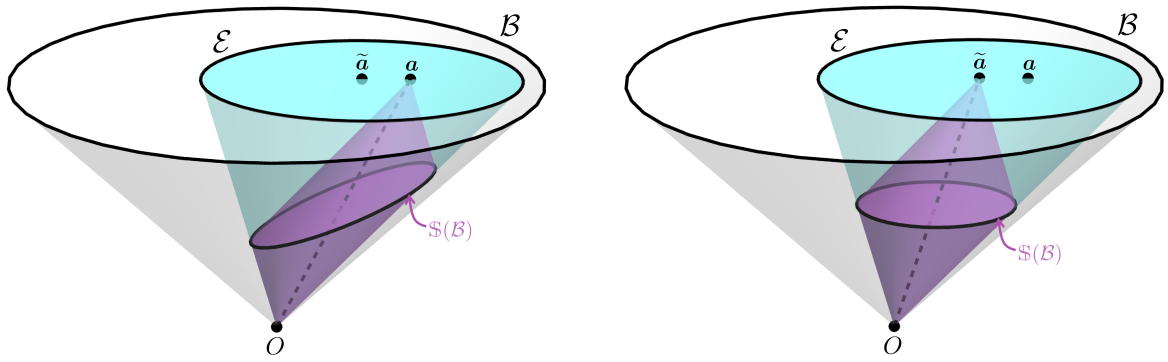

Figure 2.5: The steering outcomes for a two-qubit state before (left) and after (right) the canonical transformation. Note that $\mathbb{S}(\mathcal{M}^-)$ and hence $\mathbb{S}(\mathcal{M})$ is not invariant under the transformation. Crucially, however, $\mathbb{S}(\mathcal{M}^+)$ is, and so the steering ellipsoid $\mathcal{E} = \mathbb{P}(\mathbb{S}(\mathcal{M}^+))$ is also invariant. The canonical transformation aligns the equator $\mathbb{S}(\mathcal{B})$ parallel to the Bloch ball $\mathcal{B}$. It also transforms Alice's Bloch vector as $\boldsymbol{a} \mapsto \tilde{\boldsymbol{a}} = \boldsymbol{c}$, so that the vertex of $\mathbb{S}(\mathcal{M}^-)$ moves to the centre of $\mathcal{E}$.

$S_B = 1/\sqrt{\rho_B}$. We term this the *canonical transformation*, and it yields a *canonical state* $\widetilde{\rho}$:

$$\rho \mapsto \widetilde{\rho} = \left(\mathbb{1} \otimes \frac{1}{\sqrt{2\rho_B}}\right) \rho \left(\mathbb{1} \otimes \frac{1}{\sqrt{2\rho_B}}\right). \tag{2.20}$$

The normalisation factor of $\frac{1}{2}$ can be determined by noting that $\operatorname{tr}\left[\rho\left(\mathbb{1} \otimes \rho_B^{-1}\right)\right] = 2$. This transformation can be performed for any non-singular ρ_B. When ρ_B^{-1} does not exist then ρ_B must be a pure state, and hence ρ is a product state; then no steering is possible and $\mathcal{E}$ is simply a point. Such cases will usually not be of interest to us. We will therefore generally assume $b \neq 1$ and apply the canonical transformation without further discussion of the matter, instead noting any exceptions when product states do in fact need to be considered separately.

As the calculation in Ref. [11] shows, the canonical transformation $\Theta \mapsto \widetilde{\Theta} = \Theta\Lambda_B^{\intercal}$ corresponds to performing a Lorentz boost with 'velocity' $\boldsymbol{b}$. On transforming to the canonical 'rest frame', Bob's Bloch vector vanishes: $\boldsymbol{b} \mapsto \widetilde{\boldsymbol{b}} = \boldsymbol{0}$. In addition to the simplification of Bob's marginal becoming maximally mixed, the canonical state has a particular significance in the steering ellipsoid formalism. In the canonical frame, Alice's Bloch vector is the centre of $\mathcal{E}$: $\boldsymbol{a} \mapsto \widetilde{\boldsymbol{a}} = \boldsymbol{c}$. Hence, in the form of (1.5), we have

$$\widetilde{\rho} = \frac{1}{4}(\mathbb{1} \otimes \mathbb{1} + \boldsymbol{c} \cdot \boldsymbol{\sigma} \otimes \mathbb{1} + \sum_{i,j=1}^{3} \widetilde{T}_{ij}\, \sigma_i \otimes \sigma_j). \tag{2.21}$$

Furthermore, the steering ellipsoid matrix for a two-qubit state ρ may be expressed in terms of its canonical correlation matrix as $Q = \widetilde{T}\widetilde{T}^{\intercal}$ [11]. Indeed, as previously noted, a traditional derivation of the steering ellipsoid formalism is intimately connected with the canonical transformation: one notes that $\mathcal{E}$ is invariant under the transformation and may find the parameters $(\boldsymbol{c}, Q)$ in terms of $\widetilde{\boldsymbol{a}}$, $\widetilde{\boldsymbol{b}}$ and $\widetilde{T}$; converting these expressions back to the non-canonical variables gives the expressions for $(\boldsymbol{c}, Q)$ that we derived above using projective geometry.

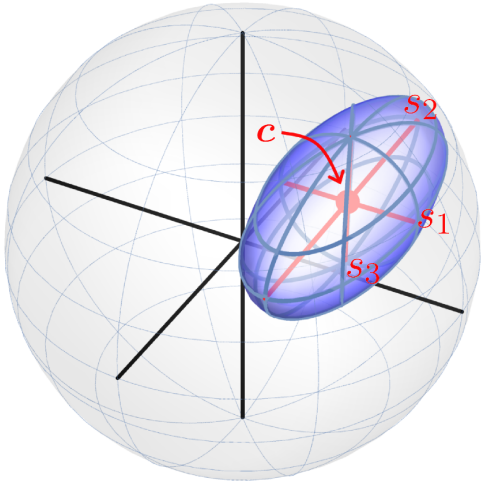

Figure 2.6: An example of a canonical, aligned $\mathcal{E}$. The centre $\boldsymbol{c}$ and the semiaxes s_1, s_2, s_3 are marked in red. Note that the semiaxes are aligned with the coordinate axes shown in black.

The significance of the canonical transformation is perhaps best seen in this geometric picture, as shown in Figure 2.5. Recall from Section 2.1.2 that the equator of the steering outcomes bicone $\mathbb{S}(\mathcal{M})$ corresponds to the image of the Bloch ball, $\mathbb{S}(\mathcal{B})$, and that the steering ellipsoid $\mathcal{E}$ is given by the projection of this back onto the Bloch ball. When we have a canonical state, Bob's Bloch vector vanishes and then, following (2.6), $\mathbb{S}(\mathcal{B})$ will be composed of four-vectors of the form $\frac{1}{2}(1, \boldsymbol{a} + T\boldsymbol{m})$ with $m \leq 1$. Crucially, the timelike component of these operators (i.e. the trace) is constant, and so $\mathbb{S}(\mathcal{M})$ is not skewed, i.e. $\mathbb{S}(\mathcal{B})$ is parallel to the Bloch hyperplane. Hence projecting $\mathbb{S}(\mathcal{B})$ back onto $\mathcal{B}$ to find $\mathcal{E}$ is greatly simplified in this canonical frame.

2.2.3 THE CANONICAL, ALIGNED STATE

Since a steering ellipsoid is invariant under the canonical transformation, the set of all possible $\mathcal{E}$ may be studied simply by examining canonical states $\widetilde{\rho}$ of the form (2.21). We perform one further manipulation to transform such a state into an *aligned* form.

Applying state-dependent local unitary operations to $\widetilde{\rho}$ (a special case of local filtering), we can achieve the transformations $\widetilde{\boldsymbol{a}} \mapsto O_A\widetilde{\boldsymbol{a}}$, $\widetilde{\boldsymbol{b}} \mapsto O_B\widetilde{\boldsymbol{b}}$ and $\widetilde{T} \mapsto O_A\widetilde{T}O_B^\intercal$ with $O_A, O_B \in \mathrm{SO}(3)$ [30]. We can always find O_A and O_B that perform a signed singular value decomposition on $\widetilde{T}$, i.e. ones that realise $O_A\widetilde{T}O_B^\intercal = \mathrm{diag}(\boldsymbol{t})$ with $\boldsymbol{t} \in \mathbb{R}^3$.[1] Bob's rotation O_B has no effect on Alice's steering ellipsoid $\mathcal{E}$, but O_A rotates $\mathcal{E}$ about the origin (treating $\boldsymbol{c}$ as a rigid rod) to align the semiaxes of $\mathcal{E}$ parallel to the coordinate axes. Note that there is some freedom in performing this rotation: the elements of $\boldsymbol{t}$ can be permuted and two signs can be flipped, but

[1] This is a slight variant on the usual singular value decomposition, which uses $O_A, O_B \in \mathrm{O}(3)$. By restricting the transformation to proper rotations, the elements of $\boldsymbol{t}$ can be positive or negative.

the product $t_1 t_2 t_3$ is fixed.

Since important physical properties such as entanglement are invariant under local unitary transformation, we can often restrict our analysis to states which have a diagonal correlation matrix. Such a canonical, aligned state has $\widetilde{T} = \mathrm{diag}(t_1, t_2, t_3)$ and hence steering ellipsoid matrix $Q = \mathrm{diag}(t_1^2, t_2^2, t_3^2)$. The semiaxes of $\mathcal{E}$ are of length $s_i = |t_i|$. We thus arrive at our standard form of a canonical, aligned state, illustrated in Figure 2.6.

Steering ellipsoid for a canonical, aligned state

Any two-qubit state ρ may be transformed by local filtering operations into the form

$$\widetilde{\rho} = \frac{1}{4}(\mathbb{1} \otimes \mathbb{1} + \boldsymbol{c} \cdot \boldsymbol{\sigma} \otimes \mathbb{1} + \sum_{i=1}^{3} t_i \, \sigma_i \otimes \sigma_i).$$

For such a state, Alice's steering ellipsoid $\mathcal{E}$ is the same as that of ρ up to a rigid rotation. The centre of $\mathcal{E}$ is $\boldsymbol{c}$, and the correlation matrix is $Q = \mathrm{diag}(t_1^2, t_2^2, t_3^2)$. $\mathcal{E}$ has semiaxes of length $s_i = |t_i|$.

This form of two-qubit state will be used throughout the thesis. Note that we now have only 6 parameters as opposed to the original 15 for describing a generic two-qubit state. These 6 parameters describe precisely the steering ellipsoid $\mathcal{E}$ by giving its centre and semiaxes. The other 3 parameters that give the Euler angles for a general ellipsoid are no longer required, since $\mathcal{E}$ is aligned with the coordinate axes. As noted in Section 1.5.3, most of the interesting behaviour of a two-qubit state is associated with its steering ellipsoid rather than the local Bloch vectors. Transforming to a canonical, aligned state distils out precisely this information.

The canonical transformation does not alter $\mathcal{E}$, whilst the alignment corresponds to a rigid rotation, which can alternatively be understood as a rotation of the Pauli basis. We can thus effectively study the set of all $\mathcal{E}$ by focusing purely on canonical, aligned $\mathcal{E}$. Of course, before making any statements about a general two-qubit state ρ based on its canonical, aligned state $\widetilde{\rho}$, one must ensure that the property of interest is also invariant under local filtering operations. We have already mentioned that entanglement is invariant under the alignment transformation (which corresponds to local unitaries). In fact, we shall see that several other important properties are invariant, or can at least be straightforwardly converted, under the whole transformation. It is this invariance of $\mathcal{E}$ together with the invariance of physical properties that makes the much simpler set of canonical, aligned states so powerful for studying two-qubit states in general.

SUMMARY AND DISCUSSION OF CHAPTER 2

We have shown how projective geometry can be used to find the steering ellipsoid for a two-qubit state. The procedure may be summarised as follows:

(1) Define the 4D bicone of measurement outcomes $\mathcal{M}$.
(2) Find the 4D skewed bicone of steering outcomes $\mathbb{S}(\mathcal{M})$.
(3) Project this onto the Bloch ball to find the 3D steering ellipsoid $\mathcal{E} = \mathbb{P}(\mathbb{S}(\mathcal{M}))$.
(4) Find explicit expressions for the parameters $(\boldsymbol{c}, Q)$ that describe the geometry of $\mathcal{E}$.

A full consideration of the 4D geometry is essential to a study of EPR-steerability [35, 43]. For our purposes, however, we refer to the 4D picture only for the purpose of presenting this derivation. In the work that follows, we shall focus purely on the properties of the 3D steering ellipsoid $\mathcal{E}$. It is worth bearing in mind that the underlying geometry is in fact 4D, but a complete understanding of this is certainly not essential to understand what follows.

On the other hand, the canonical transformation will be essential to what follows. We have seen that the study of steering ellipsoids can be boiled down to a consideration of a standard family of canonical, aligned states. Up to an arbitrary rotation of basis, these states describe every possible steering ellipsoid. We will therefore study any given $\mathcal{E}$ by examining the canonical state $\widetilde{\rho}$ that describes it and, if desired, transform expressions back to a general two-qubit state ρ.

CHAPTER 3

PHYSICAL AND ENTANGLED STATES

We are now ready to develop further the characterisation of the steering ellipsoid given by Jevtic et al. [11]. We begin by answering the crucial question of when $\mathcal{E}$ represents a valid or *physical* quantum state, i.e. an operator that is Hermitian, unit trace and positive semidefinite. Although any two-qubit state can be represented by some ellipsoid, not every ellipsoid corresponds to a two-qubit state. Clearly any $\mathcal{E}$ that punctures the Bloch sphere cannot be valid, but the criterion $\mathcal{E} \subseteq \mathcal{B}$ is not sufficient for physicality. In this chapter we derive necessary and sufficient conditions for $\mathcal{E}$ to be physical. The derivation makes heavy use of the standard form of the canonical, aligned state presented in the preceding chapter.

We also find conditions to determine whether $\mathcal{E}$ describes an entangled or a separable state. This is based on an interpretation of the Peres-Horodecki criterion in the steering ellipsoid picture. We introduce the notion of ellipsoid *chirality*, which plays a role in the conditions for physicality and for separability. In fact, owing to the relationship between chirality and the partial transposition operation, we find that entangled and separable states may be distinguished according to the chirality of $\mathcal{E}$ alone.

3.1 PHYSICALITY OF A TWO-QUBIT STATE

We begin by finding conditions for when a two-qubit operator $\rho \in \mathrm{L}(\mathbb{C}^2 \otimes \mathbb{C}^2)$ represents a valid quantum state. Let us restate the general form of such an operator (Equation (1.5)):

$$\rho = \frac{1}{4}(\mathbb{1} \otimes \mathbb{1} + \boldsymbol{a} \cdot \boldsymbol{\sigma} \otimes \mathbb{1} + \mathbb{1} \otimes \boldsymbol{b} \cdot \boldsymbol{\sigma} + \sum_{i,j=1}^{3} T_{ij}\, \sigma_i \otimes \sigma_j). \tag{3.1}$$

In order to be a density matrix, ρ must be Hermitian ($\rho = \rho^\dagger$), unit trace ($\mathrm{tr}\,\rho = 1$) and positive semidefinite ($\rho \geq 0$). The first two of these requirements are satisfied by construction owing to the properties of the Pauli matrices. Positivity, however, is a far less trivial condition.

In principle, one could form the characteristic polynomial $p(\lambda) = \det(\rho - \lambda\mathbb{1})$ and solve the resulting quartic equation $p(\lambda) = 0$ to find the eigenvalues λ. Finding conditions such that $\lambda \geq 0$ would then give necessary and sufficient conditions for $\rho \geq 0$. Indeed, previous analyses have studied precisely this question of finding the eigenvalues of a unit trace, 4×4 Hermitian matrix [44]. However, the solutions are extremely complicated. Moreover, they are effectively impossible to interpret in the steering ellipsoid picture, and we wish to find conditions for physicality that can be identified with geometric features of $\mathcal{E}$. We achieve this by transforming the problem into one involving the canonical state $\widetilde{\rho}$, finding conditions for $\widetilde{\rho} \geq 0$, and then translating these conditions into the parameters $(\boldsymbol{c}, Q)$ that describe $\mathcal{E}$.

3.1.1 TRANSFORMATION TO THE CANONICAL STATE

We first note that constraints on the local Bloch vectors are essentially trivial, allowing us to focus on the more interesting part of the steering ellipsoid itself. Define $\mathcal{E}'$ as the ellipsoid with same centre as Alice's steering ellipsoid $\mathcal{E}$ but with axes scaled down by a factor b, i.e. compared to $\mathcal{E}$ parametrised by $(\boldsymbol{c}, Q)$, the parameters describing $\mathcal{E}'$ are $(\boldsymbol{c}, b^2 Q)$. Alice's Bloch vector $\boldsymbol{a}$ must lie within $\mathcal{E}'$. This was established as part of the discussion of complete and incomplete steering in Ref. [11].[1]

Aside from these straightforward, necessary restrictions on $\boldsymbol{a}$ and $\boldsymbol{b}$, we must find some more complicated constraints involving the correlation matrix T. Before doing this, however, we transform to the canonical, aligned state, which we repeat here for convenience:

$$\widetilde{\rho} = \frac{1}{4}(\mathbb{1} \otimes \mathbb{1} + \boldsymbol{c} \cdot \boldsymbol{\sigma} \otimes \mathbb{1} + \sum_{i=1}^{3} t_i\, \sigma_i \otimes \sigma_i). \tag{3.2}$$

The transformation $\rho \mapsto \widetilde{\rho}$ leaves $\mathcal{E}$ invariant. As we now establish, it also leaves positivity

[1] Bob's steering of Alice is said to be *complete* when, for any convex decomposition of $\boldsymbol{a}$ into states in $\mathcal{E}$, there exists a POVM for Bob that steers to it [11]. All nondegenerate $\mathcal{E}$ correspond to states that are completely steerable by Bob. When Bob's steering is complete, $\boldsymbol{a}$ lies on $\partial\mathcal{E}'$; for incomplete steering, $\boldsymbol{a}$ lies strictly inside $\mathcal{E}'$.

invariant, allowing us to restrict our analysis to canonical, aligned states alone.[1]

Lemma 3.1: Local filtering preserves positivity

For any $\rho \in \mathrm{L}(\mathbb{C}^2 \otimes \mathbb{C}^2)$, the local filtering operation (2.17),

$$\rho \mapsto \widetilde{\rho} = \frac{(S_A \otimes S_B)\,\rho\,(S_A \otimes S_B)^\dagger}{\mathrm{tr}\left[(S_A \otimes S_B)\,\rho\,(S_A \otimes S_B)^\dagger\right]},$$

with $S_A, S_B \in \mathrm{GL}(2,\mathbb{C})$, preserves positivity: $\rho \geq 0$ if and only if $\widetilde{\rho} \geq 0$.

Proof. Clearly positivity of the numerator of $\widetilde{\rho}$ is sufficient for positivity of $\widetilde{\rho}$. Define $S := S_A \otimes S_B$, so that this numerator is $S\rho S^\dagger$. Say that $\rho \geq 0$; a well-known equivalent condition for this states that we can write $\rho = XX^\dagger$ for some $X \in \mathrm{L}(\mathbb{C}^2 \otimes \mathbb{C}^2)$. Then $S\rho S^\dagger = SX(SX)^\dagger \geq 0$, and so $\widetilde{\rho} \geq 0$. The converse follows using precisely the same logic and considering instead the map S^{-1}. ■

The canonical, aligning transformation was exactly such a local filtering operation, and hence to find conditions for physicality we need consider only the canonical, aligned state $\widetilde{\rho}$.

3.1.2 DESCARTES' RULE OF SIGNS

To find simple conditions for $\widetilde{\rho} \geq 0$ we will use Descartes' rule of signs. This method is employed to find conditions for positivity in, for example, Refs. [31, 32, 45]. The treatment here follows these presentations (in particular, that of Gamel [31]) with some modifications.

For our purposes, Descartes' rule states that the roots of a polynomial are all non-negative if and only if its coefficients alternate signs [46]. The characteristic polynomial may be expanded as

$$p(\lambda) = \prod_{i=1}^{4}(\lambda - \lambda_i) = \sum_{j=0}^{4}(-1)^j a_j \lambda^{4-j}. \tag{3.3}$$

Descartes' rule then tells us that $\lambda_i \geq 0\,\forall i$ if and only if $a_j \geq 0\,\forall j$. Expanding $p(\lambda)$, one finds that a_j are given by the elementary symmetric functions of the roots:

$$\begin{aligned}
a_0 &= 1,\\
a_1 &= \lambda_1 + \lambda_2 + \lambda_3 + \lambda_4,\\
a_2 &= \lambda_1\lambda_2 + \lambda_1\lambda_3 + \lambda_1\lambda_4 + \lambda_2\lambda_3 + \lambda_2\lambda_4 + \lambda_3\lambda_4,\\
a_3 &= \lambda_1\lambda_2\lambda_3 + \lambda_1\lambda_2\lambda_4 + \lambda_1\lambda_3\lambda_4 + \lambda_2\lambda_3\lambda_4,\\
a_4 &= \lambda_1\lambda_2\lambda_3\lambda_4.
\end{aligned} \tag{3.4}$$

[1] Clearly this Lemma applies for transformations in $\mathbb{C}^{d_1} \otimes \mathbb{C}^{d_2}$ but we are interested only in the case $d_1 = d_2 = 2$.

Transforming these functions of eigenvalues into functions of $\widetilde{\rho}$ then allows one to find conditions for physicality.

Lemma 3.2: Physicality of a canonical, aligned state

$\widetilde{\rho}$ is physical if and only if

$$\det\widetilde{\rho} \geq 0 \text{ and } c^2 \leq 1 - \sum_{i=1}^{3} t_i^2 - 2t_1t_2t_3 \text{ and } c^2 + \sum_{i=1}^{3} t_i^2 \leq 3.$$

Up to a positive multiplicative factor, $\det\widetilde{\rho} = c^4 - 2uc^2 + q$, with

$$u := 1 - \sum_i t_i^2 + 2\sum_i t_i^2\hat{c}_i^2,$$

$$q := (1 + t_1 + t_2 - t_3)(1 + t_1 - t_2 + t_3)(1 - t_1 + t_2 + t_3)(1 - t_1 - t_2 - t_3),$$

where we have defined the unit vector $\hat{\boldsymbol{c}} := \boldsymbol{c}/c$.

Proof. According to Descartes' rule of signs, $\widetilde{\rho} \geq 0$ if and only if $a_j \geq 0 \,\forall j$. This is satisfied trivially for $j = 0$ and $j = 1$ (since $\operatorname{tr}\widetilde{\rho} = 1$). Note that $a_4 = \prod_{i=1}^{4}\lambda_i = \det\widetilde{\rho}$.

The coefficients a_1 and a_2 may be also be expressed in terms of matrix invariants. Recall that $\operatorname{tr}(\widetilde{\rho}^n) = \sum_{i=1}^{4}\lambda_i^n$. Using Newton's identities [47] to relate the elementary symmetric polynomials a_j to these power sums we find that

$$a_2 = \tfrac{1}{2}\left[a_1(\operatorname{tr}\widetilde{\rho})^2 - \operatorname{tr}(\widetilde{\rho}^2)\right] = \tfrac{1}{2}\left[1 - \operatorname{tr}(\widetilde{\rho}^2)\right],$$

$$a_3 = \tfrac{1}{3}\left[a_2\operatorname{tr}\widetilde{\rho} - a_1\operatorname{tr}(\widetilde{\rho}^2) + \operatorname{tr}(\widetilde{\rho}^3)\right] = \tfrac{1}{6}\left[1 - 3\operatorname{tr}(\widetilde{\rho}^2) + 2\operatorname{tr}(\widetilde{\rho}^3)\right].$$

All that remains to find the conditions $a_j \geq 0$ is the evaluation of $\det\widetilde{\rho}$, $\operatorname{tr}(\widetilde{\rho}^2)$ and $\operatorname{tr}(\widetilde{\rho}^3)$ in terms of $\boldsymbol{c}$ and $\boldsymbol{t}$. The expressions given result from this tedious, but straightforward, calculation. ■

3.1.3 CONDITIONS FOR PHYSICALITY

Thus far we have found algebraic conditions for the physicality of $\widetilde{\rho}$. We now seek to find some geometric interpretation for these conditions using the steering ellipsoid $\mathcal{E}$. We achieve this by translating our conditions into rotational invariants of the parameters $(\boldsymbol{c}, Q)$ that describe $\mathcal{E}$. Since $\mathcal{E}$ is invariant under the canonical transformation, this in fact gives us a set of necessary and sufficient condition for the physicality of *any* steering ellipsoid.

Recall that $Q = \operatorname{diag}(t_1^2, t_2^2, t_3^2)$ and that $s_i = |t_i|$ give the lengths of the ellipsoid semiaxes. Rotational invariants will be terms such as $\operatorname{tr} Q = \sum_{i=1}^{3} t_i^2$. Some care is needed with the term $t_1t_2t_3$, which could be positive or negative. Since $\sqrt{\det Q} = |t_1t_2t_3| = s_1s_2s_3$ is positive by

definition, we have that $t_1 t_2 t_3 = \chi\sqrt{\det Q}$, where χ gives the *chirality* of $\mathcal{E}$. In terms of the canonical correlation matrix, we have

$$\chi = \operatorname{sign}(t_1 t_2 t_3) = \operatorname{sign}(\det \widetilde{T}). \tag{3.5}$$

Say that Bob performs Pauli measurements on $\widetilde{\rho}$ and obtains the $+1$ eigenstates as outcomes, corresponding to Bloch vectors $\hat{\boldsymbol{x}}$, $\hat{\boldsymbol{y}}$ and $\hat{\boldsymbol{z}}$. These vectors form a right-handed set, and the measurement outcomes steer Alice to the Bloch vectors $\boldsymbol{c} + t_1\hat{\boldsymbol{x}}$, $\boldsymbol{c} + t_2\hat{\boldsymbol{y}}$ and $\boldsymbol{c} + t_3\hat{\boldsymbol{z}}$ respectively. When Bob's outcomes and Alice's steered vectors are related by an affine transformation involving a proper (improper) rotation, Alice's steered vectors form a right-handed (left-handed) set and $\chi = +1$ ($\chi = -1$). We therefore refer to $\chi = +1$ ellipsoids as *right-handed* and $\chi = -1$ ellipsoids as *left-handed*. Note that a degenerate ellipsoid corresponds to $\chi = 0$, since at least one $t_i = 0$ (equivalently $s_i = 0$).

This notion of chirality will prove to be very important when we shortly consider the conditions for entanglement, and later in Chapter 7 for our study of entanglement witnesses. More immediately, however, we are now in the position to complete our goal of finding conditions for the physicality of a steering ellipsoid.

Theorem 3.3: Physicality of the steering ellipsoid

A steering ellipsoid $\mathcal{E}$ described by parameters $(\boldsymbol{c}, Q)$ and with chirality χ corresponds to a physical two-qubit state if and only if

$$c^4 - 2uc^2 + q \geq 0 \text{ and } c^2 \leq 1 - \operatorname{tr} Q - 2\chi\sqrt{\det Q} \text{ and } c^2 + \operatorname{tr} Q \leq 3,$$

where

$$u := 1 - \operatorname{tr} Q + 2\hat{\boldsymbol{c}}^{\mathsf{T}} Q \hat{\boldsymbol{c}},$$
$$q := 1 + 2\operatorname{tr}(Q^2) - 2\operatorname{tr} Q - (\operatorname{tr} Q)^2 - 8\chi\sqrt{\det Q}.$$

Proof. Rewrite the conditions of Lemma 3.2 using the ellipsoid parameters $\boldsymbol{c}$, Q and χ. In particular, we use the correspondences $\sum_i t_i^{2n} = \operatorname{tr}(Q^n)$, $\sum_i t_i^2 \hat{c}_i^2 = \hat{\boldsymbol{c}}^{\mathsf{T}} Q \hat{\boldsymbol{c}}$ and $t_1 t_2 t_3 = \chi\sqrt{\det Q}$. ■

It should be noted that any $\mathcal{E}$ inside the Bloch ball $\mathcal{B}$ must obey $\sqrt{\det Q} \leq 1$. For such $\mathcal{E}$ the second condition given in Theorem 3.3 immediately implies that $c^2 + \operatorname{tr} Q \leq 3$, rendering the third condition redundant.

We can identify three geometric contributions influencing whether a given steering ellipsoid describes a physical state:

(1) The distance of the ellipsoid centre from the origin (through terms such as c^4 and c^2).

(2) The size of $\mathcal{E}$. 'Size' can be measured in a number of different ways, e.g. the volume of $\mathcal{E}$ (proportional to $\sqrt{\det Q}$), the sum of the semiaxes squared ($\operatorname{tr} Q$), etc. Later in this thesis we will see the relevance of some of these measures, especially steering ellipsoid volume.

(3) The skew $\hat{\boldsymbol{c}}^{\intercal} Q \hat{\boldsymbol{c}}$. This gives a measure of how the axes of $\mathcal{E}$ are oriented relative to the centre vector $\boldsymbol{c}$.

In addition, the physicality conditions also depend on the chirality of the ellipsoid. We shall now see that this relates fundamentally to the separability of the two-qubit state.

3.2 CONDITIONS FOR ENTANGLEMENT

We now consider how the key property of entanglement is encoded in the geometric properties of $\mathcal{E}$. In fact, as outlined in Section 1.5.5, this matter has already been resolved in Ref. [11]. Jevtic et al. provided both the nested tetrahedron condition and an inequality for identifying whether a given $\mathcal{E}$ describes an entangled state. This inequality is in fact rather similar to our Theorem 3.3 for physicality, and identifies a similar set of geometric contributions influencing the entanglement of a state. What is missing, however, is an observation of the crucial role played by chirality. Here we will use chirality to offer another perspective on the entanglement of a steering ellipsoid, thereby clarifying and consolidating the work of Ref. [11].

3.2.1 PERES-HORODECKI CRITERION

The Peres-Horodecki or *positive partial transpose* (PPT) criterion [48, 49] gives a necessary condition for separability of a mixed bipartite state $\rho \in \mathrm{L}(\mathbb{C}^{d_1} \otimes \mathbb{C}^{d_2})$. Crucially, for our case of a two-qubit system, $d_1 = d_2 = 2$, the criterion is also sufficient.[1] The criterion relies on the spectral properties of the partial transposed state, which we write $\rho^{\intercal_B}$.

For a two-qubit state, the original Peres-Horodecki criterion states that ρ is separable if and only if $\rho^{\intercal_B} \geq 0$. Refs. [11] and [50] independently showed that this statement can in fact be simplified to the evaluation of a single determinant:

Lemma 3.4: Determinant criterion for separability

A two-qubit state ρ is separable if and only if $\det \rho^{\intercal_B} \geq 0$.

[1] The Peres-Horodecki criterion is in fact also sufficient in a qubit-qutrit system.

Note that the equivalence $\det \rho^{\intercal_B} \geq 0 \Leftrightarrow \rho^{\intercal_B} \geq 0$ is not true for a general 4×4 Hermitian operator ρ (take, for example, an operator with two positive and two negative eigenvalues). The equivalence emerges only when we additionally impose the constraints $\mathrm{tr}\, \rho = 1$ and $\rho \geq 0$.

3.2.2 CHIRALITY AND SEPARABILITY

As with the conditions for physicality, we transform to the canonical, aligned state $\widetilde{\rho}$, which preserves separability:

Lemma 3.5: Local filtering preserves separability
A two-qubit state ρ is separable if and only if its corresponding canonical, aligned state $\widetilde{\rho}$ is.

Proof. This follows immediately from an application of Lemma 3.1 to the transformation $\rho^{\intercal_B} \mapsto \widetilde{\rho}^{\intercal_B}$, together with the fact that the Peres-Horodecki criterion is necessary and sufficient for the separability of a two-qubit state. ■

Hence, given Lemma 3.4, we see that the separability of any two-qubit state ρ is given simply by the sign of $\det \widetilde{\rho}^{\intercal_B}$. The following theorem allows us to characterise the separability any two-qubit using the chirality of the canonical state steering ellipsoid $\mathcal{E}$. The result is illustrated in Figure 3.1.

Theorem 3.6: Separability of the steering ellipsoid
$\mathcal{E}$ for any entangled state is left-handed. $\mathcal{E}$ for a separable state may be right-handed, left-handed or degenerate; for a separable left-handed $\mathcal{E}$, the corresponding right-handed $\mathcal{E}$ is also a separable state and vice-versa.

Proof. The effect of the partial transposition operation is most easily seen in the Pauli basis, since we have $\sigma_\mu^\intercal = \sigma_\mu$ for $\mu \in \{0, 1, 3\}$ and $\sigma_\mu^\intercal = -\sigma_\mu$ for $\mu = 2$ (i.e. the Pauli σ_y matrix). The partial transposition operation on a canonical state, $\widetilde{\rho} \mapsto \widetilde{\rho}^{\intercal_B}$, is thus equivalent to $t_2 \mapsto -t_2$. This in turn is equivalent to simply flipping the chirality, $\chi \mapsto -\chi$.

An entangled state $\widetilde{\rho}$ must have $\det \widetilde{\rho}^{\intercal_B} < 0$ and a non-degenerate ellipsoid, and so $\chi = \pm 1$ *a priori*. All quantum states achieve $\det \widetilde{\rho} \geq 0$, so for an entangled state

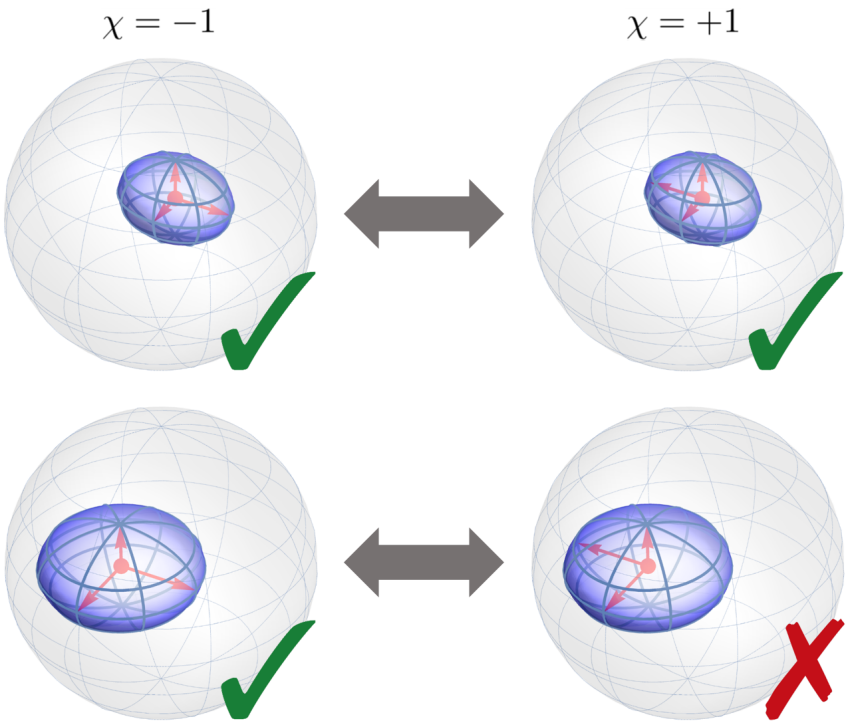

Figure 3.1: The separability of a state depends on the physicality of the different chirality steering ellipsoids. For a separable state (top), both the left-handed ($\chi = -1$) and right-handed ($\chi = +1$) ellipsoids are physical. For an entangled state (bottom), only the left-handed ellipsoid is physical. We may switch between left- and right-handed chirality using the partial transposition operation.

we have $\det \widetilde{\rho} > \det \widetilde{\rho}^{\intercal_B}$. Using the form for $\det \widetilde{\rho}$ given in Theorem 3.3, an entangled state must have $-8\chi\sqrt{\det Q} > 8\chi\sqrt{\det Q}$ and hence its chirality is restricted to $\chi = -1$.

$\mathcal{E}$ for a separable state may be degenerate or non-degenerate and so $\chi = 0$ or $\chi = \pm 1$ *a priori*. For a two-qubit separable state, the operator $\widetilde{\rho}^{\intercal_B}$ is also a separable state. Since partial transposition is equivalent to $\chi \to -\chi$, this means that both the χ and the $-\chi$ ellipsoids are separable states. For the degenerate case, $\chi = 0$. For a non-degenerate ellipsoid, both the $\chi = +1$ and $\chi = -1$ ellipsoids are separable. ■

SUMMARY AND DISCUSSION OF CHAPTER 3

We have found a set of necessary and sufficient conditions that establish when a given steering ellipsoid $\mathcal{E}$ represents a valid quantum state (Theorem 3.3), i.e. for when some $\rho \in \mathrm{L}(\mathbb{C}^2 \otimes \mathbb{C}^2)$ satisfies $\mathrm{tr}\,\rho = 1$, $\rho = \rho^\dagger$ and $\rho \geq 0$. The constraint of positivity is in fact the only nontrivial one. Finding the eigenvalues of ρ is a difficult task, and so we instead characterise positivity by employing Descartes' rule of signs.

Similarly, we have found geometric conditions to determine whether $\mathcal{E}$ represents an entangled or separable state (Theorem 3.6). This showed that the notion of ellipsoid chirality is fundamental to separability: any entangled $\mathcal{E}$ must be left-handed in order to be physical, whilst any separable $\mathcal{E}$ is physical for both left- and right-handed chirality.

Note that we have classified any $\mathcal{E}$ that does not describe a two-qubit state as unphysical. In fact, in Chapter 7, we shall see an operator with $\rho \ngeq 0$ also has a physical interpretation – not as a quantum state, but as an *entanglement witness*. This will lead to a different formulation for when $\mathcal{E}$ describes a valid quantum state, and we will find that the determinant criterion can in fact be extended to any $\mathcal{E} \subseteq \mathcal{B}$.

CHAPTER 4

EXTREMAL STATES

Given that $\mathcal{E}$ is a steering ellipsoid centred at $\boldsymbol{c}$, what is the largest volume spherical $\mathcal{E}$ that represents a separable state? What is the largest volume sphere that is physical? Are spheres the largest volume ellipsoids with a given centre and, if not, what are the largest volume ellipsoids? What is the significance of the states corresponding to such maximal ellipsoids?

The previous chapter established conditions for characterising the separability and physicality of $\mathcal{E}$. In this chapter, we will use these conditions to answer all the above and several related questions by finding $\mathcal{E}$ lying on the entangled-separable and physical-unphysical boundaries. We consider this question first in 2D by maximising areas of circles and ellipses; we then move to 3D and investigate maximal volume spheres and ellipsoids. In each case, we pose the question as a maximisation over the set of $\mathcal{E}$ with a given centre $\boldsymbol{c}$. This is a natural parameter to use in the steering ellipsoid representation, and the physical and geometric results will retrospectively confirm the relevance of such a maximisation.

Steering ellipsoid volume was first suggested as an indicator of two-qubit entanglement in Ref. [11], where it was demonstrated that any $\mathcal{E}$ with volume greater than $\frac{4\pi}{81}$ must be entangled. We will generalise and extend this result to place more sensitive, $\boldsymbol{c}$-dependent, bounds on how large an ellipsoid may be before it becomes at first entangled and then unphysical.

Although it is not evident *a priori*, we shall find that the two-qubit states corresponding to maximal volume physical $\mathcal{E}$ have particularly special properties. In Section 4.4 we introduce these so-called *maximally obese* states, which will feature heavily in Chapters 5 and 6. Investigation of these states will demonstrate more clearly the meaning of steering ellipsoid volume as a measure of quantum correlation.

4.1 METHOD FOR FINDING EXTREMAL ELLIPSOIDS

To find an extremal ellipsoid, one must solve a maximisation problem. As an example, consider the case of finding the maximal volume physical $\mathcal{E}$. As discussed in Section 2.2.3, the question of searching over all $\mathcal{E}$ is precisely equivalent to searching over canonical, aligned states. Recall that the corresponding $\mathcal{E}$ have centre $\boldsymbol{c}$ and ellipsoid matrix $Q = \mathrm{diag}(s_1^2, s_2^2, s_3^2)$, where s_i give the lengths of the semiaxes. The volume of $\mathcal{E}$ is simply given by $V = \frac{4\pi}{3} s_1 s_2 s_3$. The question of finding a maximal volume physical steering ellipsoid is then equivalent to the following optimisation problem: over all $\mathcal{E}$ centred at $\boldsymbol{c}$, find the one that maximises V subject to the physical state conditions given in Theorem 3.3.

This is much like a problem with Lagrange multipliers but with inequality constraints, which adds to the complexity. The Karush-Kuhn-Tucker (KKT) conditions provide a method to deal with such an optimisation problem [36]. Before outlining how the maximal ellipsoid optimisation problems can be solved, we demonstrate how chirality plays a crucial role in developing the results.

4.1.1 CHIRALITY AS A FLAG

Let us first consider non-degenerate $\mathcal{E}$. Recall from Theorem 3.6 that an entangled state must be left-handed ($\chi = -1$) to be physical, whilst a separable state is physical in both its right- and left-handed forms ($\chi = \pm 1$). In other words, the separable-entangled boundary corresponds to extremal right-handed physical $\mathcal{E}$, whilst the physical-unphysical boundary corresponds to extremal left-handed physical $\mathcal{E}$. We can therefore switch between these two boundaries by solving the same set of KKT conditions and altering only the chirality. We thus use chirality as a 'flag' to specify which boundary we wish to probe: for the separable-entangled boundary we use $\chi = +1$, and for the physical-unphysical boundary we use $\chi = -1$.

For the case of degenerate $\mathcal{E}$ with $\chi = 0$, any physical ellipsoid must be separable and so there is only the physical-unphysical boundary to find.

4.1.2 KARUSH-KUHN-TUCKER CONDITIONS

We consider a canonical, aligned state $\widetilde{\rho}$. Let us rephrase the conditions for physicality given in Theorem 3.3, recalling that for $\mathcal{E}$ inside the Bloch ball the condition $c^2 + \mathrm{tr}\, Q \leq 3$ is redundant. We have that $\widetilde{\rho} \geq 0$ if and only if $g_1 \geq 0$ and $g_2 \geq 0$, where

$$g_1 = c^4 - 2uc^2 + q,$$

$$g_2 = 1 - \operatorname{tr} Q - 2\chi\sqrt{\det Q} - c^2, \tag{4.1}$$

with the variables u and q given by

$$\begin{aligned} u &:= 1 - \operatorname{tr} Q + 2\hat{\boldsymbol{c}}^\mathsf{T} Q \hat{\boldsymbol{c}}, \\ q &:= 1 + 2\operatorname{tr}(Q^2) - 2\operatorname{tr} Q - (\operatorname{tr} Q)^2 - 8\chi\sqrt{\det Q}. \end{aligned} \tag{4.2}$$

We wish to maximise $V = \frac{4\pi}{3} s_1 s_2 s_3$ subject to the inequality constraints $g_1 \geq 0$ and $g_2 \geq 0$. According to the KKT conditions we form the Lagrangian

$$\mathcal{L} = V + \lambda_1 g_1 + \lambda_2 g_2, \tag{4.3}$$

where λ_1 and λ_2 are KKT multipliers [36]. Setting $Q = \operatorname{diag}(s_1^2, s_2^2, s_3^2)$, we then solve in terms of $\boldsymbol{c}$ the system of equations and inequalities given by

$$\begin{aligned} \frac{\partial \mathcal{L}}{\partial \boldsymbol{s}} &= \mathbf{0}, \\ \lambda_1 g_1 = \lambda_2 g_2 &= 0, \\ \lambda_1, \lambda_2, g_1, g_2 &\geq 0. \end{aligned} \tag{4.4}$$

This system can in fact be simplified before solving. In particular, the skew term $\hat{\boldsymbol{c}}^\mathsf{T} Q \hat{\boldsymbol{c}}$ is awkward to deal with in full generality. However, by symmetry, any maximal ellipsoid must have one of its axes aligned radially and the other two non-radial axes equal. Since we are looking at ellipsoids aligned with the coordinate axes, we may therefore take $\boldsymbol{c} = (0, 0, c)$ and $s_1 = s_2$. Maximal solutions could then have $s_1 = s_2 > s_3$ (an oblate spheroid), $s_1 = s_2 < s_3$ (a prolate spheroid) or $s_1 = s_2 = s_3$ (a sphere).

Even after this simplification, solving the system (4.4) is quite a laborious process, and the exact algebra involved is not of any particular interest. As an example, we will work through the conditions fully for our first non-trivial example of maximal area steering ellipsoids; the other cases are solved similarly.

4.2 MAXIMAL AREA STEERING ELLIPSOIDS

We begin by finding the physical-unphysical boundary for a degenerate $\mathcal{E}$ lying in the equatorial plane of $\mathcal{B}$.[1] This serves as a useful warm-up to the more important case of finding extremal 3D ellipsoids, but also provides some interesting results in its own right.

[1] In theory, we could find the maximal area ellipses lying in any plane of $\mathcal{B}$. However, clearly the overall largest ellipse will lie within the largest such plane, which without loss of generality we may orient to be equatorial, i.e. the disc $\{(x, y, z) \mid x^2 + y^2 \leq 1, z = 0\}$. The maximal $\mathcal{E}$ in other planes may then be found by scaling down the solutions to this overall maximum.

4.2.1 CIRCLES

For a circle of radius r, we take $Q = \mathrm{diag}(r^2, r^2, 0)$ and find that $\mathcal{E}$ represents a physical (and necessarily separable) state if and only if $r \leq \frac{1}{2}\left(1 - c^2\right)$, where $\boldsymbol{c}$ is the centre vector in the equatorial plane. The physical ellipse with the largest area is not however a circle for $c > 0$.

4.2.2 ELLIPSES

To find maximal ellipses, we use the KKT conditions. We describe an ellipse in the equatorial plane using $Q = \mathrm{diag}(s_1^2, s_2^2, 0)$ and $\boldsymbol{c} = (c, 0, 0)$; the area of this ellipse is $\pi s_1 s_2$. We form the Lagrangian (4.3). In fact, the algebra is simplified somewhat by including some positive constant factors and equivalently using

$$\mathcal{L} = 8\pi s_1 s_2 + \lambda_1 g_1 + 2\lambda_2 g_2. \tag{4.5}$$

Substituting Q and $\boldsymbol{c}$ into the expressions (4.1) for g_1 and g_2 gives

$$\begin{aligned} g_1 &= c^4 - 2c^2(1 + s_1^2 - s_2^2) + 1 - 2s_1^2 - 2s_2^2 - 2s_1^2 s_2^2 + s_1^4 + s_2^4, \\ g_2 &= 1 - s_1^2 - s_2^2 - c^2. \end{aligned} \tag{4.6}$$

We now solve the system (4.4). The requirement $\frac{\partial \mathcal{L}}{\partial \boldsymbol{s}} = \boldsymbol{0}$ corresponds to the two equations $\frac{\partial \mathcal{L}}{\partial s_1} = 0$ and $\frac{\partial \mathcal{L}}{\partial s_2} = 0$. Noting that the maximal solution must have $s_1 \neq 0$ and $s_2 \neq 0$, these equations can be solved simultaneously to give

$$\begin{aligned} \lambda_1 &= \frac{s_2^2 - s_1^2}{s_1 s_2 (s_2^2 - s_1^2 + c^2)}, \\ \lambda_2 &= \frac{1}{s_1 s_2}\left(s_1^2 + s_2^2 - \frac{s_2^2 - s_1^2}{s_2^2 - s_1^2 + c^2}\right). \end{aligned} \tag{4.7}$$

We now impose the constraints that $\lambda_1 g_1 = \lambda_2 g_2 = 0$ and $\lambda_1, \lambda_2, g_1, g_2 \geq 0$. The only solution to this system of equations and inequalities requires $g_1 = \lambda_2 = 0$. Using the expressions given in (4.6) and (4.7), these are solved simultaneously to find s_1 and s_2 in terms of c. Ruling out solutions that do not satisfy $0 < s_i \leq 1$ gives the unique solution

$$\begin{aligned} s_1 &= \tfrac{1}{4}\left(3 - \sqrt{1 + 8c^2}\right), \\ s_2 &= \tfrac{1}{\sqrt{8}}\sqrt{1 - 4c^2 + \sqrt{1 + 8c^2}}, \end{aligned} \tag{4.8}$$

giving the minor semiaxis s_1 and major semiaxis s_2 of the maximal area ellipse centred at $\boldsymbol{c}$.

Noting that both s_1 and s_2 are monotonically decreasing functions of c with $s_1 \leq s_2 \leq \frac{1}{2}$, we see that the overall largest ellipse is the radius $\frac{1}{2}$ circle centred on the origin. Our results then describe how a physical ellipse must shrink from this maximum as its centre is displaced towards the boundary $\partial\mathcal{B}$ (see Figure 4.1).

Note that the unit disk itself, described by $Q = \mathrm{diag}(1, 1, 0)$, does not represent a physical

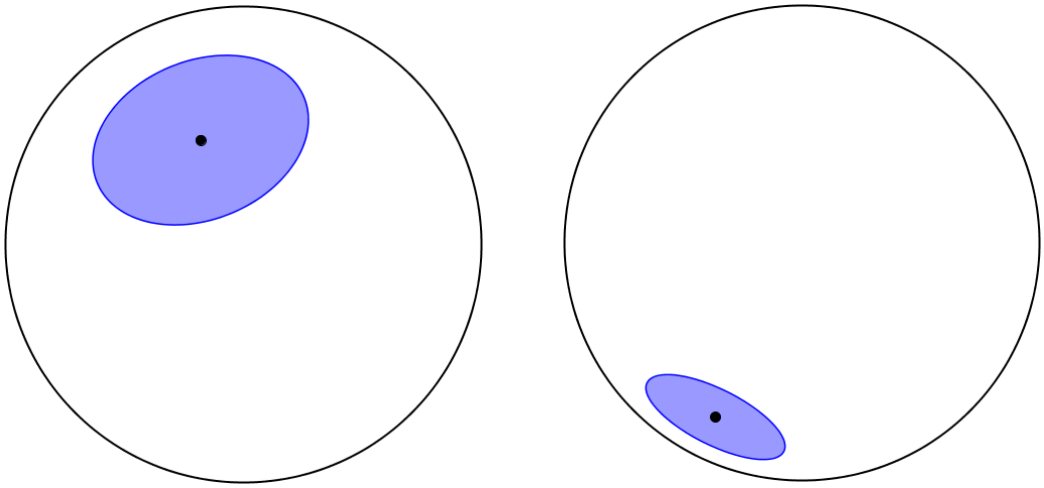

Figure 4.1: Two example steering ellipses inside the equatorial disc. These are the maximal area physical ellipses for their centre. Note, however, that these are not simply the largest ellipses that fit inside $\mathcal{B}$, owing to the stronger constraints imposed on physicality (Theorem 3.3).

state; this corresponds to the well-known result that its Choi-isomorphic single qubit map [51] is not completely positive (the so-called 'No Pancake Theorem'). In fact, Ref. [45] gives a generalisation of the No Pancake Theorem that immediately rules out such a steering ellipsoid: a physical $\mathcal{E}$ can touch the Bloch sphere at a maximum of two points unless it is the whole Bloch sphere (as will be the case for a pure entangled two-qubit state). Here we have extended the No Pancake Theorem further to find the largest possible $\mathcal{E}$ when $\boldsymbol{c}$ is displaced from the origin (corresponding in the Choi-isomorphic setting to non-unitality of the corresponding map).

4.3 MAXIMAL VOLUME STEERING ELLIPSOIDS

For non-degenerate $\mathcal{E}$ we find distinct separable-entangled and physical-unphysical boundaries. As discussed above, these boundaries may be found by studying the maximal volume physical $\mathcal{E}$ with $\chi = +1$ and $\chi = -1$ respectively. Similarly to our study of maximal area 2D steering ellipsoids, we begin with the simplest symmetric case of a spherical $\mathcal{E}$ before moving to general ellipsoids.

4.3.1 SPHERES

Inept states, originally introduced in Ref. [52], are a family of states of the form

$$\rho = r\left|\phi_\epsilon\right\rangle\left\langle\phi_\epsilon\right| + (1-r)\rho' \otimes \rho', \tag{4.9}$$

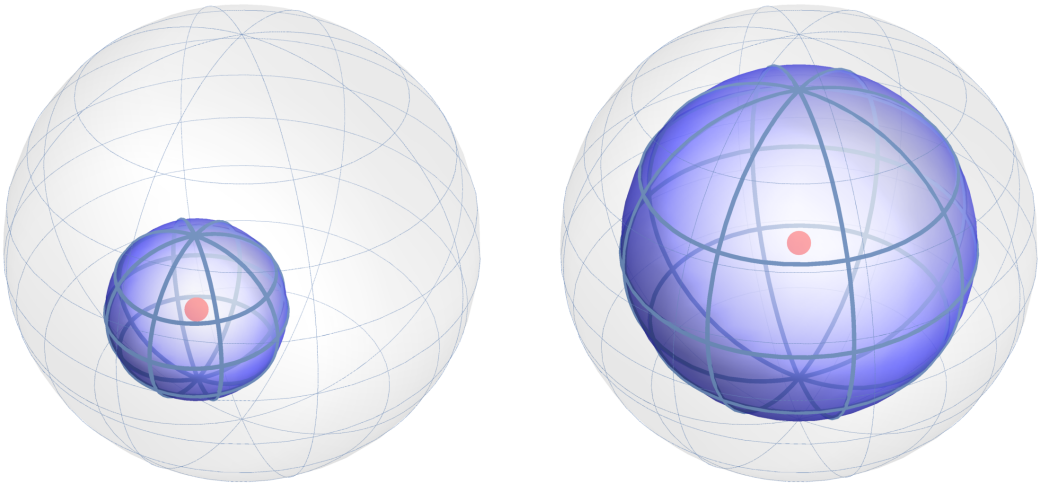

Figure 4.2: Any spherical $\mathcal{E} \subseteq \mathcal{B}$ corresponds to a physical state, given that it has appropriate chirality. Here we show an example of an inept state (left) and a Werner state (right).

where $|\phi_\epsilon\rangle := \sqrt{\epsilon}\,|00\rangle + \sqrt{1-\epsilon}\,|11\rangle$ and $\rho' := \mathrm{tr}_A\,|\phi_\epsilon\rangle\langle\phi_\epsilon| = \mathrm{tr}_B\,|\phi_\epsilon\rangle\langle\phi_\epsilon|$.[1] The two parameters r and ϵ that describe an inept state can easily be translated into a description of the steering ellipsoid: $\mathcal{E}$ has $\boldsymbol{c} = (0, 0, (2\epsilon - 1)(1 - r))$ and $Q = \mathrm{diag}(r^2, r^2, r^2)$. Thus an inept state corresponds to a spherical $\mathcal{E}$ of radius r, as illustrated in Figure 4.2. Note that inept states with $\epsilon = \frac{1}{2}$ have vanishing Bloch vectors for Alice and Bob and are equivalent to Werner states. The corresponding $\mathcal{E}$ are centred on the origin.

From the KKT conditions, we find that the separable-entangled boundary for a spherical $\mathcal{E}$ with centre $\boldsymbol{c}$ is given by

$$r = \tfrac{1}{3}\left(\sqrt{4 - 3c^2} - 1\right). \tag{4.10}$$

As described in Theorem 3.6, any left- or right-handed sphere smaller than this bound describes a separable state.

The physical-unphysical boundary is found to be $r = 1 - c$. In fact, a spherical $\mathcal{E}$ on this boundary touches the surface of the Bloch ball $\mathcal{B}$, and so this simply gives the constraint that $\mathcal{E}$ should lie inside $\mathcal{B}$. Any left-handed spherical $\mathcal{E} \subseteq \mathcal{B}$ therefore represents an inept state. A right-handed sphere whose r exceeds the separable-entangled bound cannot describe a physical state since any entangled $\mathcal{E}$ must be left-handed. Note how simple the physical state criteria are for spherical $\mathcal{E}$: subject to these conditions on chirality, all spherical $\mathcal{E} \subseteq \mathcal{B}$ are physical. The same is not true for ellipsoids in general: there are some ellipsoids inside the Bloch ball for which both the left- and right-handed forms are unphysical.

[1] The name 'inept' derives from the scenario of an inept entanglement delivery service. The service aims to deliver entangled qubits in the state $|\phi_\epsilon\rangle$ to pairs of customers but is inept: although a qubit is always delivered to each customer, any given pair of customers receives the correct pair of qubits only with probability r. The resulting state will be the inept state ρ given.

4.3.2 ELLIPSOIDS

Again, using the KKT conditions, one can find the maximal volume ellipsoids that lie on the separable-entangled and physical-unphysical boundaries. We find that such ellipsoids are oblate spheroids ($s_1 = s_2 \geq s_3$) with the minor axis aligned radially. The largest volume separable $\mathcal{E}$ centred at $\boldsymbol{c} = (0, 0, c)$ has semiaxes

$$\begin{aligned} s_1 = s_2 &= \tfrac{1}{\sqrt{18}}\sqrt{1 - 3c^2 + \sqrt{1 + 3c^2}}, \\ s_3 &= \tfrac{1}{3}\left(2 - \sqrt{1 + 3c^2}\right). \end{aligned} \tag{4.11}$$

The largest volume physical $\mathcal{E}$ centred at $\boldsymbol{c} = (0, 0, c)$ has

$$\begin{aligned} s_1 = s_2 &= \sqrt{1 - c}, \\ s_3 &= 1 - c. \end{aligned} \tag{4.12}$$

These extremal ellipsoids are in fact the largest volume ellipsoids with centre $\boldsymbol{c}$ that fit inside the Bloch ball.

The volume V of these maximal ellipsoids can be used as an indicator for entanglement and unphysicality. Our calculations have been carried out for canonical $\widetilde{\rho}$, but since steering ellipsoids are invariant under the canonical transformation, the results are directly applicable to two-qubit states in general. The maximal ellipsoids for a general $\boldsymbol{c}$ are of course simply rotations of those found above for $\boldsymbol{c} = (0, 0, c)$, and so the below theorem depends only on the distance of the centre of $\mathcal{E}$ from the origin, $c = |\boldsymbol{c}|$.

Theorem 4.1: Steering ellipsoid volume as an indicator

Any two-qubit state ρ, described by steering ellipsoid $\mathcal{E}$ with volume V and centre $\boldsymbol{c}$, is subject to the following boundaries:

(i) If $V > V_c^{\max}$ then ρ must be unphysical;

(ii) If ρ is physical and $V > V_c^{\text{sep}}$ then ρ must be entangled.

The critical volumes of $\mathcal{E}$ on the physical-unphysical and separable-entangled boundaries are given by

$$\begin{aligned} V_c^{\max} &:= \tfrac{4\pi}{3}(1 - c)^2, \\ V_c^{\text{sep}} &:= \tfrac{2\pi}{81}\left(1 - 9c^2 + (1 + 3c^2)^{3/2}\right). \end{aligned}$$

Proof. Find $V_c^{\max}$ and V_c^{sep} using $V = \frac{4\pi}{3} s_1 s_2 s_3$ and the expressions for semiaxes

given in (4.11) and (4.12). ■

This result extends the notion of using volume as an indicator for entanglement, as was introduced in Ref. [11]. There it was demonstrated that the largest volume separable ellipsoid is the Werner state on the separable-entangled boundary, which has a spherical $\mathcal{E}$ of radius $\frac{1}{3}$ and $c = 0$. We have tightened this bound by introducing the dependence on c as well as developing the analogous notion of a physicality indicator. In fact, Theorem 4.1 gives the tightest possible such bounds, since we have identified the extremal $\mathcal{E}$ that lie on the boundaries. Note that for all c we have $V_c^{\text{sep}} \leq V_c^{\max}$, with equality achieved only for $c = 1$ when $\mathcal{E}$ is a point with $V = 0$ and ρ is a product state. This confirms that, as expected, the two boundaries are indeed distinct and that the set of separable $\mathcal{E}$ is a strict subset of physical $\mathcal{E}$.

4.4 MAXIMALLY OBESE STATES

The largest volume ellipsoid with $\boldsymbol{c} = (0, 0, c)$ has major semiaxes $s_1 = s_2 = \sqrt{1-c}$ and minor semiaxis $s_3 = 1 - c$. We will call this $\mathcal{E}_c^{\max}$. With the exception of $c = 1$, which describes a product state, such ellipsoids correspond to entangled states. Using (3.2), the canonical state for $\mathcal{E}_c^{\max}$ can be then be found explicitly. We refer to such states as *maximally obese*.[1] This family of states will be central to our work in the following two chapters, and some illustrative examples are shown in Figure 4.3.

Maximally obese states

The canonical state for the largest volume physical ellipsoid with a given centre $\boldsymbol{c}$ is the maximally obese state

$$\widetilde{\rho}_c^{\max} = \left(1 - \frac{c}{2}\right) |\psi_c\rangle \langle\psi_c| + \frac{c}{2} |00\rangle \langle 00|, \tag{4.13}$$

where $|\psi_c\rangle := \frac{1}{\sqrt{2-c}} \left(|01\rangle + \sqrt{1-c}\,|10\rangle\right)$. Such states form a single parameter family with $0 \leq c \leq 1$.

A maximally obese state is a rank-2 *X state*.[2] X states were introduced in Ref. [53] as a large class of two-qubit states for which certain correlation properties can be found analytically. In fact, steering ellipsoids have already been used to study the quantum discord of X states [21].

[1] We have not yet made precise the distinction between ellipsoid *obesity* and volume. Full details will be given in Section 5.1, where we explain why a state $\widetilde{\rho}_c^{\max}$ is maximally obese rather than simply maximal volume.

[2] The density matrix of an X state in the computational basis has non-zero elements only on the diagonal and anti-diagonal, giving it a characteristic 'X' shape.

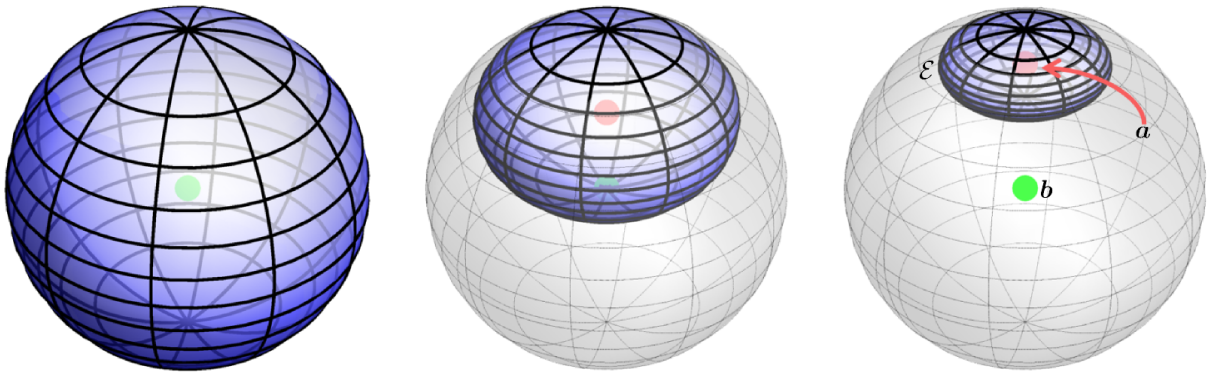

Figure 4.3: The geometric data for three maximal obese states $\widetilde{\rho}_c^{\max}$ with $c = 0$ (left), $c = 0.5$ (middle) and $c = 0.8$ (right). Since these are canonical states we have $\boldsymbol{b} = \boldsymbol{0}$ and $\boldsymbol{c} = \boldsymbol{a}$. Note that $\mathcal{E} = \mathcal{E}_c^{\max}$ touches the pole of the Bloch sphere at $|0\rangle$ for any c.

In the steering ellipsoid formalism, $\mathcal{E}$ for an X state will be radially aligned, having a semiaxis collinear with $\boldsymbol{c}$.

The state $\widetilde{\rho}_c^{\max}$ should be compared to the Horodecki state [54]

$$\rho^{\mathrm{H}} = p\,|\psi^+\rangle\langle\psi^+| + (1-p)\,|00\rangle\langle 00|\,, \tag{4.14}$$

where $|\psi^+\rangle = \frac{1}{\sqrt{2}}(|01\rangle + |10\rangle)$. This is the same as $\widetilde{\rho}_c^{\max}$ when we reparametrise $c = 2(1-p)$ and also make the change $|\psi^+\rangle \mapsto |\psi_c\rangle$. The Horodecki state is a rank-2 maximally entangled mixed state [55]. ρ^{H} may be extended (see, for example, Refs. [56–58]) to the generalised Horodecki state

$$\rho^{\mathrm{GH}} = p\,|\psi_\alpha\rangle\langle\psi_\alpha| + (1-p)\,|00\rangle\langle 00|\,, \tag{4.15}$$

where $|\psi_\alpha\rangle := \sqrt{\alpha}\,|01\rangle + \sqrt{1-\alpha}\,|10\rangle$. Note that this has two free parameters, α and p. Setting $\alpha = \frac{1}{2p}$ and reparametrising $c = 2(1-p)$, we see that our maximally obese states form a special class of the generalised Horodecki states described by the single parameter c.

The maximally obese states have a clear physical interpretation when we consider the Choi-isomorphic channel: $\widetilde{\rho}_c^{\max}$ is isomorphic to the single qubit amplitude-damping (AD) channel with decay probability c [56]. For a single qubit state η, this channel is [7]

$$\Phi_{\mathrm{AD}}(\eta) = E_0 \eta E_0^\dagger + E_1 \eta E_1^\dagger, \tag{4.16}$$

where $E_0 := |0\rangle\langle 0| + \sqrt{1-c}\,|1\rangle\langle 1|$ and $E_1 := \sqrt{c}\,|0\rangle\langle 1|$. If Alice and Bob share the Bell state $|\psi^+\rangle$ and Alice passes her qubit through this channel, we obtain a maximally obese state centred at $\boldsymbol{c} = (0, 0, c)$, i.e. $\widetilde{\rho}_c^{\max} = (\Phi_{\mathrm{AD}} \otimes \mathbb{1})\,|\psi^+\rangle\langle\psi^+|$.

SUMMARY AND DISCUSSION OF CHAPTER 4

We have found families of extremal steering ellipsoids, i.e. those lying on the separable-entangled and physical-unphysical boundaries, for a variety of scenarios: circles, ellipses, spheres and ellipsoids. For 2D $\mathcal{E}$, this allowed us to extend the No Pancake Theorem of Ref. [45]; for 3D $\mathcal{E}$, we extended the use of steering volume as an indicator of entanglement, as proposed in Ref. [11].

Our study of the 3D scenario concerning the largest volume physical ellipsoids will prove to be particularly important. Such ellipsoids describe a new family of maximally obese two-qubit states. In the following chapters, we will see that these states are very significant for the study of quantum correlations and monogamy.

In fact, perhaps the most remarkable application of the work in this chapter lies outside quantum information altogether: by exploiting the nested tetrahedron condition we can use the extremal states on the entangled-separable boundary to derive results in classical Euclidean geometry. The method relies critically on the steering ellipsoid formalism, but the results are of interest in pure geometry. In the following chapters we focus on the physical interpretation of the maximal ellipsoids, and so we defer our discussion of this purely geometric work to Chapter 8.

CHAPTER 5

MONOGAMY OF STEERING ELLIPSOID VOLUME

We have seen that the steering ellipsoid offers a powerful geometric approach to exploring the two-qubit state space. We will now demonstrate that the formalism can be applied to scenarios beyond this bipartite setting. In particular, we consider a tripartite scenario by investigating the volumes of the steering ellipsoids for the two-qubit marginals when Alice, Bob and Charlie share a three-qubit state.

Originally termed *obesity*, steering ellipsoid volume was first proposed as a measure of two-qubit correlation in Ref. [11]. Volume was shown to be distinct from both entanglement and discord, but the precise meaning of obesity was not made clear. In this chapter we propose a formal definition for obesity, which is closely related to but subtly different from steering ellipsoid volume.

The volume of a set of Bloch vectors in Euclidean space may *a priori* seem like a rather arbitrary measure of correlation strength. Our study of a monogamy scenario will demonstrate the physical relevance of this measure. We will see that steering ellipsoid volume obeys a remarkable *monogamy of steering* relationship,[1] and that from this relationship we may derive the well-known Coffman-Kundu-Wootters (CKW) inequality for the monogamy of concurrence [60]. Thus steering ellipsoid volume provides a novel derivation of this classic result, as well as a more geometrically intuitive form of monogamy.

The monogamy of steering is perhaps the most significant result of this thesis. In order to develop the result, we first derive a bound for concurrence in terms of steering ellipsoid volume. We will see that the maximally obese states presented in the previous chapter saturate this bound by maximising concurrence for a given ellipsoid centre. Given this observation, the derivation of steering monogamy will then follow quite straightforwardly.

[1] In Ref. [59], Reid studies the monogamy of EPR-steering inequalities; this may also be described as the monogamy of steering. Here we discuss only monogamy associated with the steering ellipsoids.

5.1 STEERING ELLIPSOID VOLUME AND CONCURRENCE

We begin by establishing an inequality that bounds the concurrence of a two-qubit state using the steering ellipsoid volume V. Physically motivated by its connection to the entanglement of formation, concurrence is an entanglement monotone that may be easily calculated for any two-qubit state ρ [24]. Define the spin-flipped state as

$$\bar{\rho} := (\sigma_y \otimes \sigma_y)\rho^*(\sigma_y \otimes \sigma_y), \tag{5.1}$$

and let $\lambda_1, ..., \lambda_4$ be the eigenvalues of the Hermitian matrix $\sqrt{\sqrt{\rho}\,\bar{\rho}\sqrt{\rho}}$ in non-increasing order. The concurrence is then given by

$$C(\rho) = \max(0, \lambda_1 - \lambda_2 - \lambda_3 - \lambda_4). \tag{5.2}$$

Concurrence ranges from 0 for a separable state to 1 for a maximally entangled state.

5.1.1 BOUNDING CONCURRENCE

In principle one may find $C(\rho)$ in terms of the parameters describing the corresponding steering ellipsoid by explicitly computing λ_i. However, the resulting expressions are very complicated and difficult to interpret. When we found conditions for $\rho \geq 0$ in Chapter 3, we saw that it was possible to present a much more comprehensible solution without finding the eigenvalues of a 4×4 matrix. Similarly, here we will derive a simple bound for $C(\rho)$ in terms of steering ellipsoid volume without actually computing λ_i for a general two-qubit state. We achieve this by first establishing a bound that applies to the special family of Bell-diagonal states.

A Bell-diagonal state is equivalent under local unitary operations to a T state, i.e. a two-qubit state which has both marginals maximally mixed ($\boldsymbol{a} = \boldsymbol{b} = \mathbf{0}$) [30]. Such states are particularly straightforward to manipulate algebraically and enable us to establish the following bound for concurrence.

Lemma 5.1: Concurrence of Bell-diagonal states

Let τ be a Bell-diagonal state given by

$$\tau = \frac{1}{4}(\mathbb{1} \otimes \mathbb{1} + \sum_{i=1}^{3} t_i\, \sigma_i \otimes \sigma_i).$$

The concurrence is bounded as $C(\tau) \leq \sqrt{|t_1 t_2 t_3|}$. This bound is tight: there exists a state τ achieving equality for every value $0 \leq C(\tau) \leq 1$.

Proof. Without loss of generality, order $|t_1| \geq |t_2| \geq t_3$. Ref. [40] then gives

$$C(\tau) = \max\{0, \tfrac{1}{2}(t_1 + t_2 - t_3 - 1)\}.$$

For a separable state τ, we have $C(\tau) = 0$ and so the bound holds.

An entangled state τ must have $C(\tau) > 0$. Recalling that the ellipsoid semiaxes are $s_i = |t_i|$ and that an entangled state must have $\chi = -1$ (Theorem 3.6), we take $t_1 = s_1$, $t_2 = s_2$ and $t_3 = -s_3$ to obtain

$$C(\tau) = \tfrac{1}{2}(s_1 + s_2 + s_3 - 1).$$

Ref. [30] gives necessary and sufficient conditions for the physicality and separability of τ. For τ to be an entangled state, the vector $\boldsymbol{s} = (s_1, s_2, s_3)$ must lie inside the tetrahedron with vertices $\boldsymbol{r}_0 = (1, 1, 1)$, $\boldsymbol{r}_1 = (1, 0, 0)$, $\boldsymbol{r}_2 = (0, 1, 0)$ and $\boldsymbol{r}_3 = (0, 0, 1)$. Treating the tetrahedron $(\boldsymbol{r}_0, \boldsymbol{r}_1, \boldsymbol{r}_2, \boldsymbol{r}_3)$ as a probability simplex, we may uniquely decompose any point inside it as $\boldsymbol{s} = p_0\boldsymbol{r}_0 + p_1\boldsymbol{r}_1 + p_2\boldsymbol{r}_2 + p_3\boldsymbol{r}_3$, where $\sum_i p_i = 1$ and $p_i \geq 0$. This gives $\boldsymbol{s} = (p_0 + p_1, p_0 + p_2, p_0 + p_3)$. Evaluating $s_1 + s_2 + s_3$, we obtain $C(\tau) = p_0$, as $\sum_i p_i = 1$.

We now evaluate the right hand side of the inequality. We have

$$\begin{aligned} |t_1 t_2 t_3| &= s_1 s_2 s_3 \\ &= (p_0 + p_1)(p_0 + p_2)(p_0 + p_3) \\ &= p_0^2 + p_0(p_1 p_2 + p_2 p_3 + p_3 p_1) + p_1 p_2 p_3, \end{aligned}$$

where we have again used $\sum_i p_i = 1$. Since all the terms are positive, we see that $\sqrt{|t_1 t_2 t_3|} \geq p_0 = C(\tau)$, as required. The bound is saturated by states whose $\boldsymbol{s}$ vectors lie on the edges of the tetrahedron $(\boldsymbol{r}_0, \boldsymbol{r}_1, \boldsymbol{r}_2, \boldsymbol{r}_3)$. For example, by choosing $p_1 = p_2 = 0$, we obtain the set of states $\boldsymbol{s} = (p_0, p_0, 1)$. These saturate the bound for every value of the parameter $0 \leq p_0 \leq 1$. ■

Using the transformations given by Verstraete et al. in Ref. [40], we may use the above lemma to give a bound on the concurrence of a general two-qubit state. This will be of central importance when we later demonstrate that the monogamy of steering implies the CKW inequality.

Theorem 5.2: Bound for concurrence using ellipsoid volume

The concurrence of any two-qubit state is bounded as

$$C(\rho) \leq \gamma^{-1} \left(\frac{3V}{4\pi}\right)^{1/4},$$

where $\gamma := 1/\sqrt{1-b^2}$ and V is the volume of Alice's steering ellipsoid.

Proof. Any state ρ can be transformed into a Bell-diagonal state τ by local filtering operations [40]. Recall equation (2.18), which states that such transformations may be written as

$$\rho \mapsto \tau = \frac{1}{N}(S_A \otimes S_B)\,\rho\,(S_A \otimes S_B)^\dagger,$$

where $S_A, S_B \in \mathrm{GL}(2,\mathbb{C})$. The normalisation factor $N = \mathrm{tr}\left[(S_A \otimes S_B)\,\rho\,(S_A \otimes S_B)^\dagger\right]$. Under such a local filtering operation, concurrence transforms as [40]

$$C(\rho) \mapsto C(\tau) = \frac{|\det S_A||\det S_B|}{N} C(\rho).$$

Express the state ρ in the Pauli basis using the matrix $\Theta(\rho)$ whose elements are given by $[\Theta(\rho)]_{\mu\nu} = \mathrm{tr}(\rho\,\sigma_\mu \otimes \sigma_\nu)$. Similarly, τ is represented by $\Theta(\tau)$. For a Bell-diagonal state, we have $\Theta = \mathrm{diag}(1, t_1, t_2, t_3)$. As outlined in Section 2.2.1, the above local filtering operation achieves

$$\Theta(\rho) \mapsto \Theta(\tau) = \frac{|\det S_A||\det S_B|}{N} \Lambda_A \Theta(\rho) \Lambda_B^\intercal,$$

where Λ_i are proper, orthochronous Lorentz transformations given by

$$\Lambda_i = \frac{\Upsilon(S_i \otimes S_i^*)\Upsilon^\dagger}{|\det S_i|},$$

$$\Upsilon = \frac{1}{\sqrt{2}} \begin{pmatrix} 1 & 0 & 0 & 1 \\ 0 & 1 & 1 & 0 \\ 0 & i & -i & 0 \\ 1 & 0 & 0 & -1 \end{pmatrix}.$$

For a general state ρ, the volume $V = \frac{4\pi}{3}\gamma^4 |\det \Theta(\rho)|$ [11]. From the local filtering transformation, and using $\det \Lambda_A = \det \Lambda_B = 1$, we have

$$\begin{aligned} |\det \Theta(\tau)| &= |\det \Theta(\rho)| \left(\frac{|\det S_A||\det S_B|}{N}\right)^4 \\ &= |\det \Theta(\rho)| \left(\frac{C(\tau)}{C(\rho)}\right)^4. \end{aligned}$$

For a Bell-diagonal state $|\det\Theta(\tau)| = |t_1t_2t_3|$, and so we obtain

$$V = \frac{4\pi}{3}\gamma^4|t_1t_2t_3|\left(\frac{C(\rho)}{C(\tau)}\right)^4.$$

Hence $C(\tau) = \left(\frac{4\pi}{3V}\right)^{1/4}\gamma|t_1t_2t_3|^{1/4}C(\rho)$. Since $|t_1t_2t_3| \leq 1$, Lemma 5.1 implies that $C(\tau) \leq |t_1t_2t_3|^{1/4}$, from which the result then follows. ■

5.1.2 OBESITY

The above work suggests precisely how ellipsoid volume might be interpreted as a quantum correlation feature. We define the *obesity* Ω of a two-qubit state as

$$\Omega(\rho) = |\det\Theta(\rho)|^{1/4}, \tag{5.3}$$

so that Theorem 5.2 gives the bound $C(\rho) \leq \Omega(\rho)$.

Obesity is related to the volume of Alice's steering ellipsoid as $V = \frac{4\pi}{3}\gamma^4\Omega^4$. Hence obesity is a rescaled measure of steering ellipsoid volume. In addition to a constant scaling factor, which ensures that $0 \leq \Omega(\rho) \leq 1$, the Lorentz factor γ also plays a role. Crucially, this ensures that obesity is a measure that is invariant under swapping Alice and Bob. Whilst Alice's and Bob's steering ellipsoids do not in general have the same volume, the obesity is a direct function of the two-qubit correlation data itself. Additionally, whilst steering ellipsoid volume is constant for all pure entangled states,[1] the measure of obesity distinguishes between pure states. These properties suggest that obesity might be a more physically meaningful measure of quantum correlation than the raw steering ellipsoid volume itself.

Recently the notion of obesity was proposed entirely independently of the steering ellipsoid formalism. Ref. [61] suggests a quantity denoted R_{12} as a measure of quantum correlation based on the realignment criterion for entanglement. In fact, it may be seen that R_{12} is precisely the same as Ω for a two-qubit state. The authors of Ref. [61] were not aware of our previous work on this quantity or its connection to the steering ellipsoid, again suggesting that the measure may be of general interest. Moreover, Ref. [61] suggests an extension of the definition of obesity to the higher-dimensional Hilbert space $\mathcal{H} = \mathbb{C}^d \otimes \mathbb{C}^d$ as $\Omega(\rho) = d|\det\Theta(\rho)|^{1/d^2}$.[2]

[1] Recall that $\mathcal{E}$ for any pure entangled state is the whole Bloch ball, so that $V = \frac{4\pi}{3}$.

[2] The generalisation $\Omega(\rho) = |\det\Theta(\rho)|^{1/d^2}$ was also originally proposed in the context of steering ellipsoids in Ref. [1]. Later, Ref. [61] independently suggested the same generalisation but with a factor of d that ensures $0 \leq \Omega(\rho) \leq 1$.

5.1.3 MAXIMALLY OBESE STATES MAXIMISE CONCURRENCE

We now demonstrate an important property of the maximally obese state $\widetilde{\rho}_c^{\max}$ given in (4.13). Recall that this is the canonical state corresponding to $\mathcal{E}_c^{\max}$, the maximal volume steering ellipsoid with centre $\boldsymbol{c}$. In the following theorem we show that $\widetilde{\rho}_c^{\max}$ maximises concurrence for a given ellipsoid centre. This will also serve to demonstrate the tightness of the bound given in Theorem 5.2.

Consider inverting the local filtering transformation described in Section 2.2.2 to convert the canonical $\widetilde{\rho}_c^{\max}$, which has $\widetilde{\boldsymbol{b}} = \boldsymbol{0}$, to some state with $\boldsymbol{b} \neq \boldsymbol{0}$:

$$\widetilde{\rho}_c^{\max} \mapsto \rho_c^{\max} = \left(\mathbb{1} \otimes \sqrt{2\rho_B}\right) \widetilde{\rho}_c^{\max} \left(\mathbb{1} \otimes \sqrt{2\rho_B}\right). \tag{5.4}$$

This transformation alters Bob's Bloch vector to $\boldsymbol{b}$, where $\rho_B = \frac{1}{2}(\mathbb{1} + \boldsymbol{b} \cdot \boldsymbol{\sigma}) = \mathrm{tr}_A\, \rho_c^{\max}$ is Bob's new reduced state. Recall that Bob's local filtering operation leaves Alice's steering ellipsoid $\mathcal{E}$ invariant, and so $\mathcal{E}$ for $\rho_c^{\max}$ is still the maximal volume ellipsoid $\mathcal{E}_c^{\max}$.

Theorem 5.3: Maximally obese states maximise concurrence

From the set of all two-qubit states that have $\mathcal{E}$ centred at $\boldsymbol{c}$, the one with the highest concurrence is the maximally obese state $\widetilde{\rho}_c^{\max}$. The bound of Theorem 5.2 is saturated for any $0 \leq b \leq 1$ by a state $\rho_c^{\max}$ corresponding to the maximal volume ellipsoid $\mathcal{E}_c^{\max}$.

Proof. Recall that under the local filtering operation

$$\rho \mapsto \frac{1}{N}(S_A \otimes S_B)\, \rho\, (S_A \otimes S_B)^\dagger,$$

concurrence transforms as [40]

$$C(\rho) \mapsto \frac{|\det S_A||\det S_B|}{N} C(\rho),$$

where $N := \mathrm{tr}\left[(S_A \otimes S_B)\, \rho\, (S_A \otimes S_B)^\dagger\right]$. For the canonical transformation (2.20), we have $S_A = \mathbb{1}$ and $S_B = 1/\sqrt{2\rho_B}$. This gives $\det S_A = 1$, $\det S_B = 1/\sqrt{1-b^2} =: \gamma$ and $N = 1$ so that $C(\widetilde{\rho}) = \gamma C(\rho)$. Computing the concurrence of the maximally obese state given in (4.13) yields $C(\widetilde{\rho}_c^{\max}) = \sqrt{1-c}$. Hence for a state of the form (5.4) we have $C(\rho_c^{\max}) = \gamma^{-1}\sqrt{1-c}$.

Since $\mathcal{E}$ is invariant under Bob's local filtering operation, the same $\mathcal{E}_c^{\max}$ describes a state $\rho_c^{\max}$ with any $\boldsymbol{b}$. From Theorem 4.1 we know that the maximal ellipsoid $\mathcal{E}_c^{\max}$ has volume $V_c^{\max} = \frac{4\pi}{3}(1-c)^2$. Substituting $C(\rho_c^{\max})$ and $V_c^{\max}$ into

the result of Theorem 5.2 shows that the bound is saturated by states $\rho_c^{\max}$ for any $0 \leq b \leq 1$.

Any physical ρ with $\mathcal{E}$ centred at $\boldsymbol{c}$ must obey the bounds $V \leq \frac{4\pi}{3}(1-c)^2$ (Theorem 4.1) and $C(\rho) \leq \gamma^{-1}\left(\frac{3V}{4\pi}\right)^{1/4}$ (Theorem 5.2), and hence $C(\rho) \leq \gamma^{-1}\sqrt{1-c}$. For a given $\boldsymbol{c}$, the state that maximises concurrence has $\boldsymbol{b} = \boldsymbol{0}$. The state $\widetilde{\rho}_c^{\max}$ achieves this maximum possible concurrence, $C(\widetilde{\rho}_c^{\max}) = \sqrt{1-c}$. Hence, from the set of all two-qubit states that have $\mathcal{E}$ centred at $\boldsymbol{c}$, the state with the highest concurrence is the maximally obese state $\widetilde{\rho}_c^{\max}$. ■

It should be emphasised that $\widetilde{\rho}_c^{\max}$ maximises obesity from the set of all two-qubit states that have $\mathcal{E}$ centred at $\boldsymbol{c}$, achieving $\Omega(\widetilde{\rho}_c^{\max}) = \sqrt{1-c}$. Although the maximal volume $\mathcal{E}_c^{\max}$ describes states $\rho_c^{\max}$ with any $\boldsymbol{b}$, the maximally obese state is uniquely the canonical $\widetilde{\rho}_c^{\max}$. This explains why we refer to such states as maximally obese rather than simply maximal volume.

5.2 MONOGAMY OF STEERING

We now turn to our derivation of the monogamy of steering ellipsoid volume, the key result of this chapter. We consider a three-qubit state shared between Alice, Bob and Charlie, and so we reintroduce subscripts labelling the qubits A, B and C. Thus Alice's ellipsoid $\mathcal{E}$ is now labelled $\mathcal{E}_A$, the maximal volume state $\rho_c^{\max}$ is $\rho_{c_A}^{\max}$, the Lorentz factor $\gamma = 1/\sqrt{1-b^2}$ is γ_b, and so on.

5.2.1 MUTUALLY MAXIMAL VOLUME STEERING

We begin by considering a maximal volume two-qubit state shared between Alice and Bob.

Lemma 5.4: Bipartite mutually maximal volume steering
When Alice and Bob share a state $\rho_{c_A}^{\max}$ given by (5.4), both $\mathcal{E}_A$ and $\mathcal{E}_B$ are maximal volume for their respective centres $\boldsymbol{c}_A$ and $\boldsymbol{c}_B$, and the centres obey $\gamma_b^2(1-c_B) = \gamma_a^2(1-c_A)$.

Proof. $\mathcal{E}_A = \mathcal{E}_{c_A}^{\max}$ by construction, so $V_A = V_{c_A}^{\max} = \frac{4\pi}{3}(1-c_A)^2$. From Theorem 5.2 we know that $C(\rho_{c_A}^{\max}) = \gamma_b^{-1}\sqrt{1-c_A}$. Since concurrence is a symmetric function with respect to swapping Alice and Bob we must also have $C(\rho_{c_A}^{\max}) = \gamma_a^{-1}\sqrt{1-c_B}$,

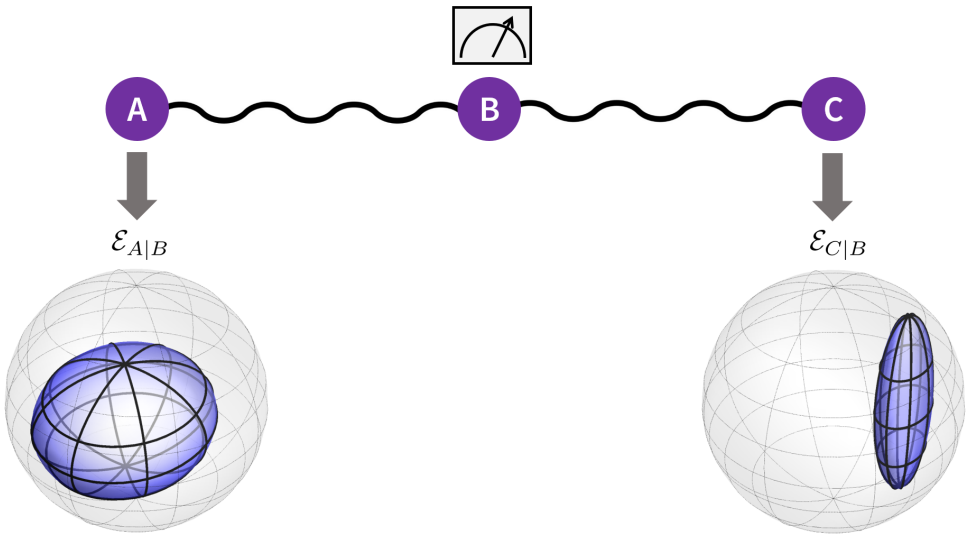

Figure 5.1: Monogamy scenario where Bob is the steering party. Bob performs a measurement to steer Alice and Charlie, with corresponding steering ellipsoids $\mathcal{E}_{A|B}$ and $\mathcal{E}_{C|B}$.

which gives $\gamma_b^2(1-c_B) = \gamma_a^2(1-c_A)$. For any two-qubit state, the volumes of $\mathcal{E}_A$ and $\mathcal{E}_B$ are related by $\gamma_b^4 V_B = \gamma_a^4 V_A$ [11], so $V_B = \frac{4\pi}{3}(1-c_B)^2$. This means that $V_B = V_{c_B}^{\max}$ and so $\mathcal{E}_B$ is also maximal volume for the centre $\boldsymbol{c}_B$, i.e. $\mathcal{E}_B = \mathcal{E}_{c_B}^{\max}$. ■

Now consider the scenario shown in Figure 5.1. Alice, Bob and Charlie share a pure three-qubit state, and Bob can perform a measurement to steer Alice and Charlie. Let $\mathcal{E}_{A|B}$, with volume $V_{A|B}$ and centre $\boldsymbol{c}_{A|B}$, be the ellipsoid for Bob steering Alice, and similarly for the ellipsoid $\mathcal{E}_{C|B}$ with Bob steering Charlie. We show that Bob can simultaneously steer Alice and Charlie to maximal volume ellipsoids.

Lemma 5.5: Tripartite mutually maximal volume steering

When Alice, Bob and Charlie share a pure three-qubit state and $\mathcal{E}_{A|B}$ is maximal volume for its centre $\boldsymbol{c}_{A|B}$, the ellipsoid $\mathcal{E}_{C|B}$ is also maximal volume for its centre $\boldsymbol{c}_{C|B}$, and the centres obey $c_{A|B} + c_{C|B} = 1$.

Proof. Consider first the case that Alice and Bob's state is the canonical $\rho_{AB} = \widetilde{\rho}_{c_{A|B}}^{\max}$ given by (4.13), which means that $\mathcal{E}_{A|B} = \mathcal{E}_{c_{A|B}}^{\max}$ by construction. Call the pure three-qubit state $|\widetilde{\phi}_{ABC}\rangle$, so that $\rho_{AB} = \mathrm{tr}_C |\widetilde{\phi}_{ABC}\rangle\langle\widetilde{\phi}_{ABC}|$, with Bob's local state being maximally mixed. Performing a purification over Charlie's qubit, we obtain the rank-

2 state

$$|\widetilde{\phi}_{ABC}\rangle = \frac{1}{\sqrt{2}}\left(\sqrt{c_{A|B}}\,|001\rangle + |010\rangle + \sqrt{1-c_{A|B}}\,|100\rangle\right).$$

Computing $\rho_{BC} = \mathrm{tr}_A\,|\widetilde{\phi}_{ABC}\rangle\langle\widetilde{\phi}_{ABC}|$, we see that the state ρ_{BC} corresponds to a maximal volume $\mathcal{E}_{C|B} = \mathcal{E}^{\max}_{c_{C|B}}$ with centre $c_{C|B} = 1 - c_{A|B}$.

Transforming out of the canonical frame, as in (5.4), we perform the local filtering operation

$$|\widetilde{\phi}_{ABC}\rangle \mapsto |\phi_{ABC}\rangle = (\mathbb{1}\otimes\sqrt{2\rho_B}\otimes\mathbb{1})\,|\widetilde{\phi}_{ABC}\rangle\,.$$

This 'boosts' Bob's Bloch vector to an arbitrary $\boldsymbol{b}$, with $\rho_B = \frac{1}{2}(\mathbb{1} + \boldsymbol{b}\cdot\boldsymbol{\sigma})$. The local filtering operation leaves both $\mathcal{E}_{A|B}$ and $\mathcal{E}_{C|B}$ invariant. Therefore the relationship $c_{A|B} + c_{C|B} = 1$ must also hold for the general case that $\rho_{AB} = \rho^{\max}_{c_{A|B}}$ with any $\boldsymbol{b}$. ■

5.2.2 MONOGAMY RELATIONS

Everything is now in place to derive a monogamy relation for steering ellipsoid volume. Referring to Figure 5.1, we are interested in the trade-off relationship between $V_{A|B}$ and $V_{C|B}$: does Bob's steering of Alice limit the extent to which he can steer Charlie? The following theorem quantifies precisely this trade-off.[1]

Theorem 5.6: Monogamy of steering

When Alice, Bob and Charlie share a pure three-qubit state, the ellipsoids steered by Bob obey the monogamy of steering relation

$$\sqrt{V_{A|B}} + \sqrt{V_{C|B}} \leq \sqrt{\frac{4\pi}{3}}.$$

The bound is saturated when $\mathcal{E}_{A|B}$ and $\mathcal{E}_{C|B}$ are maximal volume.

Proof. Alice, Bob and Charlie hold the pure three-qubit state $|\phi_{ABC}\rangle$. The canonical transformation $|\phi_{ABC}\rangle \mapsto |\widetilde{\phi}_{ABC}\rangle$ leaves $\mathcal{E}_{A|B}$ and $\mathcal{E}_{C|B}$ invariant. We therefore need consider only canonical states for which $\widetilde{\boldsymbol{b}} = \boldsymbol{0}$. (When ρ_B is singular and the canonical transformation cannot be performed, no steering by Bob is possible; we then have $V_{A|B} = V_{C|B} = 0$ so that the bound holds trivially.)

[1] Note that the original proof of this theorem, published in Ref. [1], is incorrect; the corrected version presented here appears in Ref. [62]. The author is very grateful to Michael Hall for pointing out the error and assisting with the correction.

We begin by showing that $V_{A|B} = \frac{4\pi}{3} c_{C|B}^2$. Denote the eigenvalues of $\widetilde{\rho}_{AB} = \mathrm{tr}_C \left|\widetilde{\phi}_{ABC}\right\rangle \left\langle\widetilde{\phi}_{ABC}\right|$ as $\{\lambda_i\}$. For a canonical state Charlie's Bloch vector coincides with $\boldsymbol{c}_{C|B}$, and so

$$\widetilde{\rho}_C = \mathrm{tr}_{AB} \left|\widetilde{\phi}_{ABC}\right\rangle \left\langle\widetilde{\phi}_{ABC}\right| = \tfrac{1}{2}(\mathbb{1} + \boldsymbol{c}_{C|B} \cdot \boldsymbol{\sigma}).$$

By Schmidt decomposition of $|\widetilde{\phi}_{ABC}\rangle$ we therefore have

$$\{\lambda_i\} = \left\{\tfrac{1}{2}(1 + c_{C|B}), \tfrac{1}{2}(1 - c_{C|B}), 0, 0\right\}.$$

From the expression for $V_{A|B}$ given in Ref. [11] we obtain $V_{A|B} = \frac{64\pi}{3} |\det \widetilde{\rho}_{AB}^{\mathsf{T}_A}|$.

Define the reduction map [63, 64] as $\Lambda(X) := \mathbb{1}\mathrm{tr}X - X$. Following Ref. [50] we note that

$$\begin{aligned}
\det \widetilde{\rho}_{AB}^{\mathsf{T}_A} &= \det\left[(\sigma_y \otimes \mathbb{1})\, \widetilde{\rho}_{AB}^{\mathsf{T}_A} (\sigma_y \otimes \mathbb{1})\right] \\
&= \det\left[(\Lambda \otimes \mathbb{1})\, \widetilde{\rho}_{AB}\right] \\
&= \det\left[\tfrac{1}{2}\mathbb{1} \otimes \mathbb{1} - \widetilde{\rho}_{AB}\right],
\end{aligned}$$

where we have used the fact that Bob's local state is maximally mixed, $\mathrm{tr}_A\, \widetilde{\rho}_{AB} = \frac{1}{2}\mathbb{1}$. Since the eigenvalues of $\frac{1}{2}\mathbb{1} \otimes \mathbb{1} - \widetilde{\rho}_{AB}$ are $\left\{\frac{1}{2} - \lambda_i\right\}$, we obtain

$$\begin{aligned}
\det \widetilde{\rho}_{AB}^{\mathsf{T}_A} &= \prod_{i=1}^{4} \left(\tfrac{1}{2} - \lambda_i\right) \\
&= \left(-\tfrac{1}{2} c_{C|B}\right) \left(\tfrac{1}{2} c_{C|B}\right) \left(\tfrac{1}{2}\right) \left(\tfrac{1}{2}\right) \\
&= -\tfrac{1}{16} c_{C|B}^2.
\end{aligned}$$

Hence $V_{A|B} = \frac{64\pi}{3} |\det \widetilde{\rho}_{AB}^{\mathsf{T}_A}| = \frac{4\pi}{3} c_{C|B}^2$.

From Theorem 4.1 we have $V_{C|B} \leq V_{c_{C|B}}^{\max} = \frac{4\pi}{3} \left(1 - c_{C|B}\right)^2$. This allows us to complete the proof of the bound:

$$\sqrt{V_{A|B}} + \sqrt{V_{C|B}} \leq \sqrt{\frac{4\pi}{3}} c_{C|B} + \sqrt{\frac{4\pi}{3}} \left(1 - c_{C|B}\right) = \sqrt{\frac{4\pi}{3}}.$$

■

The significance of $\sqrt{\frac{4\pi}{3}}$ in this bound is of course directly inherited from the fact that the volume of the entire Bloch ball is $\frac{4\pi}{3}$.

We can also formulate a monogamy relation for the 'inverse' scenario depicted in Figure 5.2, in which Alice and Charlie can perform local measurements to steer Bob. Labelling the corresponding steering ellipsoids $\mathcal{E}_{B|A}$ and $\mathcal{E}_{B|C}$ respectively, it is straightforward to derive a bound for the volumes $V_{B|A}$ and $V_{B|C}$.

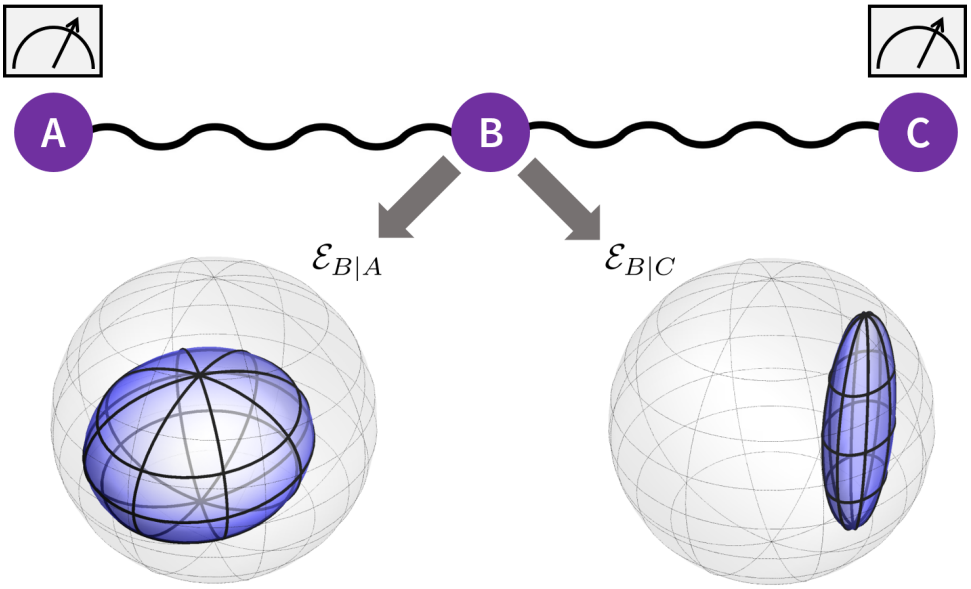

Figure 5.2: Monogamy scenario where Bob is the steered party. Alice and Charlie perform measurements to steer Bob, with corresponding steering ellipsoids $\mathcal{E}_{B|A}$ and $\mathcal{E}_{B|C}$.

Corollary 5.7: Monogamy of steering (inverse scenario)

When Alice, Bob and Charlie share a pure three-qubit state, the ellipsoids steered by Alice and Charlie obey the monogamy of steering relation

$$\gamma_a^{-2}\sqrt{V_{B|A}} + \gamma_c^{-2}\sqrt{V_{B|C}} \leq \gamma_b^{-2}\sqrt{\frac{4\pi}{3}},$$

where γ_i gives the Lorentz factor for each party. The bound is saturated when $\mathcal{E}_{A|B}$ and $\mathcal{E}_{C|B}$ are maximal volume.

Proof. The bound follows immediately from Theorem 5.6 and the relationships

$$\gamma_b^4 V_{B|A} = \gamma_a^4 V_{A|B},$$
$$\gamma_b^4 V_{B|C} = \gamma_c^4 V_{C|B},$$

which apply to any two-qubit state [11]. The bound is saturated for maximal volume $\mathcal{E}_{B|A}$ and $\mathcal{E}_{B|C}$ owing to Lemma 5.4, since the bound for the scenario in which Bob is the steering party is saturated by maximal volume $\mathcal{E}_{A|B}$ and $\mathcal{E}_{C|B}$. ■

The monogamy relations given in Theorem 5.6 and Corollary 5.7 are remarkably elegant; it was not at all obvious that there should be such simple bounds for ellipsoid volume. The simplicity of the result is a consequence of the mutuality of maximal volume steering. If we have $\mathcal{E}_{A|B} = \mathcal{E}^{\max}_{c_{A|B}}$ then we must also have $\mathcal{E}_{B|A} = \mathcal{E}^{\max}_{c_{B|A}}$, $\mathcal{E}_{C|B} = \mathcal{E}^{\max}_{c_{C|B}}$ and $\mathcal{E}_{B|C} = \mathcal{E}^{\max}_{c_{B|C}}$, i.e. all

of $\mathcal{E}_{A|B}$, $\mathcal{E}_{B|A}$, $\mathcal{E}_{C|B}$ and $\mathcal{E}_{B|C}$ are simultaneously maximal volume for their respective centres.

The monogamy of steering can easily be rephrased in terms of obesity. Although Alice's and Bob's steering ellipsoid volumes are in general different, obesity is a party-independent measure. When expressed using obesity, the two steering scenarios therefore give the same bound:

$$\Omega^2(\rho_{AB}) + \Omega^2(\rho_{BC}) \leq \gamma_b^{-2}. \tag{5.5}$$

We now show that the CKW inequality for monogamy of concurrence [60] follows as an immediate corollary of the monogamy of steering. The steering ellipsoid thus provides a very novel and more geometrically intuitive derivation of this classic result in quantum information theory.

Corollary 5.8: Monogamy of concurrence

When Alice, Bob and Charlie share a pure three-qubit state, the squared concurrences obey the CKW inequality

$$C^2(\rho_{AB}) + C^2(\rho_{BC}) \leq 4 \det \rho_B.$$

Proof. Note that $\gamma_b^{-2} = 4 \det \rho_B$. The result then follows immediately from (5.5) and Theorem 5.2, which gave $C(\rho) \leq \Omega(\rho)$ for any two-qubit state ρ. ■

Finally, we note that the tangle of a three-qubit state may be written as [60]

$$\tau_{ABC} = \gamma_b^{-2} - C^2(\rho_{AB}) - C^2(\rho_{BC}). \tag{5.6}$$

When there is maximal steering, so that the bounds in Theorems 5.6 and 5.8 are saturated, we have $\tau_{ABC} = 0$. The corresponding three-qubit state belongs to the class of W states [39] (assuming that we have genuine tripartite entanglement). The W state itself,

$$|W\rangle = \frac{1}{\sqrt{3}}(|001\rangle + |010\rangle + |001\rangle), \tag{5.7}$$

corresponds to the case that $\boldsymbol{c}_{A|B} = \boldsymbol{c}_{B|A} = \boldsymbol{c}_{C|B} = \boldsymbol{c}_{B|C} = (0, 0, \frac{1}{2})$.

SUMMARY AND DISCUSSION OF CHAPTER 5

In this chapter we have provided a definition of obesity as a measure of two-qubit correlation. Crucially, we found that the maximally obese states $\widetilde{\rho}_c^{\max}$ maximise concurrence for a fixed ellipsoid centre (Theorem 5.3). In the following chapter we shall see that these states also maximise several other measures of quantum correlation.

Our most important result quantifies the extent to which Bob's steering of Alice and Charlie must be monogamous. This is one of the key results of the thesis, which we highlight again below.

Monogamy of steering ellipsoid volume

When Alice, Bob and Charlie share a pure three-qubit state, the volume of the ellipsoids steered by Bob obey the inequality

$$\sqrt{V_{A|B}} + \sqrt{V_{C|B}} \leq \sqrt{\frac{4\pi}{3}}.$$

As well as providing a novel route to the CKW inequality for concurrence monogamy, this result is of considerable interest in its own right. Recent work in Ref. [6] has extended the investigation of monogamy of steering ellipsoid volume. In particular, monogamy results are established for the case of mixed three-qubit states and further multi-qubit scenarios.[1] Furthermore, Ref. [6] demonstrates the robustness of the monogamy of steering under local noise and explores further the connection to the classification of three-qubit states that we alluded to above in our discussion of the W state.

Lastly, we note that the monogamy of steering may have an application in the quantum marginals problem [65]. By using steering ellipsoid volume monogamy to place bounds on the consistency of overlapping quantum marginals, we can find conditions that are stronger than the well-known ones obtained from the CKW inequality.

[1] In fact, it is shown that the relationship in terms of $\sqrt{V}$ that we found for pure three-qubit does not hold in general for a mixed state; instead, one can establish a weaker bound involving terms of the form $V^{2/3}$.

CHAPTER 6

CORRELATIONS OF MAXIMALLY OBESE STATES

In this chapter we uncover some remarkable properties of the maximally obese states introduced in Section 4.4. Such states were originally presented as the canonical ones corresponding to the maximum volume ellipsoids $\mathcal{E}_{\boldsymbol{c}}^{\max}$. We have already seen that, in addition to this geometric significance, $\widetilde{\rho}_{\boldsymbol{c}}^{\max}$ is the one that maximises concurrence for a given ellipsoid centre $\boldsymbol{c}$. Here we find that $\widetilde{\rho}_{\boldsymbol{c}}^{\max}$ maximises three more measures of quantum correlation – CHSH violation, fully entangled fraction, and negativity – over the set of all canonical two-qubit states with some fixed $\boldsymbol{c}$.

Chapter 5 emphasised the importance of steering ellipsoid volume, $V = \frac{4\pi}{3} s_1 s_2 s_3$, which was found to relate intimately to the concurrence of a two-qubit state. However, volume is one of many measures for the 'size' of an ellipsoid. Here we will find that other measures of ellipsoid size, such as the sum of the semiaxes $s_1 + s_2 + s_3$, can also be interpreted as expressions of quantum correlation. Furthermore, we find that the maximally obese state has geometric properties that give it maximal values for these different correlation measures. In turn, this makes maximally obese states optimal for certain quantum information tasks.

In addition to showing that maximally obese states maximise several measures of quantum correlation, we prove that any maximally obese state must be either CHSH nonlocal or symmetrically extendible. Finally, we place necessary bounds on $\boldsymbol{c}$ for a general two-qubit state (i.e. one without any restriction on Bob's marginal) to be CHSH violating or useful for quantum teleportation.

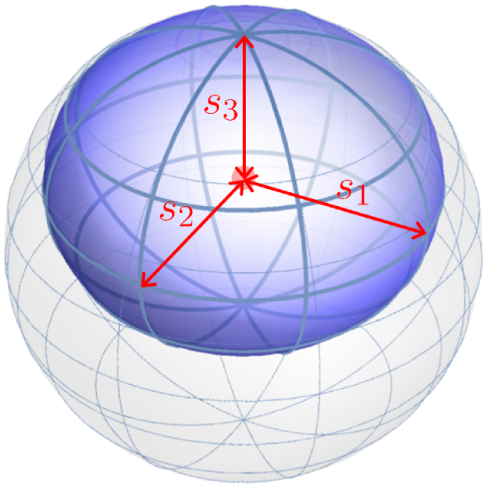

Figure 6.1: An example $\mathcal{E}_c^{\max}$ with $c = \frac{1}{3}$. $\mathcal{E}_c^{\max}$ has centre $\boldsymbol{c} = (0, 0, c)$ and semiaxes $s_1 = s_2 = \sqrt{1-c}$, $s_3 = 1 - c$.

6.1 CANONICAL AND MAXIMALLY OBESE STATES: A REMINDER

For convenience, we begin by recalling some properties of canonical states $\widetilde{\rho}$ and maximally obese states $\widetilde{\rho}_c^{\max}$. A canonical state is one for which Bob's marginal is maximally mixed:

$$\widetilde{\rho} = \frac{1}{4}(\mathbb{1} \otimes \mathbb{1} + \boldsymbol{c} \cdot \boldsymbol{\sigma} \otimes \mathbb{1} + \sum_{i,j=1}^{3} \widetilde{T}_{ij}\, \sigma_i \otimes \sigma_j). \tag{6.1}$$

For such a state, Alice's Bloch vector coincides with the ellipsoid centre $\boldsymbol{c}$. The ellipsoid matrix of a general two-qubit state ρ is defined using its canonical state by $Q = \widetilde{T}\widetilde{T}^{\intercal}$. The ellipsoid semiaxes are therefore given by the singular values of $\widetilde{T}$, which we denote s_i.[1] Without loss of generality we will say that the semiaxes are ordered such that $s_1 \geq s_2 \geq s_3$.

A maximally obese state is given by

$$\widetilde{\rho}_c^{\max} = \left(1 - \frac{c}{2}\right) |\psi_c\rangle \langle\psi_c| + \frac{c}{2} |00\rangle \langle 00|\,, \tag{6.2}$$

where $|\psi_c\rangle := \frac{1}{\sqrt{2-c}} \left(|01\rangle + \sqrt{1-c}\,|10\rangle\right)$. The corresponding steering ellipsoid $\mathcal{E}_c^{\max}$ has major semiaxes $s_1 = s_2 = \sqrt{1-c}$ and minor semiaxis $s_3 = 1 - c$ (see Figure 6.1). With the exception of $c = 1$, the maximally obese states are entangled and hence have chirality $\chi = -1$.

6.2 CORRELATIONS OF CANONICAL AND MAXIMALLY OBESE STATES

We now consider a number of quantum correlation measures and properties: CHSH nonlocality, symmetric extendibility, fully entangled fraction, concurrence and negativity. We consider how the measures can be bounded by Alice's Bloch vector $\boldsymbol{c}$ for canonical states and demon-

[1] Recall that the *signed* singular values are given by t_i; the singular values are $s_i = |t_i|$.

strate the special role played by maximally obese states in saturating these bounds.

6.2.1 CHSH NONLOCALITY AND SYMMETRIC EXTENDIBILITY

Consider the Clauser-Horne-Shimony-Holt (CHSH) scenario [66] with Alice and Bob sharing a canonical two-qubit state $\widetilde{\rho}$. Alice can measure her qubit in one of the two directions $\boldsymbol{\alpha}$ or $\boldsymbol{\alpha}'$, and Bob can measure his qubit in $\boldsymbol{\beta}$ or $\boldsymbol{\beta}'$. We define the operator

$$B := \boldsymbol{\alpha}\cdot\boldsymbol{\sigma}\otimes(\boldsymbol{\beta}+\boldsymbol{\beta}')\cdot\boldsymbol{\sigma} + \boldsymbol{\alpha}'\cdot\boldsymbol{\sigma}\otimes(\boldsymbol{\beta}-\boldsymbol{\beta}')\cdot\boldsymbol{\sigma}. \tag{6.3}$$

The maximal CHSH violation is a measure of Bell nonlocality given by

$$\beta(\widetilde{\rho}) = \max_{B} |\mathrm{tr}(\widetilde{\rho}\, B)|\,, \tag{6.4}$$

where the maximisation is performed over all directions $\boldsymbol{\alpha}, \boldsymbol{\alpha}', \boldsymbol{\beta}, \boldsymbol{\beta}'$. This gives [67]

$$\beta(\widetilde{\rho}) = 2\sqrt{s_1^2 + s_2^2}, \tag{6.5}$$

where s_1 and s_2 are the two largest singular values of $\widetilde{T}$.

In the steering ellipsoid picture, the entanglement of a state depends on the centre vector $\boldsymbol{c}$, the size of $\mathcal{E}$ and its skew $\boldsymbol{c}^{\intercal}Q\boldsymbol{c}$ [11]. In contrast to this, the CHSH nonlocality of a canonical state has a remarkably simple geometric interpretation: it depends on only the two longest semiaxes of $\mathcal{E}$ and not on the position or orientation of $\mathcal{E}$ inside the Bloch ball. We now see that for canonical states with some fixed ellipsoid centre, it is the maximally obese state that maximises CHSH nonlocality.

Theorem 6.1: Maximally obese states maximise CHSH nonlocality
From the set of all canonical states with a given $\boldsymbol{c}$, the most CHSH nonlocal state is the maximally obese state $\widetilde{\rho}_c^{\max}$.

Proof. According to (6.5), we need to bound $s_1^2 + s_2^2$. The most CHSH nonlocal state will be entangled and so has $\chi = -1$. From the conditions for physicality given in Theorem 3.3 we have

$$s_1^2 + s_2^2 \leq 1 - c^2 + 2s_1s_2s_3 - s_3^2.$$

As described in Section 4.1.2 we can use the Karush-Kuhn-Tucker conditions to show that the maximal volume $\mathcal{E}_c^{\max}$ also maximises $2s_1s_2s_3 - s_3^2$ for a given $\boldsymbol{c} = (0,0,c)$. This $\mathcal{E}_c^{\max}$ has $s_1 = s_2 = \sqrt{1-c}$ and $s_3 = 1-c$. We therefore see that $2s_1s_2s_3 - s_3^2 \leq$

$(1-c)^2$, so

$$s_1^2 + s_2^2 \leq 1 - c^2 + (1-c)^2 = 2(1-c).$$

This gives the bound $\beta(\widetilde{\rho}) \leq 2\sqrt{2(1-c)}$, which is met by $\widetilde{\rho}_c^{\max}$. ■

Let us also consider the symmetric extendibility of a maximally obese state. A bipartite quantum state ρ_{AB} is *symmetrically extendible* with respect to Alice if there exists a tripartite state $\rho_{AA'B}$ for which $\mathrm{tr}_A \rho_{AA'B} = \mathrm{tr}_{A'} \rho_{AA'B}$ [68]. Originally introduced as a test for entanglement [69] (symmetrically extendibility is a necessary condition for separability), symmetric extendibility has a number of operational interpretations. For example, a symmetrically extendible state cannot be used for one-way entanglement distillation [70] or one-way secret key distillation [71].

Some previous work has studied the relationship between symmetric extendibility and Bell nonlocality; in particular, Ref. [72] shows that a two-qubit state cannot be both symmetrically extendible and CHSH nonlocal. In general there exist (necessarily entangled) two-qubit states that are neither symmetrically extendible nor CHSH nonlocal. However, we observe that a maximally obese state must possess one of these properties.

Corollary 6.2: Maximally obese states are either symmetrically extendible or CHSH nonlocal

The family of maximally obese states is partitioned into states that are symmetrically extendible and states that are CHSH nonlocal. $\widetilde{\rho}_c^{\max}$ is symmetrically extendible for $\frac{1}{2} \leq c \leq 1$ and CHSH nonlocal for $0 \leq c < \frac{1}{2}$.

Proof. The necessary and sufficient condition for a two-qubit state ρ_{AB} to be symmetrically extendible with respect to Alice is $\mathrm{tr}\,\rho_A^2 \geq \mathrm{tr}\,\rho_{AB}^2 - 4\sqrt{\det \rho_{AB}}$ [68]. For $\rho_{AB} = \widetilde{\rho}_c^{\max}$, as given in Eq. (4.13), we find that

$$\mathrm{tr}(\rho_A^2) = \tfrac{1}{2}(1+c^2),$$
$$\mathrm{tr}\,\rho_{AB}^2 = \tfrac{1}{2}(2-2c+c^2),$$
$$\det \rho_{AB} = 0.$$

$\widetilde{\rho}_c^{\max}$ is therefore symmetrically extendible if and only if $\frac{1}{2}(1+c^2) \geq \frac{1}{2}(2-2c+c^2)$, which gives $c \geq \frac{1}{2}$.

The necessary and sufficient condition for a state ρ_{AB} to be CHSH nonlocal is $\beta(\rho_{AB}) > 2$. From Theorem 6.1, we have that $\beta(\widetilde{\rho}_c^{\max}) = 2\sqrt{2(1-c)}$, and hence $\beta(\widetilde{\rho}_c^{\max}) > 2$ if and only if $c < 1/2$. ■

6.2.2 FULLY ENTANGLED FRACTION

The fully entangled fraction of a bipartite state ρ is a measure of correlation given by [73]

$$f(\rho) = \max_{|\phi\rangle} \langle\phi| \rho |\phi\rangle , \tag{6.6}$$

where the maximum is taken over all maximally entangled states $|\phi\rangle$. For a canonical state $\widetilde{\rho}$, the fully entangled fraction can be computed as [74]

$$f(\widetilde{\rho}) = \tfrac{1}{4}(1 + s_1 + s_2 - \chi s_3), \tag{6.7}$$

where we recall the ordering $s_1 \geq s_2 \geq s_3$. An entangled state must have $\chi = -1$; in this case $f(\widetilde{\rho})$ depends only on the sum of the steering ellipsoid semiaxes, $\sum_i s_i = \operatorname{tr}\sqrt{Q}$. As with CHSH nonlocality, the fully entangled fraction of a canonical state depends only on the size of $\mathcal{E}$ and not on its position or orientation. Like CHSH nonlocality, the fully entangled fraction is maximised by $\widetilde{\rho}_c^{\max}$.

Theorem 6.3: Maximally obese states maximise fully entangled fraction
From the set of all canonical states with a given $\boldsymbol{c}$, the state with the highest fully entangled fraction is the maximally obese $\widetilde{\rho}_c^{\max}$.

Proof. According to (6.7), we need to bound $s_1 + s_2 - \chi s_3$. Since χ takes a value -1, 1 or 0, we have $s_1 + s_2 - \chi s_3 \leq s_1 + s_2 + s_3$. As s_3 is the minor axis of a physical $\mathcal{E}$, we must have $s_3 \leq 1 - c$ in order for $\mathcal{E}$ to lie inside the Bloch ball, and so

$$s_1 + s_2 + s_3 \leq s_1 + s_2 + 1 - c.$$

The Cauchy-Schwarz inequality allows us to place a bound on the 1-norm of any n-dimensional vector $\boldsymbol{v}$ using the 2-norm: $\|v\|_1 \leq \sqrt{n}\|v\|_2$ [75]. Applying this to $\boldsymbol{v} = (s_1, s_2)$, we have $s_1 + s_2 \leq \sqrt{2(s_1^2 + s_2^2)}$. From Theorem 6.1, $s_1^2 + s_2^2 \leq 2(1-c)$. We therefore see that

$$s_1 + s_2 + s_3 \leq 2\sqrt{1-c} + 1 - c.$$

This gives the bound $f(\widetilde{\rho}) \leq \frac{1}{4}(1 + \sqrt{1-c})^2$, which is met by $\widetilde{\rho}_c^{\max}$. ■

Fully entangled fraction relates directly to the fidelity of quantum teleportation [76]: when Alice and Bob share a two-qubit state ρ to use as a resource for quantum teleportation, the average fidelity achieved is $F(\rho) = \frac{1}{3}(2f(\rho) + 1)$. Since $F(\rho)$ increases monotonically with $f(\rho)$, Theorem 6.3 shows that $\widetilde{\rho}_c^{\max}$ is the optimal state to use for teleportation over all states that have Bob's marginal maximally mixed and Alice's Bloch vector equal to $\boldsymbol{c}$.

We can also consider this result in the Choi-isomorphic setting, using the property presented in Section 4.4 that $\widetilde{\rho}_c^{\max}$ is isomorphic to the amplitude-damping channel Φ_{AD}, i.e. $\widetilde{\rho}_c^{\max} = (\Phi_{\mathrm{AD}} \otimes \mathbb{1}) |\psi^+\rangle \langle\psi^+|$. Let us say that Alice prepares a Bell state and sends one qubit to Bob through a trace-preserving quantum channel Φ, intending the resulting shared state to act as a resource for teleportation. From the set of all non-unital maps Φ for which $\Phi(\frac{1}{2}\mathbb{1}) = \frac{1}{2}(\mathbb{1} + \boldsymbol{c}\cdot\boldsymbol{\sigma})$ and $\boldsymbol{c} = (0, 0, c)$, the one that will maximise teleportation fidelity is the amplitude-damping channel Φ_{AD}.

These results complement previous studies of teleportation, which have shown that passing a resource state through a dissipative channel can enhance the average teleportation fidelity [74] as well as identifying the filtering operations that achieve optimal fidelity for a given resource state [77, 78].

6.2.3 CONCURRENCE AND NEGATIVITY

We now consider two entanglement monotones, both of which range from 0 for a separable state to 1 for a maximally entangled state. A method for computing the concurrence $C(\rho)$ of a two-qubit state ρ was explained in Section 5.1. Negativity provides another measure for entanglement, based on the Peres-Horodecki criterion [48, 49]. Let $\mu_{\min}$ be the smallest eigenvalue of the partially transposed state ρ^{T_B}; the negativity is then given by [79]

$$N(\rho) = \max(0, -2\mu_{\min}). \tag{6.8}$$

In Theorem 5.2 we bounded the concurrence of any two-qubit state in terms of the volume of its steering ellipsoid. This gave us the bound $C(\widetilde{\rho}) \leq \sqrt{1-c}$ for a canonical state $\widetilde{\rho}$. The bound is saturated by maximally obese states $\widetilde{\rho}_c^{\max}$. The above results on CHSH violation allow us to derive another result that is neither stronger nor weaker than this bound. Ref. [80] gives the inequality $2\sqrt{2}C(\widetilde{\rho}) \leq \beta(\widetilde{\rho})$. From (6.5) and the ordering $s_1 \geq s_2 \geq s_3$ we then obtain $C(\widetilde{\rho}) \leq s_1$. Although this bound is distinct from $C(\widetilde{\rho}) \leq \sqrt{1-c}$, it is also saturated by maximally obese states.

Numerical results show that the negativity of a canonical state is bounded as $N(\widetilde{\rho}) \leq s_3$. As discussed in Theorem 6.3 we have $s_3 \leq 1 - c$, and so $N(\widetilde{\rho}) \leq 1 - c$. Explicit computation of

$N(\widetilde{\rho}_c^{\max})$ shows that this bound is again saturated by maximally obese states.

We therefore see that in the steering ellipsoid picture, the concurrence of a canonical state is upper bounded by the length of the major semiaxis while the negativity is upper bounded by the length of the minor semiaxis.[1] For maximally obese states, these entanglement measures are in fact equal to the lengths of these semiaxes and can thus be directly obtained from a geometric visualisation of $\mathcal{E}_c^{\max}$. This again demonstrates the particular significance of maximally obese states in the steering ellipsoid representation.

As discussed in Section 4.4, maximally obese states form a special single-parameter class of the generalised Horodecki state (see, for example, Refs. [56–58]). Other classes of the generalised Horodecki state have been studied before and were seen to have certain extremal properties. For example, the Verstraete-Verschelde states [81] minimise the fully entangled fraction for a given concurrence and negativity, obeying the relationship $C = \frac{1}{2}(N + \sqrt{N(4+5N)})$. Our maximally obese states $\widetilde{\rho}_c^{\max}$ maximise concurrence for a given CHSH nonlocality and obey $C = \sqrt{N}$.

6.3 NONLOCALITY AND TELEPORTATION FOR GENERAL STATES

We now consider briefly how we might bound quantum correlation measures for a general two-qubit state ρ using the steering ellipsoid centre $\boldsymbol{c}$. Unlike concurrence, CHSH nonlocality and fully entangled fraction are measures that do not transform straightforwardly under local filtering operations. The bounds given in Theorems 6.1 and 6.3 for canonical states cannot therefore be used to analytically derive bounds for $\beta(\rho)$ and $f(\rho)$ for a general (i.e. not necessarily canonical) two-qubit state ρ. However, numerical investigations lead us to conjecture remarkably simple expressions for these bounds (see Figure 6.2).

Conjecture 6.4: CHSH nonlocality for a general two-qubit state
For any two-qubit state ρ with steering ellipsoid $\mathcal{E}$ centred at $\boldsymbol{c}$, the CHSH nonlocality is tightly bounded as $\beta(\rho) \leq \max[2\sqrt{2(1-c)}, 2]$.

This allows us to place a necessary bound on the steering ellipsoid for a general two-qubit state ρ to be CHSH violating: to violate the CHSH inequality we need $\beta(\rho) > 2$ and so $c < 1/2$. We therefore see that a two-qubit state whose $\mathcal{E}$ is centred too close to the surface of the Bloch

[1] As proven in Theorem 5.3, for any given steering ellipsoid $\mathcal{E}$, the state with highest concurrence is the canonical state. The concurrence of *any* two-qubit state is therefore upper bounded by the length of the major semiaxis.

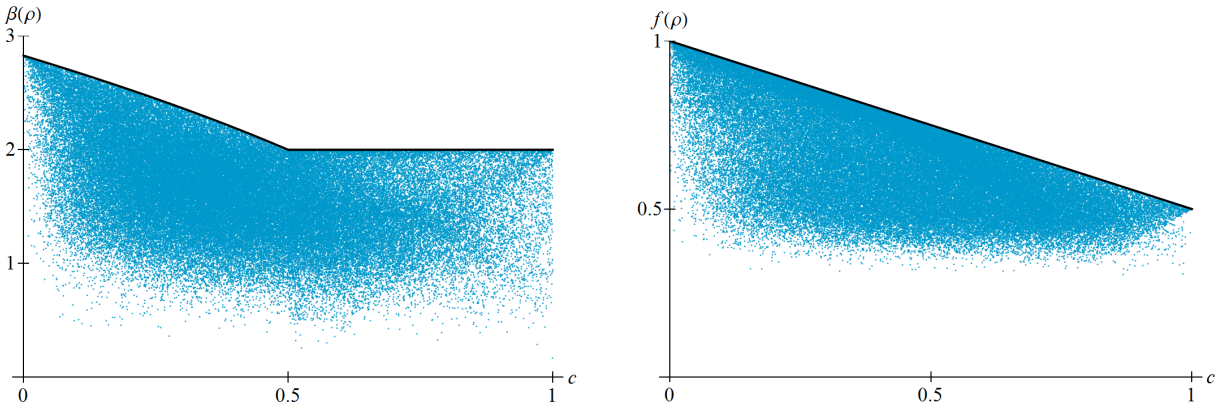

Figure 6.2: The numerical evidence for Conjecture 6.4 (left) and Conjecture 6.5 (right). Using 10^5 random two-qubit states ρ, we plot the CHSH nonlocality $\beta(\rho)$ and fully entangled fraction $f(\rho)$ against the magnitude of the steering ellipsoid centre. The conjectured bounds are shown as black lines.

ball cannot exhibit CHSH nonlocality.

Conjecture 6.5: Fully entangled fraction for a general two-qubit state

For any two-qubit state ρ with steering ellipsoid $\mathcal{E}$ centred at $\boldsymbol{c}$, the fully entangled fraction is tightly bounded as $f(\rho) \leq 1 - \frac{c}{2}$.

Recall that teleportation teleportation is directly related to the fully entangled fraction of the resource state as $F(\rho) = \frac{1}{3}(2f(\rho) + 1)$. Using only state estimation and classical communication, it is possible to achieve a teleportation fidelity of $\frac{2}{3}$ [76]. To beat this classical limit we require $f(\rho) > \frac{1}{2}$, and so we see that for all $c < 1$ there exists $\mathcal{E}$ describing a state that achieves truly quantum teleportation. An optimal universal cloning machine achieves a fidelity of $\frac{5}{6}$ [82, 83]. To beat this limit we require $f(\rho) > \frac{3}{4}$ and hence $c < \frac{1}{2}$, which is the same bound that we obtained as a necessary condition for $\mathcal{E}$ to be CHSH violating.

SUMMARY AND DISCUSSION OF CHAPTER 6

The results of this chapter place bounds on the quantum correlation of canonical states, i.e. states that have a single marginal maximally mixed. Canonical states are intermediate between the set of T states encountered in Lemma 5.1, which have both marginals maximally mixed, and general two-qubit states, which have unconstrained marginals. Algebraically, a T state is much simpler to work with than a general two-qubit state.[1] It is thus often possible to derive analytic results for T states that are inaccessible for general states – see, for example, Refs. [30, 43, 84, 85].

The set of canonical states, however, has not been investigated in such detail. Our work here gives important expressions for correlation measures in terms of the canonical state's non-vanishing marginal:

Bounds on quantum correlations for canonical states

A canonical state $\widetilde{\rho}$ is subject to the following bounds in terms of the non-vanishing Bloch vector $\boldsymbol{c}$:

$$C(\widetilde{\rho}) \leq \sqrt{1-c}, \qquad \text{(Theorem 5.2)}$$

$$\beta(\widetilde{\rho}) \leq 2\sqrt{2(1-c)}, \qquad \text{(Theorem 6.1)}$$

$$f(\widetilde{\rho}) \leq \tfrac{1}{4}(1+\sqrt{1-c})^2, \qquad \text{(Theorem 6.3)}$$

where C is concurrence, β is CHSH nonlocality and f is fully entangled fraction. In each case the bound is saturated by the maximally obese state $\widetilde{\rho}_c^{\max}$.

These results are significant both in the context of steering ellipsoids, where correlation measures for canonical states have particularly simple geometric interpretations, and for the general study of two-qubit states with a single mixed marginal.

Whether these results can be easily extended to higher dimensional quantum systems remains to be seen. In particular, what would be the analogous family of maximally obese states in higher dimensions, and what properties would these states have? It seems likely that the set of states Choi-isomorphic to higher dimensional amplitude-damping channels [86] will also have interesting features in terms of maximising quantum correlation.

[1] As a simple example, consider the task of finding the eigenvalues of ρ. We saw in Section 3.1 that this is in general a very non-trivial problem, but for the case of a T state, analytic expressions may easily be obtained. Thus one may derive a particularly simple set of necessary and sufficient conditions for $\rho \geq 0$ [30] (equivalently, consider the great simplification to the conditions for physicality given in Theorem 3.3 when one sets $\boldsymbol{c} = \boldsymbol{0}$).

CHAPTER 7

ENTANGLEMENT WITNESSES

So far we have investigated steering ellipsoids for two-qubit states. We now explore a point that was mentioned but not fully developed in Chapter 3: any two-qubit state can be represented by some $\mathcal{E}$, but not every $\mathcal{E}$ represents a valid state satisfying $\rho \geq 0$. What then is the meaning of an ellipsoid $\mathcal{E}$ that does not represent a quantum state? Previously we referred to these ellipsoids as 'unphysical'; in this chapter we will see that such an ellipsoid does in fact have a physical interpretation – not as a quantum state, but as an *entanglement witness*.

We will prove that an ellipsoid inside the Bloch ball $\mathcal{B}$ must represent a *block positive* operator B, i.e. one which achieves a positive expectation value over all separable states.[1] Using this, we take inspiration from the determinant criterion for separability given in Lemma 3.4 to derive a classification scheme based on the positivity of $\det B$ and $\det B^{\intercal_B}$. This gives a remarkably elegant physical interpretation to *all* ellipsoids $\mathcal{E} \subseteq \mathcal{B}$.

The previous chapters examined two-qubit states of particular significance in the steering ellipsoid picture; this chapter will examine two-qubit entanglement witnesses from a similar geometric perspective. We find that properties such as witness optimality are naturally manifest in this geometric representation and look at several important examples of two-qubit entanglement witnesses. Finally, we give a conjecture that relates the ellipsoid representation to the notion of optimality within a set of entanglement witnesses.

[1] A positive operator, on the other hand, must achieve a positive expectation value over *all* states, separable or entangled.

7.1 PRELIMINARIES

7.1.1 INTRODUCTION TO ENTANGLEMENT WITNESSES

Entanglement witnesses are an important approach to the characterisation, classification and detection of entanglement in a mixed quantum system [87]. An entanglement witness [88] is an operator that detects the presence of entanglement through the expectation value of an observable; any entangled state can be detected using an appropriate witness. Experimentally, entanglement witnesses provide a method for characterising a quantum state without needing full tomographic knowledge of the system [89]. Mathematically, the theory of entanglement witnesses gives a very nontrivial generalisation of positive semidefinite operators (for a recent review, see Ref. [90]).

As discussed in Chapter 3, for a system of two qubits the Peres-Horodecki criterion gives a simple necessary and sufficient condition for detecting entanglement. However, two-qubit entanglement witnesses are still of interest in a variety of scenarios such as secure quantum key distribution [91, 92], the investigation of Bell nonlocality [93], and the experimental characterisation of entanglement [94].

7.1.2 POSITIVITY AND BLOCK POSITIVITY

We review some basic definitions and set out the notation. Let R be a Hermitian operator acting on the finite-dimensional Hilbert space $\mathcal{H}$, i.e. $R \in \mathrm{L}(\mathcal{H})$. R is *positive semidefinite* ($R \geq 0$) when $\langle\psi| R |\psi\rangle \geq 0$ for all $|\psi\rangle \in \mathcal{H}$. To be a quantum state we also require that R has unit trace. R is *block positive* when $\langle\psi| R |\psi\rangle \geq 0$ for all product $|\psi\rangle = |\phi\rangle \otimes |\nu\rangle \in \mathcal{H}$. An entanglement witness is block positive but not positive semidefinite [88] and can without loss of generality be taken to have unit trace [95].[1]

As usual, we denote a state ρ. Similarly, we denote a Hermitian operator R, a block positive operator B, and an entanglement witness W. All of these will be unit trace operators acting on the two-qubit Hilbert space $\mathcal{H} = \mathbb{C}^2 \otimes \mathbb{C}^2$.

The most general unit trace Hermitian operator may be written in the Pauli basis as

$$R = \frac{1}{4}(\mathbb{1} \otimes \mathbb{1} + \boldsymbol{a} \cdot \boldsymbol{\sigma} \otimes \mathbb{1} + \mathbb{1} \otimes \boldsymbol{b} \cdot \boldsymbol{\sigma} + \sum_{i,j=1}^{3} T_{ij}\, \sigma_i \otimes \sigma_j), \tag{7.1}$$

where $\boldsymbol{a} = \mathrm{tr}(R\, \boldsymbol{\sigma} \otimes \mathbb{1})$, $\boldsymbol{b} = \mathrm{tr}(R\, \mathbb{1} \otimes \boldsymbol{\sigma})$ and $T_{ij} = \mathrm{tr}(R\, \sigma_i \otimes \sigma_j)$. When R is a state, $\boldsymbol{a}$ and $\boldsymbol{b}$ give the local Bloch vectors and T encodes correlations between the qubits held by Alice and Bob.

[1] Clearly there do not exist operators that are positive semidefinite but not block positive: block positivity is necessary but not sufficient for positivity.

The steering ellipsoid $\mathcal{E}$ then describes the set of Bloch vectors to which Alice can be steered given all local measurements by Bob.

When R is not a state, we can still define $\mathcal{E}$ using the same parameters $(\boldsymbol{c}, Q)$ given in Section 2.1.4. These give the centre and semiaxes of $\mathcal{E}$. However, for a general $R \not\geq 0$, this $\mathcal{E}$ no longer represents the set of steered states. Indeed, we are no longer even guaranteed that $\mathcal{E}$ will lie inside the Bloch ball.

7.1.3 CANONICAL TRANSFORMATION

When considering states, we found it useful to perform a local filtering operation to transform to a canonical frame. We will use the same transformation for our consideration of more general two-qubit operators. Recall the local filtering transformation given in (2.17), which we now apply to a general Hermitian operator R:

$$R \mapsto \widetilde{R} = \frac{(S_A \otimes S_B)\, R\, (S_A \otimes S_B)^\dagger}{\operatorname{tr}\left[(S_A \otimes S_B)\, R\, (S_A \otimes S_B)^\dagger\right]}, \tag{7.2}$$

with $S_A, S_B \in \mathrm{GL}(2, \mathbb{C})$.

We have seen that this local filtering operation preserves positivity (Lemma 3.1); we now prove that is also preserves block positivity.

Lemma 7.1: Local filtering preserves block positivity
For any $R \in \mathrm{L}(\mathbb{C}^2 \otimes \mathbb{C}^2)$, the local filtering operation (7.2) preserves block positivity: R is block positive if and only if $\widetilde{R}$ is.

Proof. R is block positive when $\langle\psi|\, R\, |\psi\rangle \geq 0$ for all $|\psi\rangle = |\phi\rangle \otimes |\nu\rangle \in \mathbb{C}^2 \otimes \mathbb{C}^2$. Any separable state can be decomposed as $\sigma = \sum_i p_i\, |\phi_i\rangle\langle\phi_i| \otimes |\nu_i\rangle\langle\nu_i|$ with $\sum_i p_i = 1$ and $p_i \geq 0$; it follows from this that block positivity of R is equivalent to $\operatorname{tr}(R\,\sigma) \geq 0$ for all separable σ.

Block positivity of the numerator of $\widetilde{R}$ is sufficient for block positivity of $\widetilde{R}$ since the denominator

$$\operatorname{tr}\left[(S_A \otimes S_B)\, R\, (S_A \otimes S_B)^\dagger\right] = \operatorname{tr}\left[R\, (S_A^\dagger S_A \otimes S_B^\dagger S_B)\right]$$

is positive for any block positive R (consider $\operatorname{tr}(R\,\sigma)$ with the unnormalised separable state $\sigma = S_A^\dagger S_A \otimes S_B^\dagger S_B$). Define $S := S_A \otimes S_B$, so that the numerator is $SRS^\dagger$. Then

$$\operatorname{tr}(SRS^\dagger\sigma) = \operatorname{tr}(RS^\dagger\sigma S) = \operatorname{tr}(R\bar{\sigma}), \tag{7.3}$$

where $\bar{\sigma} := S^\dagger\sigma S$. By Lemma 3.5, local filtering preserves separability, so that $\bar{\sigma}$ is

separable if and only if σ is. Hence $\mathrm{tr}(\widetilde{R}\,\sigma) \geq 0$ for all separable σ if and only if $\mathrm{tr}(R\,\bar{\sigma}) \geq 0$ for all separable $\bar{\sigma}$, i.e. $\widetilde{R}$ is block positive if and only if R is. ■

Thus positivity, block positivity and separability are all invariant under local filtering operations, and hence any categorisation of a Hermitian operator as a state, block positive operator or entanglement witness will be preserved. As with our study of two-qubit states, we can restrict much of our analysis to the set of canonical operators $\widetilde{R}$ which have $\widetilde{\boldsymbol{b}} = \mathbf{0}$. Such an operator is obtained through the local filtering operation (7.2) with $S_A = \mathbb{1}$ and $S_B = 1/\sqrt{\mathrm{tr}_A\, R}$ and may be written

$$\widetilde{R} = \frac{1}{4}(\mathbb{1}\otimes\mathbb{1} + \boldsymbol{c}\cdot\boldsymbol{\sigma}\otimes\mathbb{1} + \sum_{i,j=1}^{3} \widetilde{T}_{ij}\,\sigma_i\otimes\sigma_j). \tag{7.4}$$

As $\mathcal{E}$ is invariant under transformation to the canonical frame, in order to characterise any ellipsoid $\mathcal{E}$ describing a general two-qubit operator R, we need consider only the canonical operator $\widetilde{R}$. The ellipsoid $\mathcal{E}$ of such an operator has centre $\boldsymbol{c}$, ellipsoid matrix $Q = \widetilde{T}\widetilde{T}^{\intercal}$ and chirality $\chi = \mathrm{sign}(\det\widetilde{T})$. Recall that we may have $\chi = +1$ (right-handed), $\chi = -1$ (left-handed) or $\chi = 0$ (degenerate).

7.2 GEOMETRIC CHARACTERISATION OF TWO-QUBIT OPERATORS

7.2.1 BLOCK POSITIVITY

Although the ellipsoid $\mathcal{E}$ is defined for any Hermitian, unit trace two-qubit operator R, block positive operators have a particular geometric significance.

Theorem 7.2: Geometric interpretation of block positivity
R is block positive if and only if its corresponding ellipsoid $\mathcal{E}$ lies inside the Bloch ball $\mathcal{B}$, i.e. $\mathcal{E} \subseteq \mathcal{B}$.

Proof. Since $\mathcal{E}$ and block positivity of R are both invariant under the canonical transformation, it suffices to consider a canonical operator $\widetilde{R}$. $\widetilde{R}$ is block positive when $\langle\psi|\,\widetilde{R}\,|\psi\rangle \geq 0$ for all product $|\psi\rangle = |\phi\rangle\otimes|\nu\rangle$. Let $\boldsymbol{\phi} = \langle\phi|\,\boldsymbol{\sigma}\,|\phi\rangle$ and $\boldsymbol{\nu} = \langle\nu|\,\boldsymbol{\sigma}\,|\nu\rangle$ be the Bloch vectors, where we must have $|\boldsymbol{\phi}| = |\boldsymbol{\nu}| = 1$. We compute

$$\langle\psi|\,\widetilde{R}\,|\psi\rangle = \tfrac{1}{4}(1 + \boldsymbol{\phi}\cdot\boldsymbol{r}^{(\boldsymbol{\nu})}),$$

where $\boldsymbol{r}^{(\boldsymbol{\nu})}$ has components $r_i^{(\boldsymbol{\nu})} = c_i + \sum_j \widetilde{T}_{ij}\nu_j$. Since $|\boldsymbol{\nu}| = 1$, this describes the linear transformation of the unit ball $\mathcal{B}$; in fact, referring to Section 2.1.3, we see that our expression gives precisely $\mathcal{E}$. The vector $\boldsymbol{r}^{(\boldsymbol{\nu})}$ is therefore a point on the surface of $\mathcal{E}$, parametrised by $\boldsymbol{\nu}$.

So $\langle\psi|\,\widetilde{R}\,|\psi\rangle \geq 0$ for all $|\psi\rangle = |\phi\rangle \otimes |\nu\rangle$ if and only if $\boldsymbol{\phi}\cdot\boldsymbol{r}^{(\boldsymbol{\nu})} \geq -1$ for all $|\boldsymbol{\phi}| = |\boldsymbol{\nu}| = 1$. This inequality is satisfied if and only if $|\boldsymbol{r}^{(\boldsymbol{\nu})}| \leq 1$ for all $\boldsymbol{\nu}$, i.e. if and only if every point on $\mathcal{E}$ lies within $\mathcal{B}$. ■

It should be noted that determining whether a general $\mathcal{E}$ is contained within $\mathcal{B}$ is a difficult problem in Euclidean geometry [96]. In fact, given Theorem 7.2, the problem is clearly equivalent in difficulty to determining whether R is block positive. This is known to be a hard problem, and there is no straightforward test that gives necessary and sufficient conditions for block positivity even in this simplest case of a 4×4 matrix [97]. In the Choi-isomorphic setting, the question is equivalent to determining whether a single-qubit map is positive, which is again known to be a hard problem (see, for example, Refs. [98, 99]). However, often it will be plainly apparent whether $\mathcal{E}$ lies inside the Bloch ball from a visualisation, and hence it will be immediately possible to determine block positivity of R from the ellipsoid representation.

7.2.2 DETERMINANT CRITERIA FOR BLOCK POSITIVE OPERATORS

We now present a novel way of characterising a unit trace block positive operator B. This allows two-qubit states and entanglement witnesses to be distinguished based on the positivity of the determinant alone.

Lemma 7.3: Determinant criterion for states and entanglement witnesses
Let B be a two-qubit block positive operator. B is a state if and only if $\det B \geq 0$; otherwise B is an entanglement witness.

Proof. By definition B is a state when $B \geq 0$. Since B is block positive, it is an entanglement witness when $B \ngeq 0$. Clearly an operator $B \geq 0$ achieves $\det B \geq 0$. A two-qubit entanglement witness B must have exactly one negative and three positive eigenvalues [100] and hence $\det B < 0$. The condition $\det B \geq 0$ is therefore necessary and sufficient for $B \geq 0$. ■

Having classified block positive operators using the sign of $\det B$, we can now provide a further classification of states and entanglement witnesses by considering the sign of $\det B^{\intercal_B}$. The partially transposed operator $B^{\intercal_B}$ is block positive if and only if B is block positive.[1] In Lemma 3.4 we noted that a two-qubit state B is entangled if and only if $\det B^{\intercal_B} < 0$. Using Lemma 7.3, the positivity of $\det B$ and $\det B^{\intercal_B}$ can then be used to classify all block positive two-qubit operators. For convenience we label these Classes A, B, C and D.

Determinant classification of block positive operators

Any two-qubit block positive operator B can be placed into one of four classes according to the signs of $\det B$ and $\det B^{\intercal_B}$:

$$B \text{ and } B^{\intercal_B} \text{ are separable states} \iff \det B \geq 0 \text{ and } \det B^{\intercal_B} \geq 0, \quad \text{(Class A)}$$

$$\left.\begin{array}{r} B \text{ is an entangled state} \\ B^{\intercal_B} \text{ is an entanglement witness} \end{array}\right\} \iff \det B \geq 0 \text{ and } \det B^{\intercal_B} < 0, \quad \text{(Class B)}$$

$$\left.\begin{array}{r} B \text{ is an entanglement witness} \\ B^{\intercal_B} \text{ is an entangled state} \end{array}\right\} \iff \det B < 0 \text{ and } \det B^{\intercal_B} \geq 0, \quad \text{(Class C)}$$

$$B \text{ and } B^{\intercal_B} \text{ are entanglement witnesses} \iff \det B < 0 \text{ and } \det B^{\intercal_B} < 0. \quad \text{(Class D)}$$

Note that an operator B belonging to Class B is equivalent to the operator $B^{\intercal_B}$ belonging to Class C, and so the above classification essentially consists of three classes: operators that are separable states and remain so under partial transposition (Class A); operators that are entanglement witnesses and remain so under partial transposition (Class D); and operators that flip between entangled states and entanglement witnesses under partial transposition (Class B/C).

7.2.3 CLASSIFICATION OF BLOCK POSITIVE ELLIPSOIDS

Due to Theorem 7.2, any $\mathcal{E} \subseteq \mathcal{B}$ describes a block positive two-qubit operator B and can therefore be classified using the scheme presented above. Recall that the canonical transformation maintains positivity and block positivity. This means that for block positive B we have $\det B \geq 0 \Leftrightarrow \det \widetilde{B} \geq 0$ and $\det B^{\intercal_B} \geq 0 \Leftrightarrow \det \widetilde{B}^{\intercal_B} \geq 0$. Since expressions involving $\widetilde{B}$ can be written in terms of the ellipsoid centre $\boldsymbol{c}$, matrix Q and chirality χ, this allows us to characterise *any* block positive two-qubit operator using geometric features of $\mathcal{E}$.

[1] This follows from the identity $\operatorname{tr}(B^{\intercal_B}\sigma) = \operatorname{tr}(B\sigma^{\intercal_B})$ and the fact that the partial transpose of a separable state is also a separable state.

Expressions for $\det \widetilde{B}$ and $\det \widetilde{B}^{\intercal_B}$ in terms of the ellipsoids parameters were given in Theorems 3.3 and 3.6. Recall that partial transposition is equivalent to flipping the ellipsoid chirality ($\chi \mapsto -\chi$), and so these two expressions are in fact identical apart from the sign of one term:

$$\begin{aligned} \det \widetilde{B} \geq 0 &\iff c^4 - 2uc^2 + v - \chi w \geq 0, \\ \det \widetilde{B}^{\intercal_B} \geq 0 &\iff c^4 - 2uc^2 + v + \chi w \geq 0, \end{aligned} \tag{7.5}$$

where

$$\begin{aligned} u &:= 1 - \operatorname{tr} Q + 2\hat{\boldsymbol{c}}^{\intercal} Q \hat{\boldsymbol{c}}, \\ v &:= 1 + 2\operatorname{tr}(Q^2) - 2\operatorname{tr} Q - (\operatorname{tr} Q)^2, \\ w &:= 8\sqrt{\det Q}, \end{aligned} \tag{7.6}$$

with the unit vector $\hat{\boldsymbol{c}} = \boldsymbol{c}/c$.[1]

With this we can now classify any $\mathcal{E} \subseteq \mathcal{B}$ using simple expressions in terms of the ellipsoid parameters.

Theorem 7.4: Ellipsoid classification of block positive operators

A two-qubit block positive operator B can be classified according to the parameters of its corresponding $\mathcal{E}$ (the centre $\boldsymbol{c}$, matrix Q and chirality χ):

$$B \text{ and } B^{\intercal_B} \text{ are separable states} \iff c^4 - 2uc^2 + v - w \geq 0, \tag{Class A}$$

$$\left.\begin{array}{l} B \text{ is an entangled state} \\ B^{\intercal_B} \text{ is an entanglement witness} \end{array}\right\} \iff \begin{cases} c^4 - 2uc^2 + v - \chi w \geq 0 \\ c^4 - 2uc^2 + v + \chi w < 0, \end{cases} \tag{Class B}$$

$$\left.\begin{array}{l} B \text{ is an entanglement witness} \\ B^{\intercal_B} \text{ is an entangled state} \end{array}\right\} \iff \begin{cases} c^4 - 2uc^2 + v - \chi w < 0 \\ c^4 - 2uc^2 + v + \chi w \geq 0, \end{cases} \tag{Class C}$$

$$B \text{ and } B^{\intercal_B} \text{ are entanglement witnesses} \iff c^4 - 2uc^2 + v + w < 0. \tag{Class D}$$

Proof. Since $\det B \geq 0 \Leftrightarrow \det \widetilde{B} \geq 0$ and $\det B^{\intercal_B} \geq 0 \Leftrightarrow \det \widetilde{B}^{\intercal_B} \geq 0$, we can directly convert the determinant-based classification scheme given above to canonical operators and use (7.5). The necessary and sufficient conditions for $\mathcal{E}$ to belong to Class A are therefore

$$c^4 - 2uc^2 + v - \chi w \geq 0,$$

[1] Compared to Theorem 3.3, we have separated out the term q as $q = v - \chi w$ to isolate the chirality dependence.

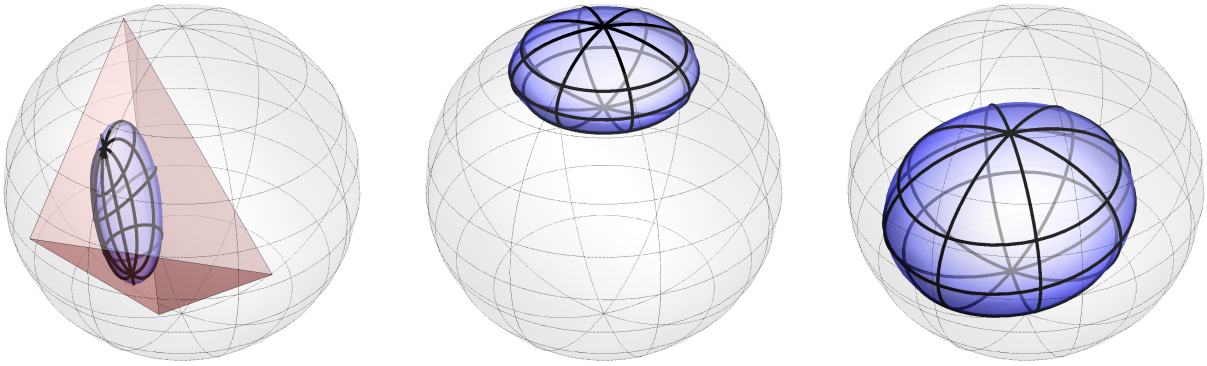

Figure 7.1: Visualisation of example $\mathcal{E}$ belonging to the different Classes given in Theorem 7.4. Left: $\mathcal{E}$ belongs to Class A if and only if it fits inside a tetrahedron inside $\mathcal{B}$. Both the left- and right-handed $\mathcal{E}$ are separable states. Centre: The same surface describes $\mathcal{E}$ belonging to Class B and $\mathcal{E}$ belonging to Class C. The left-handed $\mathcal{E}$ represents an entangled state; the right-handed $\mathcal{E}$ represents an entanglement witness. Right: $\mathcal{E}$ belonging to Class D represents an entanglement witness in both its left- and right-handed forms.

$$c^4 - 2uc^2 + v + \chi w \geq 0.$$

These two inequalities are equivalent to $c^4 - 2uc^2 + v - |\chi w| \geq 0$. However, $w \geq 0$ and $\chi = \pm 1, 0$, and so $|\chi w| = w$, where the case of a degenerate $\mathcal{E}$ holds as χ and w vanish simultaneously. Hence the single inequality $c^4 - 2uc^2 + v - w \geq 0$ is necessary and sufficient for Class A. The two inequalities for Class D simplify similarly. ■

Any $\mathcal{E}$ lying inside $\mathcal{B}$ can thus be straightforwardly classified according to its geometric features. As in Section 3.1.3, where we examined conditions for positivity, we can identify three geometric contributions: the distance of the centre of $\mathcal{E}$ from the origin, the size of $\mathcal{E}$ (through terms such as $\operatorname{tr} Q$ and $\det Q$) and the skew $\hat{\boldsymbol{c}}^\intercal Q \hat{\boldsymbol{c}}$ (which gives a measure of the orientation of $\mathcal{E}$ relative to $\boldsymbol{c}$).

Figure 7.1 shows example ellipsoids for each class. We now make a few remarks to highlight how Theorem 7.4 and the notion of ellipsoid chirality can be used to classify any ellipsoid inside the Bloch ball.

- As discussed in Theorem 3.6, $\mathcal{E}$ for an entangled state (Class B) must be left-handed, as it obeys $\chi w < -\chi w$. We see similarly that $\mathcal{E}$ belonging to Class C must obey $\chi w > -\chi w$ and therefore be right-handed.
- Any degenerate $\mathcal{E}$ inside the Bloch ball must belong to Class A or Class D. The nested tetrahedron condition states that $\mathcal{E}$ fits inside a tetrahedron inside the Bloch ball if and only if it corresponds to a separable state (Class A) [11]. For the case of degenerate $\mathcal{E}$, the

nested tetrahedron may be taken to be a triangle. Degenerate $\mathcal{E}$ belonging to Class D are therefore those which do not fit inside a triangle inside the Bloch ball.

- Non-degenerate $\mathcal{E}$ belonging to Class A are those for which both the left- and right-handed ellipsoids represent separable states. Non-degenerate $\mathcal{E}$ belonging to Class D are those for which both the left- and right-handed ellipsoids represent entanglement witnesses.
- Any $\mathcal{E}$ that meets the surface of the Bloch ball at a circle cannot represent a state regardless of its chirality (recall the No Pancake Theorem of Section 4.2). Such ellipsoids must therefore belong to Class D.

In Chapter 3 we gave necessary and sufficient conditions for a two-qubit operator to represent a state (separable or entangled). Theorem 7.4 gives an alternative formulation of this: given that $\mathcal{E}$ lies inside $\mathcal{B}$, it represents a state if and only if $\mathcal{E}$ belongs to Class A or Class B. Any $\mathcal{E} \subseteq \mathcal{B}$ that does not represent a state must instead represent an entanglement witness (Class C or Class D). This gives a new physical interpretation to ellipsoids that were previously considered unphysical. For the remainder of this chapter we will investigate these ellipsoids and the corresponding entanglement witnesses in more detail.

7.3 ENTANGLEMENT WITNESS ELLIPSOIDS

7.3.1 OPTIMALITY AND WEAK OPTIMALITY

We use W to denote a unit trace two-qubit entanglement witness, which could belong to either Class C or Class D. A state ρ is detected by W when $\mathrm{tr}(\rho W) < 0$, and a witness W_1 is said to be *finer* than another witness W_2 if all the states detected by W_2 are also detected by W_1. W is called *optimal* when there does not exist a finer witness [95]. This notion can be extended to optimality within a set as follows [91]: let S be a set of entanglement witnesses; then $W \in S$ is optimal in S if there does not exist a finer entanglement witness in S. Finally, W is *weakly optimal* when there exists a product state $|\psi\rangle = |\phi\rangle \otimes |\nu\rangle \in \mathcal{H}$ such that $\langle\psi| W |\psi\rangle = 0$ [101].

For two-qubit entanglement witnesses, the properties of optimality and weak optimality can be immediately visualised using the ellipsoid representation.

Theorem 7.5: Optimality of entanglement witness ellipsoids

The optimality of any two-qubit entanglement witness is manifest through the geometry of its corresponding $\mathcal{E}$:

(i) W is optimal if and only if $\mathcal{E}$ is the whole Bloch ball $\mathcal{B}$ and right-handed;

(ii) W is weakly optimal if and only if $\mathcal{E}$ touches the Bloch sphere $\partial\mathcal{B}$.

Proof.

(i) An optimal two-qubit entanglement witness is of the form $W = |\psi_e\rangle\langle\psi_e|^{\mathsf{T}_B}$, with $|\psi_e\rangle$ an entangled state [90]. Since the steering ellipsoid for a state ρ is $\mathcal{B}$ if and only if ρ is a pure entangled state, such a steering ellipsoid must be left-handed (Theorem 3.6). An optimal entanglement witness is the partial transposition of such a state ($\rho = |\psi_e\rangle\langle\psi_e|$). Since partial transposition leaves the ellipsoid surface invariant but flips the chirality, this corresponds to the case that $\mathcal{E} = \mathcal{B}$ but right-handed.

(ii) That the property of weak optimality is preserved under the canonical transformation is clear from (7.2): there exists $|\psi\rangle = |\phi'\rangle \otimes |\nu\rangle$ such that $\langle\psi|\widetilde{W}|\psi\rangle = 0$ if and only if there exists $|\psi'\rangle = |\phi\rangle \otimes |\nu'\rangle$ such that $\langle\psi'|W|\psi'\rangle = 0$. Since $\mathcal{E}$ is invariant under the canonical transformation, it therefore suffices to consider a canonical entanglement witness $\widetilde{W}$.

The proof then proceeds similarly to Theorem 7.2. There exists $|\psi\rangle = |\phi\rangle \otimes |\nu\rangle$ such that $\langle\psi|\widetilde{W}|\psi\rangle = 0$ if and only if there exists $\boldsymbol{\phi}$ with $|\boldsymbol{\phi}| = 1$ such that $\boldsymbol{\phi}\cdot\boldsymbol{r}^{(\boldsymbol{\nu})} = -1$ for some point $\boldsymbol{r}^{(\boldsymbol{\nu})}$ on the surface of $\mathcal{E}$ parametrised by $\boldsymbol{\nu}$. Clearly $\boldsymbol{\phi}\cdot\boldsymbol{r}^{(\boldsymbol{\nu})} = -1$ implies that there exists some $\boldsymbol{\nu}$ for which $|\boldsymbol{r}^{(\boldsymbol{\nu})}| = 1$. Conversely, since the only constraint on $\boldsymbol{\phi}$ is $|\boldsymbol{\phi}| = 1$, if $|\boldsymbol{r}^{(\boldsymbol{\nu})}| = 1$ then the direction of $\boldsymbol{\phi}$ can always be chosen so that $\boldsymbol{\phi}\cdot\boldsymbol{r}^{(\boldsymbol{\nu})} = -1$. So $\widetilde{W}$ is weakly optimal if and only if $|\boldsymbol{r}^{(\boldsymbol{\nu})}| = 1$, i.e. a point on $\mathcal{E}$ is coincident with $\partial\mathcal{B}$.

■

We thus see from a geometric perspective that an optimal witness is a special case of a weakly optimal witness, since any $\mathcal{E} = \mathcal{B}$ touches $\partial\mathcal{B}$. In terms of the classification scheme given in Theorem 7.4, any optimal W must belong to Class C, since $W^{\mathsf{T}_B} = |\psi_e\rangle\langle\psi_e|$ is an entangled state. A weakly optimal W can belong to Class C or Class D (see Figure 7.2).

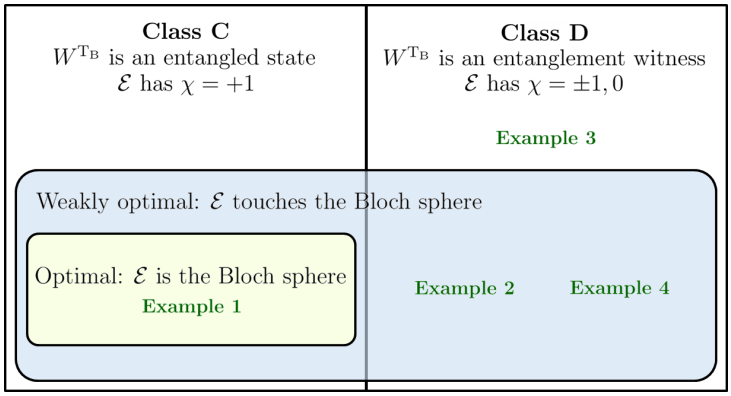

Figure 7.2: Any two-qubit entanglement witness W belongs to either Class C or Class D; these are distinguished by whether W^{T_B} is an entangled state or an entanglement witness. Witnesses represented by degenerate $\mathcal{E}$ must belong to Class D, while all witnesses in Class C must be right-handed. There are weakly optimal witnesses in Class C and Class D, but an optimal witness must belong to Class C. The optimality or weak optimality of a witness is immediately evident from a visualisation of $\mathcal{E}$ inside the Bloch sphere. Example witnesses discussed in the main text are shown.

7.3.2 EXAMPLES OF ENTANGLEMENT WITNESSES

We now present some typical examples of two-qubit entanglement witnesses to show how the geometric features of $\mathcal{E}$ relate to witness properties. This will also serve to illustrate the distinction between operators belonging to Class C and Class D (recall that W belongs to Class C when W^{T_B} is an entangled state; W belongs to Class D when W^{T_B} is an entanglement witness). The examples are shown on Figure 7.2, with the corresponding ellipsoids illustrated in Figure 7.3.

Example 1: Flip operator

The flip or swap operator $\mathbb{F}$ is defined by $\mathbb{F}\,|\phi\rangle \otimes |\nu\rangle = |\nu\rangle \otimes |\phi\rangle$ [90]. After normalisation to unit trace we have

$$W = \frac{1}{2}\mathbb{F} = |\phi^+\rangle\langle\phi^+|^{T_B}\,, \tag{7.7}$$

where $|\phi^+\rangle = \frac{1}{\sqrt{2}}(|00\rangle + |11\rangle)$. In terms of the Pauli basis (7.1), we have $\boldsymbol{a} = \boldsymbol{b} = \mathbf{0}$ and $T = \mathrm{diag}(1,1,1)$. Computing the ellipsoid parameters $\boldsymbol{c}$ and Q we see that $\mathcal{E}$ representing W is the whole Bloch ball with $\chi = +1$, as it must be for an optimal entanglement witness (Theorem 7.5). As with any optimal entanglement witness, W belongs to Class C.

Example 2: Weakly optimal witnesses

Ref. [102] presents a family of two-qubit entanglement witnesses that, after normalisation, may be decomposed as

$$W_p = pQ_1 + (1-p)Q_2^{T_B}\,, \tag{7.8}$$

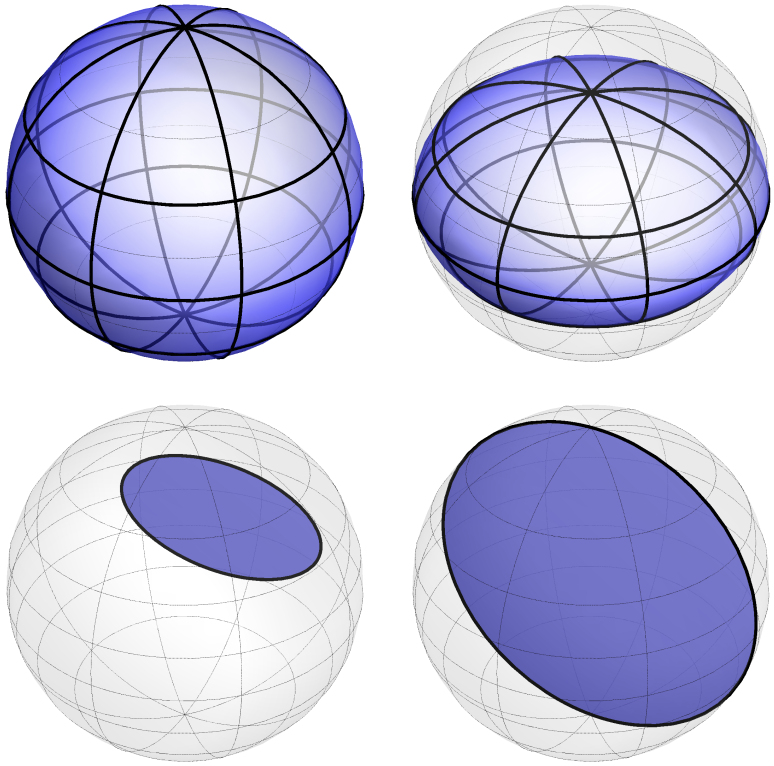

Figure 7.3: Visualisation of the example $\mathcal{E}$. Top left: Example 1 – $\mathcal{E}$ representing the optimal witness $W = |\phi^+\rangle\langle\phi^+|^{\mathsf{T}_B}$ is the whole Bloch ball with $\chi = +1$. Top right: Example 2 – $\mathcal{E}$ representing a weakly optimal witness touches the surface of the Bloch sphere. Here we show $\mathcal{E}$ for W_p with $p = \frac{1}{5}$; this meets the surface of $\mathcal{B}$ at the circle on the equatorial plane. Bottom left: Example 4 – $\mathcal{E}$ representing $W \in \mathrm{EW}_4$ is an ellipse in the xz plane. Due to the nested tetrahedron condition, there is no triangle inside the Bloch sphere that circumscribes $\mathcal{E}$. Bottom right: Example 4 – $\mathcal{E}$ representing optimal $W \in \mathrm{EW}_4$ is the xz unit disc.

where $Q_1 := |\psi^+\rangle\langle\psi^+|$ and $Q_2 := |\phi^+\rangle\langle\phi^+|$. The family W_p is studied further in Refs. [103, 104]. Explicitly, we have

$$W_p = \frac{1}{2}\begin{pmatrix} p & 0 & 0 & 0 \\ 0 & 1-p & 1 & 0 \\ 0 & 1 & 1-p & 0 \\ 0 & 0 & 0 & p \end{pmatrix}.$$

In terms of the Pauli basis, $\boldsymbol{a} = \boldsymbol{b} = \mathbf{0}$ and $T = \mathrm{diag}(1, 1, 2p-1)$. $\mathcal{E}_p$ representing W_p therefore has centre $\boldsymbol{c} = \mathbf{0}$ and chirality $\chi = \mathrm{sign}(2p-1)$. The semiaxes of $\mathcal{E}_p$ have length 1, 1 and $|2p-1|$ aligned with the x, y and z coordinate axes respectively.

$\mathcal{E}$ lies inside $\mathcal{B}$ if and only if $|2p-1| \leq 1$, and so, following Theorem 7.2, W_p is block positive if and only if $0 \leq p \leq 1$. W_p is positive semidefinite and hence a state for $p = 0$; for all other values of p, W_p is therefore an entanglement witness. Since all such $\mathcal{E}$ touch $\partial\mathcal{B}$, W_p

forms a family of weakly optimal entanglement witnesses.[1]

Furthermore, when $p = 1$, W_p reduces to the optimal witness presented in Example 1. For all other $0 < p < 1$, the ellipsoid $\mathcal{E}$ meets $\partial\mathcal{B}$ at the circle on the equatorial plane. As discussed in Section 7.2.3, such ellipsoids belong to Class D.

Example 3: EW_4 **family**

Refs. [91, 92] introduce EW_4, a set of two-qubit entanglement witnesses of interest in quantum key distribution. An entanglement witness $W \in \mathrm{EW}_4$ if and only if $W = W^{\mathsf{T}} = W^{\mathsf{T}_B}$.

From (7.1) we see that for $W \in \mathrm{EW}_4$ all terms involving σ_y must vanish[2] so that

$$\boldsymbol{a} = \begin{pmatrix} a_1 \\ 0 \\ a_3 \end{pmatrix}, \boldsymbol{b} = \begin{pmatrix} b_1 \\ 0 \\ b_3 \end{pmatrix} \text{ and } T = \begin{pmatrix} T_{11} & 0 & T_{13} \\ 0 & 0 & 0 \\ T_{31} & 0 & T_{33} \end{pmatrix}.$$

We then convert this data into the ellipsoid parameters $(\boldsymbol{c}, Q)$ to find the corresponding ellipsoid $\mathcal{E}$.

We find that $\boldsymbol{c}$ lies in the xz plane and that the ellipsoid matrix Q is rank deficient, and hence $\mathcal{E}$ is degenerate ($\chi = 0$). The support of Q spans the xz plane and so $\mathcal{E}$ itself must lie within the xz plane. $\mathcal{E}$ cannot be a line or point, as these always describe a separable state (since they correspond to degenerate tetrahedra inside the Bloch sphere and hence satisfy the nested tetrahedron condition [11]). Therefore $\mathcal{E}$ for $W \in \mathrm{EW}_4$ is an ellipse in the xz plane. As a degenerate ellipsoid, all $\mathcal{E}$ for $W \in \mathrm{EW}_4$ belong to Class D.

Example 4: Optimality within EW_4

Entanglement witnesses that are optimal within the set EW_4 are given by $W = \frac{1}{2}(\rho + \rho^{\mathsf{T}_B})$, where $\rho = |\psi_e\rangle\langle\psi_e|$ and $|\psi_e\rangle$ is a real entangled state [91]. Ref. [105] shows that $\mathcal{E}$ for such an operator is a circular disc with centre $\boldsymbol{c} = \boldsymbol{0}$ and radius 1. Any $W \in \mathrm{EW}_4$ must lie in the xz plane, and so optimal witnesses within EW_4 are represented by the xz unit disc itself. Note that these witnesses are also weakly optimal for two qubits in general, since $\mathcal{E}$ touches the surface of the Bloch sphere.

7.3.3 OPTIMALITY WITHIN A SET

The examples given above suggest an interesting new geometric perspective on optimality within a set of two-qubit entanglement witnesses. Consider the set S of all two-qubit entanglement witnesses. The ellipsoids describing $W \in S$ always lie within the Bloch ball, and the

[1] It is straightforward to verify that $\langle\psi| W_p |\psi\rangle = 0$ for $|\psi\rangle = |+\rangle \otimes |-\rangle$ with $|\pm\rangle = \frac{1}{\sqrt{2}}(|0\rangle \pm |1\rangle)$, fulfilling the defining criterion of a weakly optimal witness.

[2] This follows since $\sigma_i^{\mathsf{T}} = \sigma_i$ for $i \in \{1, 3\}$ whilst $\sigma_i^{\mathsf{T}} = -\sigma_i$ for $i = 2$.

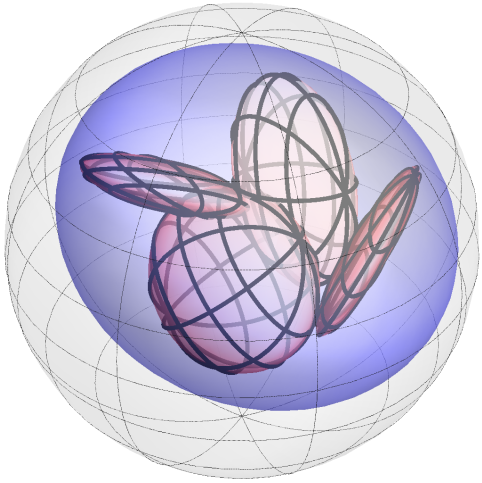

Figure 7.4: Visualisation of Conjecture 7.6. The blue ellipsoid is $\mathcal{E}^\star$; the red ellipsoids are example witnesses $W \in S$. We conjecture that the optimal $W \in S$ are described by $\mathcal{E}_W = \mathcal{E}^\star$.

optimal $W \in S$ are simply the optimal two-qubit entanglement witnesses. According to Theorem 7.5, the ellipsoid representing these optimal W is the whole Bloch ball. This $\mathcal{E}$ is the largest possible one that represents any $W \in S$.

Members of the set EW_4 are described by $\mathcal{E}$ that are ellipses within the xz plane (Example 3). The optimal $W \in \mathrm{EW}_4$ are described by the whole xz unit disc (Example 4). Again, this $\mathcal{E}$ is the largest possible ellipsoid for any $W \in \mathrm{EW}_4$. This leads us to conjecture that the optimal W within a set will always be described by the largest possible ellipsoid.

Conjecture 7.6: Geometric condition for optimality within a set
Define the set S of two-qubit entanglement witnesses: $W \in S$ if and only if $\mathcal{E}_W \subseteq \mathcal{E}^\star$, where $\mathcal{E}_W$ is the ellipsoid representing W and $\mathcal{E}^\star \subseteq \mathcal{B}$ is some ellipsoid inside the Bloch ball. The optimal $W \in S$ are then represented by $\mathcal{E}_W = \mathcal{E}^\star$.

In the case that S is the set of all two-qubit entanglement witnesses, $\mathcal{E}^\star$ is the whole Bloch sphere; and for our example $S = \mathrm{EW}_4$, $\mathcal{E}^\star$ is the xz plane. Note that this conjecture applies to any $\mathcal{E}^\star$ belonging to Class C or Class D.

Although this conjecture is easy to visualise geometrically (Figure 7.4), it is nontrivial to approach analytically. In addition to finding the optimal witnesses within a set, the conjecture involves determining whether a given W belongs to S. This means finding whether one ellipsoid $\mathcal{E}$ lies inside another $\mathcal{E}^\star$, which, as noted in Section 7.2.1, is a difficult problem.

SUMMARY AND DISCUSSION OF CHAPTER 7

In this chapter we have extended the steering ellipsoid formalism for representing two-qubit states to represent any two-qubit block positive operator B. We derived a novel classification of B using the positivity of $\det B$ and $\det B^{\mathsf{T}_B}$, and we can now classify any ellipsoid inside the Bloch ball as a separable state, entangled state or entanglement witness (Theorem 7.4). This gives a beautiful physical meaning to ellipsoids which were previously regarded as unphysical.

We have studied several examples of two-qubit entanglement witnesses and found that features such as optimality and weak optimality are clearly manifest in the ellipsoid representation (Theorem 7.5). This promotes ellipsoids as a natural and intuitive scheme for representing two-qubit entanglement witnesses.

It is also worth noting some features of the formalism that we have investigated without finding any significant results. Is there any relationship between the ellipsoid representing an entanglement witness W and the set of ellipsoids describing two-qubit states that W detects? Or, conversely, is there a relationship between the ellipsoid of an entangled two-qubit state and the set of ellipsoids describing entanglement witnesses which can detect that state? It also remains to be seen whether an analogous representation of entanglement witnesses is useful for studying higher-dimensional scenarios.

Finally, we note that Wang et al. [103, 104] have recently characterised weakly optimal entanglement witnesses and given a general procedure for their construction. The ellipsoid representation might be used to give a novel geometric interpretation of this procedure for two qubits.

CHAPTER 8

INEQUALITIES FOR A NESTED TETRAHEDRON

In the final chapter of this thesis we demonstrate how the steering ellipsoid formalism can be used to establish results in pure geometry. Recall the nested tetrahedron condition, mentioned in Section 1.5.5: a two-qubit state is separable if and only if $\mathcal{E}$ fits inside a tetrahedron that fits inside the Bloch ball. In Chapter 4 we used the physical state conditions and ellipsoid chirality to algebraically find the separable-entangled boundary. We now use the equivalence between this algebraic formulation and the nested tetrahedron condition to derive several results in classical Euclidean elementary geometry, some of which are entirely new.

We consider a ball of radius r contained inside another ball of radius R, with the centres separated by a distance d. When does there exist a 'nested' tetrahedron circumscribed about the smaller ball and inscribed in the larger ball? We derive the Grace-Danielsson inequality $d^2 \leq (R+r)(R-3r)$ as the sole necessary and sufficient condition for the existence of a nested tetrahedron. Our method also gives the Euler-Chapple inequality $d^2 \leq R(R-2r)$ for the existence of a nested triangle in the analogous 2D scenario.

We thus find a remarkable, physically motivated derivation of some very nontrivial geometric results. In fact, our work extends these results to give conditions for the existence of a nested tetrahedron for the more general, and significantly more difficult, case of an ellipsoid inside a ball.

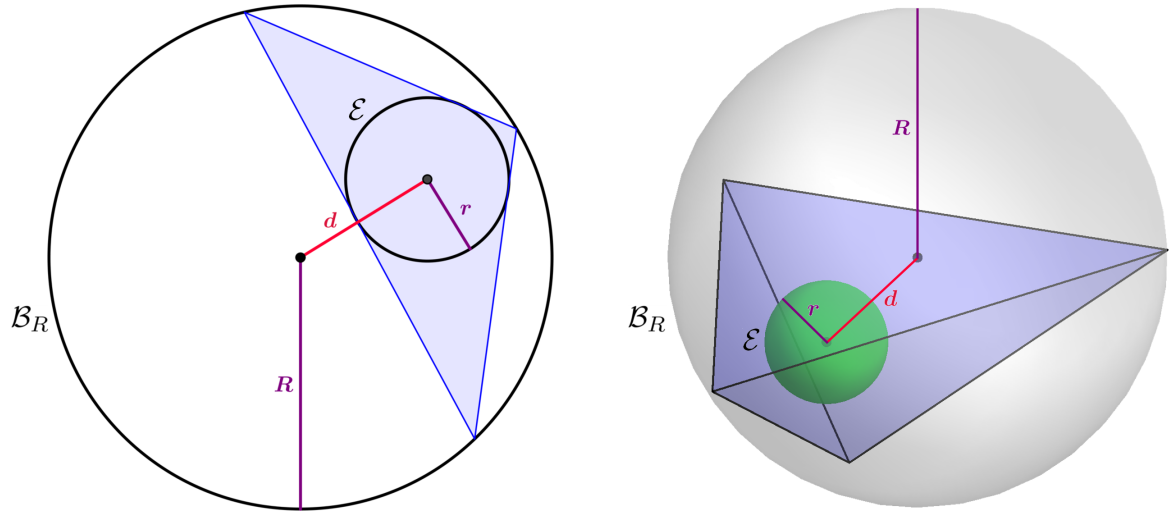

Figure 8.1: Left: 2D scenario; right: 3D scenario. A disc (ball) $\mathcal{E}$ of radius r is contained inside another disc (ball) $\mathcal{B}_R$ of radius R. The distance between the centres of $\mathcal{E}$ and $\mathcal{B}$ is d. In the examples shown here there exists a nested triangle (tetrahedron) circumscribed about $\mathcal{E}$ and inscribed in $\mathcal{B}_R$.

8.1 CLASSICAL EUCLIDEAN ELEMENTARY GEOMETRY

We begin by introducing some important results of classical Euclidean elementary geometry (CEEG). Let d be the distance between the incentre and circumcentre of a triangle with inradius r and circumradius R. Independently, Chapple (in 1746) and Euler (in 1765) found a classic result of 2D Euclidean geometry relating these quantities: $d^2 = R(R-2r)$ [106]. This relationship holds for any triangle.

The analogous scenario in 3D space involves a tetrahedron, insphere (radius r) and circumsphere (radius R), with the sphere centres separated by a distance d. In 1816, Gergonne asked whether in 3 dimensions d could be similarly expressed as a function of only R and r. Eight years later, Durrande gave the solution $d^2 = (R+r)(R-3r)$. This was widely accepted for many years but is in fact incorrect, and there cannot exist such an equality that holds for all tetrahedra (see Ref. [107] for a full discussion).

We consider a closely related question. A disc (ball) $\mathcal{E}$ of radius r is contained inside another disc (ball) $\mathcal{B}_R$ of radius R.[1] Let the distance between the centres of $\mathcal{E}$ and $\mathcal{B}_R$ be d. What are the necessary and sufficient conditions for the existence of a triangle (tetrahedron) nested between $\mathcal{E}$ and $\mathcal{B}_R$? Examples of the 2- and 3-dimensional scenarios are shown in Figure 8.1.

In 2 dimensions, the sole condition for the existence of a nested triangle is given by the *Euler-Chapple inequality* [108]

$$d^2 \leq R(R-2r). \tag{8.1}$$

[1] Following our usual notation, the Bloch ball, which has $R = 1$, will be written $\mathcal{B}$.

In 3 dimensions, Grace (in 1917, see Ref. [109]) and Danielsson (in 1949, see Ref. [110]) proved that the sole condition for the existence of a nested tetrahedron is

$$d^2 \leq (R + r)(R - 3r). \tag{8.2}$$

We shall call (8.2) the *Grace-Danielsson inequality*.

Ref. [107] notes that the statement of this problem is formulated in terms of classical Euclidean elementary geometry (CEEG) but Danielsson's proof is based on some intricate projective geometry. This poses a challenge to prove inequality (8.2) using only methods belonging to CEEG. We will prove the Grace-Danielsson inequality using the steering ellipsoid formalism. There already exist some physically motivated derivations of geometric results; for example, the generalised parallel axes theorem can be used to prove the Euler-Chapple result $d^2 = R(R - 2r)$ [111]. Our derivation is particularly remarkable since it gives a new, and highly nontrivial, generalisation of these results from CEEG.

8.2 CONDITION FOR THE EXISTENCE OF A NESTED TETRAHEDRON

We recall the nested tetrahedron condition:[1]

Lemma 8.1: Geometric condition for separability
An ellipse (ellipsoid) $\mathcal{E}$ corresponds to a separable state if and only if there exists a triangle (tetrahedron) nested between $\mathcal{E}$ and $\mathcal{B}$.

Here we outline the main ideas behind the proof; for full details, see Ref. [11].[2]

By definition, a separable state can be decomposed as $\rho = \sum_{i=1}^{n} p_i \phi_i \otimes \nu_i$ with $\sum_i p_i = 1$ and $p_i \geq 0$. For two qubits, we can always take $n \leq 4$ [24, 112]. Define Bloch vectors for Alice's states ϕ_i as $\boldsymbol{\phi}_i := \mathrm{tr}(\phi_i \boldsymbol{\sigma})$. The set $\{\boldsymbol{\phi}_i\}$ defines a (possibly degenerate) tetrahedron.

When Bob performs a measurement and obtains outcome M, Alice is steered as

$$\begin{aligned} \rho_A \mapsto \rho'_A &= \frac{\mathrm{tr}_B\left[\rho\,(\mathbb{1} \otimes M)\right]}{\mathrm{tr}\left[\rho\,(\mathbb{1} \otimes M)\right]} \\ &= \frac{\sum_i p_i \,\mathrm{tr}(\nu_i M)\,\phi_i}{\sum_i p_i \,\mathrm{tr}(\nu_i M)}. \end{aligned} \tag{8.3}$$

Alice's steered Bloch vector $\boldsymbol{a}' = \mathrm{tr}(\rho'_A \boldsymbol{\sigma})$ is thus a convex combination of $\{\boldsymbol{\phi}_i\}$. Hence her steering ellipsoid $\mathcal{E}$, which gives the set of all Bloch vectors to which she can be steered, lies

[1] Note that any physical degenerate ellipsoid must represent a separable state (Theorem 3.6). Hence the existence of a nested triangle for an ellipse $\mathcal{E}$ is equivalent to the physicality of $\mathcal{E}$.

[2] Alternatively, a derivation for the nested tetrahedron condition using the 4D bicone picture has recently been given in Ref. [35].

inside the tetrahedron with vertices $\{\boldsymbol{\phi}_i\}$.

The converse direction of the proof is more difficult and involves showing that for any $\mathcal{E}$ inside a tetrahedron one can construct a separable state ρ. The proof of the 2D nested triangle result derives from the fact that if an ellipse fits inside a tetrahedron inside $\mathcal{B}$ then it must fit inside a triangle inside $\mathcal{B}$ [113].

Independently of the nested tetrahedron condition we can also formulate an algebraic condition for separability. As usual, in order to describe any $\mathcal{E}$ inside $\mathcal{B}$ we only need consider canonical states of the form

$$\widetilde{\rho} = \frac{1}{4}(\mathbb{1}\otimes\mathbb{1} + \boldsymbol{d}\cdot\boldsymbol{\sigma}\otimes\mathbb{1} + \sum_{i,j=1}^{3}\widetilde{T}_{ij}\,\sigma_i\otimes\sigma_j), \tag{8.4}$$

which has ellipsoid matrix $Q = \widetilde{T}\widetilde{T}^{\intercal}$. The centre of $\mathcal{E}$ is $\boldsymbol{d}$ (relabelled from our normal $\boldsymbol{c}$ to match the notation conventionally used in CEEG). Since $\mathcal{B}$ is centred on the origin, the distance between the centres of $\mathcal{E}$ and $\mathcal{B}$ is $d = |\boldsymbol{d}|$.

Lemma 8.2: Algebraic condition for separability

A (possibly degenerate) ellipsoid $\mathcal{E} \subseteq \mathcal{B}$ with parameters ($\boldsymbol{d}$, Q) corresponds to a separable state if and only if $d^4 - 2ud^2 + q \geq 0$, where

$$u := 1 - \operatorname{tr} Q + 2\hat{\boldsymbol{d}}^{\intercal}Q\hat{\boldsymbol{d}},$$
$$q := 1 + 2\operatorname{tr}(Q^2) - 2\operatorname{tr} Q - (\operatorname{tr} Q)^2 - 8\sqrt{\det Q},$$

with the unit vector $\hat{\boldsymbol{d}} = \boldsymbol{d}/d$.

Proof. $\mathcal{E} \subseteq \mathcal{B}$ represents a block positive operator, and so we apply Theorem 7.4 to classify $\widetilde{\rho}$ as a separable state (Class A). ■

We thus have two equivalent necessary and sufficient conditions for the separability of ρ: the geometric condition of the existence of a nested tetrahedron and this algebraic condition. It is not at all obvious how either one of these conditions could be found directly from the other. Crucially, however, we now have an algebraic formulation for the existence of a nested tetrahedron. Converting the unit ball $\mathcal{B}$ to a ball $\mathcal{B}_R$ of radius R, we arrive at the key inequality that will be used to derive all our CEEG results.

Theorem 8.3: Algebraic condition for a nested tetrahedron

Let $\mathcal{E}$ be an ellipsoid, described by matrix Q, contained inside a ball $\mathcal{B}_R$ of radius R. The centre of $\mathcal{E}$ relative to the centre of $\mathcal{B}_R$ is $\boldsymbol{d}$. There exists a tetrahedron circumscribed about $\mathcal{E}$ and inscribed in $\mathcal{B}$ if and only if $d^4 - 2u_R d^2 + q_R \geq 0$, where

$$u_R := R^2 - \operatorname{tr} Q + 2\hat{\boldsymbol{d}}^\mathsf{T} Q \hat{\boldsymbol{d}},$$
$$q_R := R^4 + 2\operatorname{tr}(Q^2) - 2R^2 \operatorname{tr} Q - (\operatorname{tr} Q)^2 - 8R\sqrt{\det Q}.$$

When $\mathcal{E}$ is an ellipse, the tetrahedron can always be taken to be a triangle.

Proof. Lemma 8.1 and Lemma 8.2 are both necessary and sufficient for separability of $\mathcal{E}$. The result follows immediately from this, after rescaling the quantities u and q to u_R and q_R. ■

8.3 CEEG RESULTS

Theorem 8.3 is all that will be needed to derive the Euler-Chapple inequality (8.1) for the 2D scenario and the corresponding Grace-Danielsson inequality (8.2) for the 3D scenario. We also present an example that demonstrates how Theorem 8.3 can be used to establish new results for ellipses and ellipsoids.

Corollary 8.4: Euler-Chapple inequality

Let $\mathcal{E}$ be a disc of radius r contained inside a disc $\mathcal{B}_R$ of radius R. The distance between the centres of $\mathcal{E}$ and $\mathcal{B}_R$ is d. The sole necessary and sufficient condition for the existence of a nested triangle is

$$d^2 \leq R(R - 2r),$$

as given by the Euler-Chapple inequality (8.1).

Proof. $\mathcal{E}$ may be described by $Q = \operatorname{diag}(r^2, r^2, 0)$. The degenerate case of Theorem 8.3 gives a condition for the existence of a triangle circumscribed about $\mathcal{E}$ and inscribed in a ball of radius R. Setting $\boldsymbol{d} = (d_1, d_2, 0)$ ensures that $\mathcal{E}$ and $\boldsymbol{d}$ are coplanar, so that Theorem 8.3 equivalently gives a condition for the existence of a triangle circumscribed about $\mathcal{E}$ and inscribed in a disc of radius R. The skew term $\hat{\boldsymbol{d}}^\mathsf{T} Q \hat{\boldsymbol{d}} = r^2$

does not depend on the orientation of $\boldsymbol{d}$ within its plane. Evaluating u_R and q_R gives

$$u_R = R^2,$$
$$q_R = R^4 - 4R^2r^2.$$

Theorem 8.3 then tells us that a nested triangle exists if and only if

$$d^4 - 2u_R d^2 + q_R = (d^2 - R^2)^2 - 4R^2r^2 \geq 0,$$

from which the result follows. ■

The physical significance of this result in terms of steering ellipsoids inside the Bloch ball was considered in Section 4.2 as an extension to the No Pancake Theorem. Briefly, this states that the equatorial disc of the Bloch ball is not a valid steering ellipsoid; by setting $R = 1$, Corollary 8.4 extends this result to identify the largest circular $\mathcal{E}$ that is a valid steering ellipsoid for a given $\boldsymbol{d}$.

Corollary 8.5: Grace-Danielsson inequality

Let $\mathcal{E}$ be a ball of radius r contained inside a ball $\mathcal{B}_R$ of radius R. The distance between the centres of $\mathcal{E}$ and $\mathcal{B}_R$ is d. The sole necessary and sufficient condition for the existence of a nested tetrahedron is

$$d^2 \leq (R + r)(R - 3r),$$

as given by the Grace-Danielsson inequality (8.2).

Proof. $\mathcal{E}$ may be described by $Q = \text{diag}(r^2, r^2, r^2)$. The skew term $\hat{\boldsymbol{d}}^\mathsf{T} Q \hat{\boldsymbol{d}} = r^2$ does not depend on the orientation of $\boldsymbol{d}$. Evaluating u_R and q_R gives

$$u_R = R^2 - r^2,$$
$$q_R = R^4 - 6R^2r^2 - 8Rr^3 - 3r^4.$$

Theorem 8.3 then tells us that a nested tetrahedron exists if and only if

$$d^4 - 2u_R d^2 + q_R = (d - R - r)(d + R + r)(d^2 - (R + r)(R - 3r)) \geq 0,$$

from which the result follows. ■

Again, we provided a physical interpretation of this result in Section 4.3.1, where we identified the associated two-qubit states as inept states lying on the separable-entangled boundary [52].

Finally, we consider results for an ellipsoid $\mathcal{E}$. Note that Theorem 8.3 concerns *any* ellipse or ellipsoid inside a ball – in particular, this includes ellipsoids that are oriented with no semiaxis collinear with $\boldsymbol{d}$. Such ellipsoids have an awkward skew term $\hat{\boldsymbol{d}}^{\mathsf{T}} Q \hat{\boldsymbol{d}}$, which causes significant difficulties when attempting to formulate algebraic conditions for when $\mathcal{E}$ is contained inside a ball [96]. Remarkably, Theorem 8.3 works in full generality to give conditions for the existence of a nested tetrahedron for an ellipsoid with any skew. The degenerate case can be used to give conditions for the existence of a nested triangle for any ellipse inside a disc or ball. We believe this to be the first formulation of necessary and sufficient conditions for these general scenarios.

As an example of how Theorem 8.3 can be used for ellipsoids, we give a result for a specially oriented class of ellipsoid.

Corollary 8.6: Oriented ellipsoid inequality

Let $\mathcal{E}$ be an ellipsoid with semiaxes s_1, s_2, s_3 contained inside a ball $\mathcal{B}_R$ of radius R. The distance between the centres of $\mathcal{E}$ and $\mathcal{B}_R$ is d, and $\mathcal{E}$ has its s_1 axis collinear with $\boldsymbol{d}$. The sole necessary and sufficient condition for the existence of a nested tetrahedron is

$$d^2 \leq (R - s_1)^2 - (s_2 + s_3)^2.$$

Proof. $\mathcal{E}$ may be described by $Q = \operatorname{diag}(s_1^2, s_2^2, s_3^2)$ and $\boldsymbol{d} = (d, 0, 0)$. Evaluating u_R and q_R gives

$$u_R = R^2 + s_1^2 - s_2^2 - s_3^2,$$
$$q_R = R^4 - 2R^2(s_1^2 + s_2^2 + s_3^2) - 8Rs_1s_2s_3 + s_1^4 + s_2^4 + s_3^4 - 2s_1^2s_2^2 - 2s_2^2s_3^2 - 2s_3^2s_1^2.$$

Theorem 8.3 then tells us that a nested tetrahedron exists if and only if

$$d^4 - 2u_R d^2 + q_R = (d^2 - R^2 - s_1^2 + s_2^2 + s_3^2)^2 - (2Rs_1 + 2s_2s_3)^2 \geq 0,$$

from which the result follows. ■

Note that by setting $s_1 = s_2 = s_3 = r$ Corollary 8.6 reproduces the result for a spherical $\mathcal{E}$ given in Corollary 8.5.

SUMMARY AND DISCUSSION OF CHAPTER 8

In this Chapter we have used the nested tetrahedron condition to derive two classic results in CEEG:

Nested triangles and tetrahedra

A disc (ball) of radius r is contained inside a disc (ball) of radius R. The distance between the centres is d. There exists a nested triangle (tetrahedron) if and only if

$$\text{Triangle: } d^2 \leq R(R-2r), \qquad \text{(Euler-Chapple inequality)}$$

$$\text{Tetrahedron: } d^2 \leq (R+r)(R-3r). \qquad \text{(Grace-Danielsson inequality)}$$

It is particularly noteworthy that we have derived the Grace-Danielsson inequality, which remains unproven using methods from CEEG. Remarkably, both these results follow immediately from a single key inequality (Theorem 8.3). Moreover, the same inequality can be used to give a necessary and sufficient condition for the existence of a nested triangle (tetrahedron) in the general case that $\mathcal{E}$ is an ellipse (ellipsoid). This is the first time that such a condition has been formulated. As well as providing these new results in CEEG, our results are of interest purely for the novelty of the derivation.

Finally, we note that this work has led to renewed interest in the n-dimensional scenario concerning a hyperball (radius r) inside a hyperball (radius R). Egan has conjectured

$$d^2 \leq (R+(n-2)r)(R-nr) \tag{8.5}$$

to be necessary and sufficient for the existence of a nested simplex [114]. Although sufficiency of this condition has been proven, there is not yet a proof of its necessity.

REFERENCES

[1] A. Milne, S. Jevtic, D. Jennings, H. Wiseman, and T. Rudolph, "Quantum steering ellipsoids, extremal physical states and monogamy," New J. Phys. **16**, 083017 (2014).

[2] A. Milne, D. Jennings, S. Jevtic, and T. Rudolph, "Quantum correlations of two-qubit states with one maximally mixed marginal," Phys. Rev. A **90**, 024302 (2014).

[3] A. Milne, D. Jennings, and T. Rudolph, "Geometric representation of two-qubit entanglement witnesses," Phys. Rev. A **92**, 012311 (2015).

[4] A. Milne, "The Euler and Grace-Danielsson inequalities for nested triangles and tetrahedra: a derivation and generalisation using quantum information theory," J. Geom. **106**, 455–463 (2015).

[5] X. Hu, A. Milne, B. Zhang, and H. Fan, "Quantum coherence of steered states," Sci. Rep. **6**, 19365 (2016).

[6] S. Cheng, A. Milne, M. J. W. Hall, and H. M. Wiseman, "Volume monogamy of quantum steering ellipsoids for multi-qubit systems," Phys. Rev. A **94**, 042105 (2016).

[7] I. Chuang and M. Nielsen, *Quantum Computation and Quantum Information* (Cambridge University Press, 2000).

[8] A. Einstein, B. Podolsky, and N. Rosen, "Can Quantum-Mechanical Description of Physical Reality Be Considered Complete?" Phys. Rev. **47**, 777–780 (1935).

[9] E. Schrödinger, "Discussion of Probability Relations between Separated Systems," Math. Proc. Cambridge Philos. Soc. **31**, 555 (1935).

[10] E. Schrödinger, "Probability relations between separated systems," Math. Proc. Cambridge Philos. Soc. **32**, 446 (1936).

[11] S. Jevtic, M. F. Pusey, D. Jennings, and T. Rudolph, "Quantum Steering Ellipsoids," Phys. Rev. Lett. **113**, 020402 (2014).

[12] L. P. Hughston, R. Jozsa, and W. K. Wootters, "A complete classification of quantum ensembles having a given density matrix," Phys. Lett. A **183**, 14–18 (1993).

[13] N. Gisin, "Stochastic quantum dynamics and relativity," Helv. Phys. Acta **62**, 363–371 (1989).

[14] K. A. Kirkpatrick, "The Schrödinger-HJW Theorem," Found. Phys. Lett. **19**, 95–102 (2006).

[15] R. W. Spekkens and T. Rudolph, "Optimization of coherent attacks in generalizations of the BB84 quantum bit commitment protocol," Quantum Inform. Compu. **2**, 66 (2002).

[16] H. M. Wiseman, S. J. Jones, and A. C. Doherty, "Steering, Entanglement, Nonlocality, and the EPR Paradox," Phys. Rev. Lett. **98**, 140402 (2007).

[17] S. J. Jones, H. M. Wiseman, and A. C. Doherty, "Entanglement, Einstein-Podolsky-Rosen correlations, Bell nonlocality, and steering," Phys. Rev. A **76**, 052116 (2007).

[18] D. Cavalcanti and P. Skrzypczyk, "Quantum steering: a short review with focus on semidefinite programming," arXiv:1604.00501 [quant-ph] (2016).

[19] I. Bengtsson and K. Życzkowski, *Geometry of Quantum States: An Introduction to Quantum Entanglement* (Cambridge University Press, 2006).

[20] F. Verstraete, *Quantum entanglement and quantum information*, Ph.D. thesis, Katholieke Universiteit Leuven (2002).

[21] M. Shi, F. Jiang, C. Sun, and J. Du, "Geometric picture of quantum discord for two-qubit quantum states," New J. Phys. **13**, 073016 (2011).

[22] M. Shi, W. Yang, F. Jiang, and J. Du, "Quantum discord of two-qubit rank-two states," J. Phys. A: Math. Theor. **44**, 415304 (2011).

[23] J. B. Altepeter, E. R. Jeffrey, M. Medic, and P. Kumar, "Multiple-qubit quantum state visualization," in *2009 Conference on Lasers and Electro-Optics and 2009 Conference on Quantum electronics and Laser Science Conference* (2009) pp. 1–2.

[24] W. K. Wootters, "Entanglement of Formation of an Arbitrary State of Two Qubits," Phys. Rev. Lett. **80**, 2245–2248 (1998).

[25] H. Ollivier and W. H. Zurek, "Quantum discord: A measure of the quantumness of correlations," Phys. Rev. Lett. **88**, 017901 (2001).

[26] L. Henderson and V. Vedral, "Classical, quantum and total correlations," J. Phys. A: Math. Gen. **34**, 6899 (2001).

[27] R. Mosseri and R. Dandoloff, "Geometry of entangled states, Bloch spheres and Hopf fibrations," J. Phys. A: Math. Gen. **34**, 10243 (2001).

[28] J. E. Avron, G. Bisker, and O. Kenneth, "Visualizing Two Qubits," J. Math. Phys. **48**, 102107 (2007).

[29] J. E. Avron and O. Kenneth, "Entanglement and the geometry of two qubits," Ann. Phys. **324**, 470–496 (2009).

[30] R. Horodecki and M. Horodecki, "Information-theoretic aspects of inseparability of mixed states," Phys. Rev. A **54**, 1838–1843 (1996).

[31] O. Gamel, "Entangled Bloch spheres: Bloch matrix and two-qubit state space," Phys. Rev. A **93**, 062320 (2016).

[32] G. Kimura, "The Bloch vector for n-level systems," Phys. Lett. A **314**, 339–349 (2003).

[33] G. Kimura and A. Kossakowski, "The Bloch-Vector Space for n-level Systems: the Spherical-Coordinate Point of View," Open Syst. Inf. Dyn. **12**, 207–229 (2005).

[34] S. K. Goyal, B. N. Simon, R. Singh, and S. Simon, "Geometry of the generalized Bloch sphere for qutrits," J. Phys. A: Math. Theor. **49**, 165203 (2016).

[35] H. C. Nguyen and T. Vu, "Non-separability and steerability of two-qubit states from the geometry of steering outcomes," arXiv:1604.00265 [quant-ph] (2016).

[36] S. Boyd and L. Vandenberghe, *Convex Optimization* (Cambridge University Press, 2004).

[37] B. Spain, *Analytical Conics* (Dover Publications, 2007).

[38] W. H. Press, S. A. Teukolsky, W. T. Vetterling, and B. P. Flannery, *Numerical Recipes: The Art of Scientific Computing* (Cambridge University Press, 2007).

[39] W. Dür, G. Vidal, and J. I. Cirac, "Three qubits can be entangled in two inequivalent ways," Phys. Rev. A **62**, 062314 (2000).

[40] F. Verstraete, J. Dehaene, and B. De Moor, "Local filtering operations on two qubits," Phys. Rev. A **64**, 010101 (2001).

[41] R. Uola, T. Moroder, and O. Gühne, "Joint measurability of generalized measurements implies classicality," Phys. Rev. Lett. **113**, 160403 (2014).

[42] R. Gallego and L. Aolita, "The resource theory of steering," Phys. Rev. X **5**, 041008 (2015).

[43] H. C. Nguyen and T. Vu, "Necessary and sufficient condition for steerability of two-qubit states by the geometry of steering outcomes," arXiv:1604.03815 [quant-ph] (2016).

[44] A. M. Wang, "Eigenvalues, Peres' separability condition and entanglement," Comm. Theor. Phys. **42**, 206 (2004).

[45] D. Braun, O. Giraud, I. Nechita, C. Pellegrini, and M. Žnidarič, "A universal set of qubit quantum channels," J. Phys. A: Math. Theor. **47**, 135302 (2014).

[46] L. E. Dickson, *Elementary Theory of Equations* (Stanhope Press, 1914).

[47] I. Macdonald, *Symmetric Functions and Hall Polynomials* (Clarendon Press, 1995).

[48] A. Peres, "Separability Criterion for Density Matrices," Phys. Rev. Lett. **77**, 1413–1415 (1996).

[49] M. Horodecki, P. Horodecki, and R. Horodecki, "Separability of Mixed States: Necessary and Sufficient Conditions," Phys. Lett. A **223**, 1–8 (1996).

[50] R. Augusiak, M. Demianowicz, and P. Horodecki, "Universal observable detecting all two-qubit entanglement and determinant based separability tests," Phys. Rev. A **77**, 030301 (2008).

[51] M.-D. Choi, "Completely positive linear maps on complex matrices," Linear Algebr. Appl. **10**, 285–290 (1975).

[52] S. J. Jones, H. M. Wiseman, and D. T. Pope, "Entanglement distribution by an arbitrarily inept delivery service," Phys. Rev. A **72**, 022330 (2005).

[53] T. Yu and J. Eberly, "Evolution from entanglement to decoherence of bipartite mixed X states," Quantum Inf. Comput. **7**, 459–468 (2007).

[54] M. Horodecki, P. Horodecki, and R. Horodecki, *Quantum Information: An Introduction to Basic Theoretical Concepts and Experiments* (Springer, 2001).

[55] S. Ishizaka and T. Hiroshima, "Maximally entangled mixed states under nonlocal unitary operations in two qubits," Phys. Rev. A **62**, 022310 (2000).

[56] B. Horst, K. Bartkiewicz, and A. Miranowicz, "Two-qubit mixed states more entangled than pure states: Comparison of the relative entropy of entanglement for a given nonlocality," Phys. Rev. A **87**, 042108 (2013).

[57] K. Bartkiewicz, B. Horst, K. Lemr, and A. Miranowicz, "Entanglement estimation from bell inequality violation," Phys. Rev. A **88**, 052105 (2013).

[58] A. Miranowicz, S. Ishizaka, B. Horst, and A. Grudka, "Comparison of the relative entropy of entanglement and negativity," Phys. Rev. A **78**, 052308 (2008).

[59] M. D. Reid, "Monogamy inequalities for the EPR paradox and quantum steering," Phys. Rev. A **88**, 062108 (2013).

[60] V. Coffman, J. Kundu, and W. K. Wootters, "Distributed Entanglement," Phys. Rev. A **61**, 052306 (2000).

[61] U. T. Bhosale and A. Lakshminarayan, "A simple permutation based measure of quantum correlations, and maximally 3-tangled states," arXiv:1510.03656 [quant-ph] (2015).

[62] A. Milne, S. Jevtic, D. Jennings, H. Wiseman, and T. Rudolph, "Corrigendum: Quantum steering ellipsoids, extremal physical states and monogamy," New J. Phys. **17**, 019501 (2015).

[63] M. Horodecki and P. Horodecki, "Reduction criterion of separability and limits for a class of distillation protocols," Phys. Rev. A **59**, 4206–4216 (1999).

[64] N. J. Cerf and C. Adami, "Quantum extension of conditional probability," Phys. Rev. A **60**, 893–897 (1999).

[65] J. Chen and A. Milne, "Detecting consistency of overlapping quantum marginals by quantum steering ellipsoids," in preparation (2016).

[66] J. Clauser, A. Horne, A. Shimony, and R. Holt, "Proposed Experiment to Test Local Hidden-Variable Theories," Phys. Rev. Lett. **23**, 880 (1969).

[67] R. Horodecki, P. Horodecki, and M. Horodecki, "Violating Bell inequality by mixed spin-$\frac{1}{2}$ states: necessary and sufficient condition," Phys. Lett. A **200**, 340–344 (1995).

[68] J. Chen, Z. Ji, D. Kribs, N. Lütkenhaus, and B. Zeng, "Symmetric Extension of Two-Qubit States," Phys. Rev. A **90**, 032318 (2014).

[69] A. C. Doherty, P. A. Parrilo, and F. M. Spedalieri, "Distinguishing separable and entangled states," Phys. Rev. Lett. **88**, 187904 (2002).

[70] M. Nowakowski and P. Horodecki, "A simple test for quantum channel capacity," J. Phys. A: Math. Theor. **42**, 135306 (2009).

[71] G. O. Myhr, J. M. Renes, A. C. Doherty, and N. Lütkenhaus, "Symmetric extension in two-way quantum key distribution," Phys. Rev. A **79**, 042329 (2009).

[72] B. M. Terhal, A. C. Doherty, and D. Schwab, "Symmetric Extensions of Quantum States and Local Hidden Variable Theories," Phys. Rev. Lett. **90**, 157903 (2003).

[73] C. H. Bennett, D. P. DiVincenzo, J. A. Smolin, and W. K. Wootters, "Mixed-state entanglement and quantum error correction," Phys. Rev. A **54**, 3824 (1996).

[74] P. Badziąg, M. Horodecki, P. Horodecki, and R. Horodecki, "Local environment can enhance fidelity of quantum teleportation," Phys. Rev. A **62**, 012311 (2000).

[75] L. Hogben, *Handbook of Linear Algebra* (Chapman and Hall/CRC, 2014).

[76] M. Horodecki, P. Horodecki, and R. Horodecki, "General teleportation channel, singlet fraction, and quasidistillation," Phys. Rev. A **60**, 1888 (1999).

[77] F. Verstraete and H. Verschelde, "Optimal teleportation with a mixed state of two qubits," Phys. Rev. Lett. **90**, 097901 (2003).

[78] S. Adhikari and A. Kumar, "Upper bound on singlet fraction of two qubit mixed entangled states," Quantum Inf. Process. **15**, 2797 (2016).

[79] G. Vidal and R. Werner, "Computable measure of entanglement," Phys. Rev. A **65**, 032314 (2002).

[80] F. Verstraete and M. M. Wolf, "Entanglement versus Bell Violations and Their Behavior under Local Filtering Operations," Phys. Rev. Lett. **89**, 170401 (2002).

[81] F. Verstraete and H. Verschelde, "Fidelity of mixed states of two qubits," Phys. Rev. A **66**, 022307 (2002).

[82] D. Bruss, D. P. DiVincenzo, A. Ekert, C. Fuchs, C. Macchiavello, and J. A. Smolin, "Optimal universal and state-dependent quantum cloning," Phys. Rev. A **57**, 2368–2378 (1998).

[83] V. Buzek and M. Hillery, "Quantum copying: Beyond the no-cloning theorem." Phys. Rev. A **54**, 1844–1852 (1996).

[84] S. Jevtic, M. J. W. Hall, M. R. Anderson, M. Zwierz, and H. M. Wiseman, "Einstein-Podolsky-Rosen steering and the steering ellipsoid," J. Opt. Soc. Am. B **32**, A40 (2015).

[85] Q. Quan, H. Zhu, S.-Y. Liu, S.-M. Fei, H. Fan, and W.-L. Yang, "Steering Bell-diagonal states," Sci. Rep. **6**, 22025 (2016).

[86] Y. Ouyang, "Channel covariance, twirling, contraction, and some upper bounds on the quantum capacity," Quantum Inform. Compu. **14**, 917 (2014).

[87] O. Gühne and G. Tóth, "Entanglement detection," Phys. Rep. **474**, 1 (2009).

[88] B. M. Terhal, "Bell inequalities and the separability criterion," Phys. Lett. A **271**, 319–326 (2000).

[89] J. Eisert, F. G. S. L. Brandão, and K. M. R. Audenaert, "Quantitative entanglement witnesses," New J. Phys. **9**, 46 (2007).

[90] D. Chruściński and G. Sarbicki, "Entanglement witnesses: construction, analysis and classification," J. Phys. A: Math. Theor. **47**, 483001 (2014).

[91] M. Curty, M. Lewenstein, and N. Lütkenhaus, "Entanglement as a precondition for secure quantum key distribution," Phys. Rev. Lett. **92**, 217903 (2004).

[92] M. Curty, O. Gühne, M. Lewenstein, and N. Lütkenhaus, "Detecting two-party quantum correlations in quantum-key-distribution protocols," Phys. Rev. A **71**, 022306 (2005).

[93] P. Hyllus, O. Gühne, D. Bruss, and M. Lewenstein, "Relations between entanglement witnesses and bell inequalities," Phys. Rev. A **72**, 012321 (2005).

[94] H. S. Park, S.-S. B. Lee, H. Kim, S.-K. Choi, and H.-S. Sim, "Construction of an optimal witness for unknown two-qubit entanglement," Phys. Rev. Lett. **105**, 230404 (2010).

[95] M. Lewenstein, B. Kraus, J. I. Cirac, and P. Horodecki, "Optimization of entanglement witnesses," Phys. Rev. A **62**, 052310 (2000).

[96] R. Bryant, "Conditions for when an off-centre ellipsoid fits inside the unit ball," `http://mathoverflow.net/questions/140339/` (2013), accessed August 2016.

[97] N. Johnston, *Norms and Cones in the Theory of Quantum Entanglement*, Ph.D. thesis, University of Guelph (2012).

[98] K. Życzkowski and I. Bengtsson, "On duality between quantum maps and quantum states," Open Syst. Inf. Dyn. **11**, 3 (2004).

[99] S. L. Woronowicz, "Positive maps of low dimensional matrix algebras," Rep. Math. Phys. **10**, 165–183 (1976).

[100] G. Sarbicki, "Spectral properties of entanglement witnesses," J. Phys. A: Math. Theor. **41**, 375303 (2008).

[101] P. Badziąg, P. Horodecki, R. Horodecki, and R. Augusiak, "Separability in terms of a single entanglement witness," Phys. Rev. A **88**, 010301 (2013).

[102] J. K. Korbicz, M. L. Almeida, J. Bae, M. Lewenstein, and A. Acín, "Structural approximations to positive maps and entanglement-breaking channels," Phys. Rev. A **78**, 062105 (2008).

[103] B.-H. Wang and D.-Y. Long, "Structural physical approximations and entanglement witnesses," Phys. Rev. A **87**, 062324 (2013).

[104] B.-H. Wang, H.-R. Xu, S. Campbell, and S. Severini, "Characterization and properties of weakly optimal entanglement witnesses," Quantum Inform. Compu. **15**, 1109 (2015).

[105] K. Ried, M. Agnew, L. Vermeyden, D. Janzing, R. W. Spekkens, and K. J. Resch, "Inferring causal structure: a quantum advantage," Nat. Phys. **11**, 414 (2015).

[106] O. Bottema, R. Z. Djordjević, R. R. Janić, D. S. Mitrinović, and P. M. Vasić, *Geometric inequalities* (Wolters-Noordhoff Publishing, 1969).

[107] A. M. Balk and M. B. Balk, "The enigma of the triangular pyramid," J. Geom. **62**, 13–25 (1998).

[108] O. Bottema, R. Z. Djordjević, R. R. Janić, D. S. Mitrinović, and P. M. Vasić, *Recent advances in geometric inequalities* (Springer, 1989).

[109] J. H. Grace, "Tetrahedra in relation to spheres and quadrics," Proc. London Math. Soc. **17**, 259–271 (1918).

[110] G. Danielsson, "Proof of the inequality $d^2 \leq (R + r)(R - 3r)$ for the distance between the centres of the circumscribed and inscribed spheres of a tetrahedron," in *Den 11te Skandinaviske Matematikerkongress, Trondheim, 1949* (1952) pp. 101–105.

[111] G. C. Smith, "Statics and the moduli space of triangles," Forum Geom. **5**, 181–190 (2005).

[112] A. Sanpera, R. Tarrach, and G. Vidal, "Local description of quantum inseparability," Phys. Rev. A **58**, 826–830 (1998).

[113] M. Vidrighin, "Does every ellipse inside a tetrahedron inside a ball fit in a triangle inside the ball?" http://mathoverflow.net/questions/109153/ (2012), accessed August 2016.

[114] G. Egan, "An n-dimensional Grace-Danielsson inequality," http://blogs.ams.org/visualinsight/2014/06/01/grace-danielsson-inequality/ (2014), accessed August 2016.